National Aeronautics and Space Administration

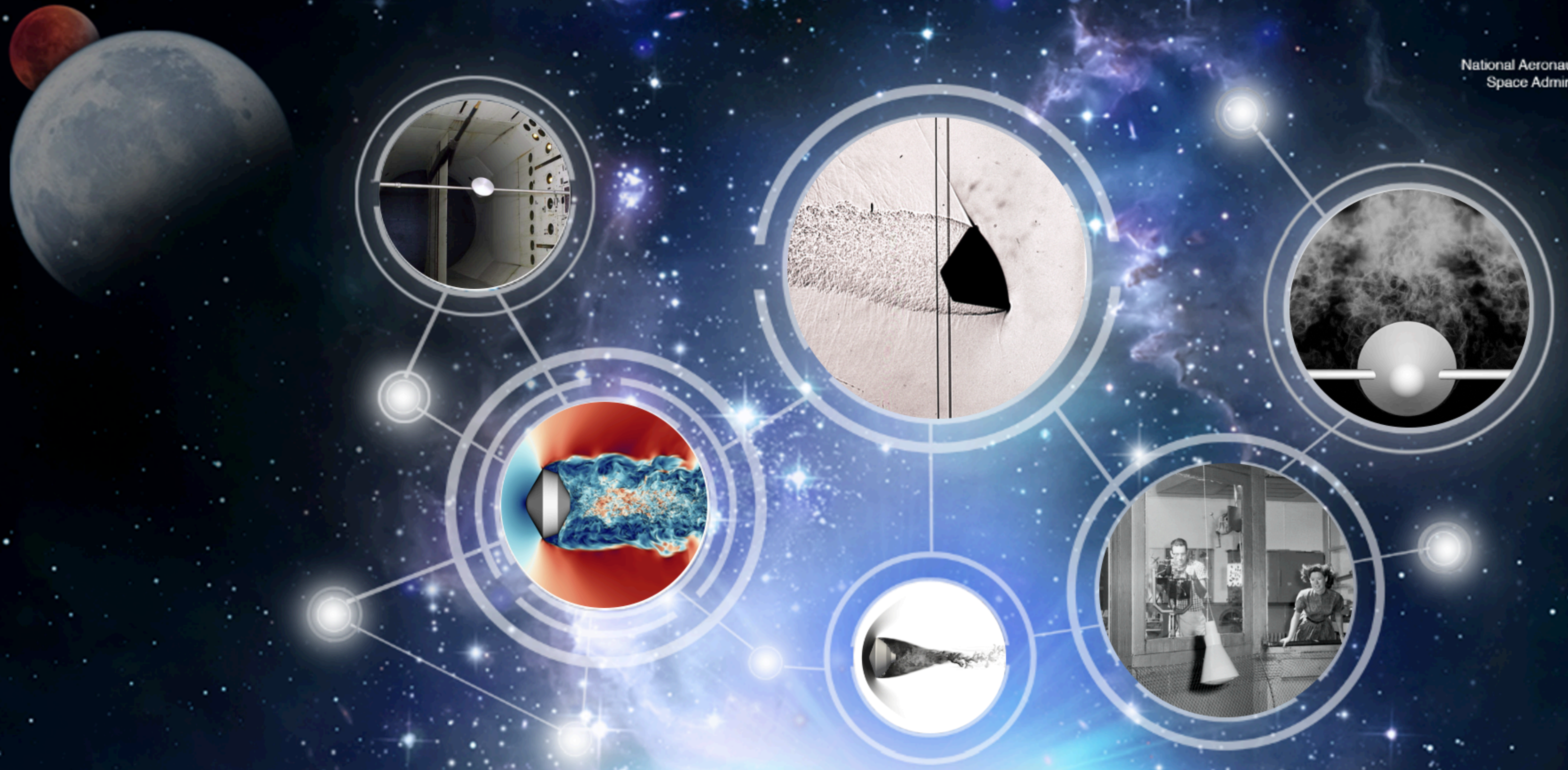

Dynamic Stability Methodologies and Capabilities

Joseph Brock
Eric Stern
Cole Kazemba
Quincy McKown
Dirk Ekelschot

Characterization of Dynamic Stability

- Blunt-body capsules are subject to dynamic instabilities at low-supersonic and transonic Mach numbers
- Dynamic stability typically characterized exclusively via experiment: forced-, free-oscillation, and ballistic range
  - These methods have a long pedigree of producing dynamic aero for missions
  - However, each method has drawbacks resulting in uncertain predictions
- Current entry missions have dynamics challenges:
  - MSR EES: dynamics during terminal descent drive impact angle which is key for containment
  - Dragonfly: coupled capsule-chute dynamics drive Lander separation event
- Mission needs motivate improved capabilities beyond what standard methods can provide
- Renewed effort on various fronts to characterize dynamics via new testing and computational methods

Mars Phoenix Lander (Desai, 2011)

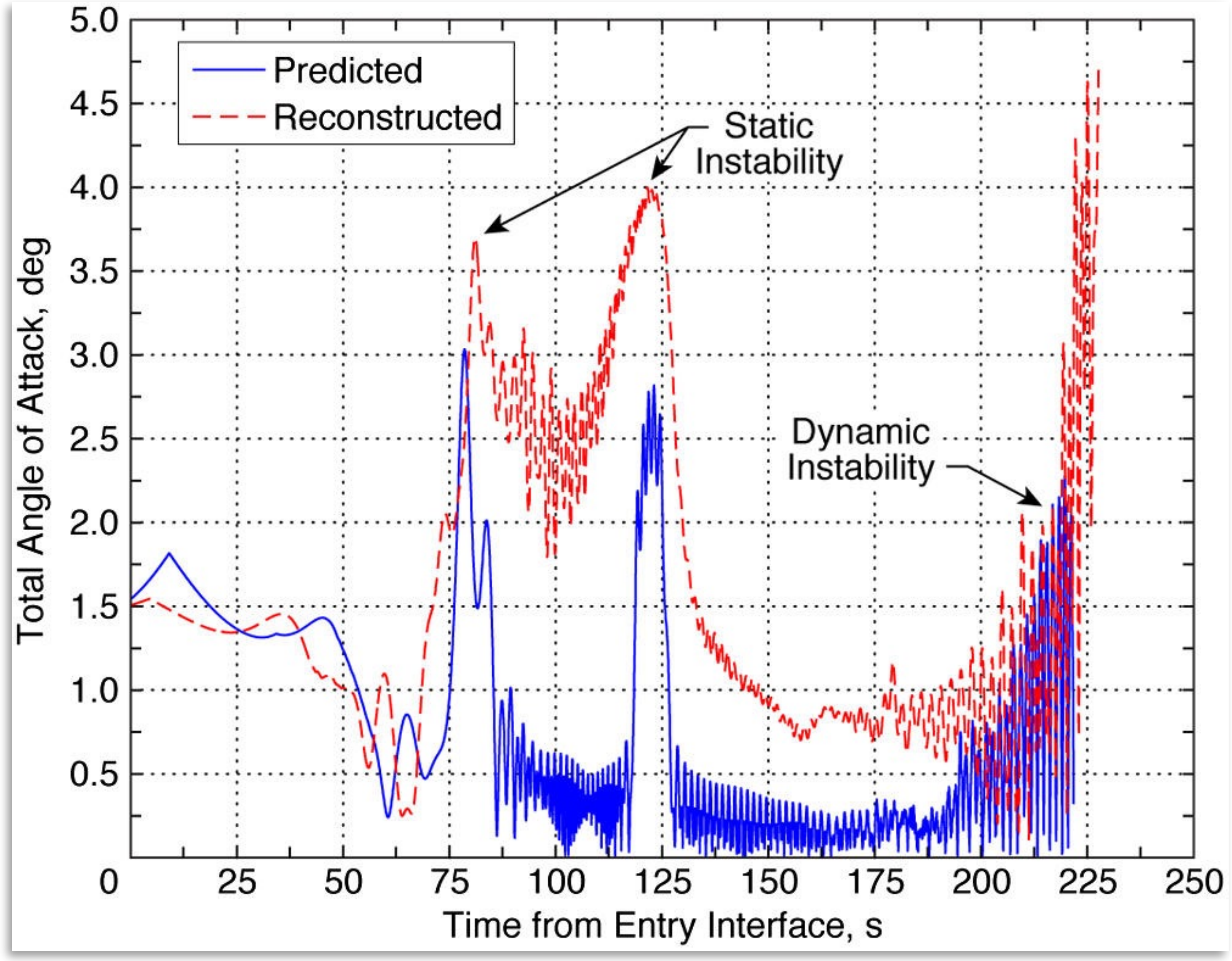

Dynamic instabilities of blunt bodies often arise at low-supersonic and transonic Mach numbers

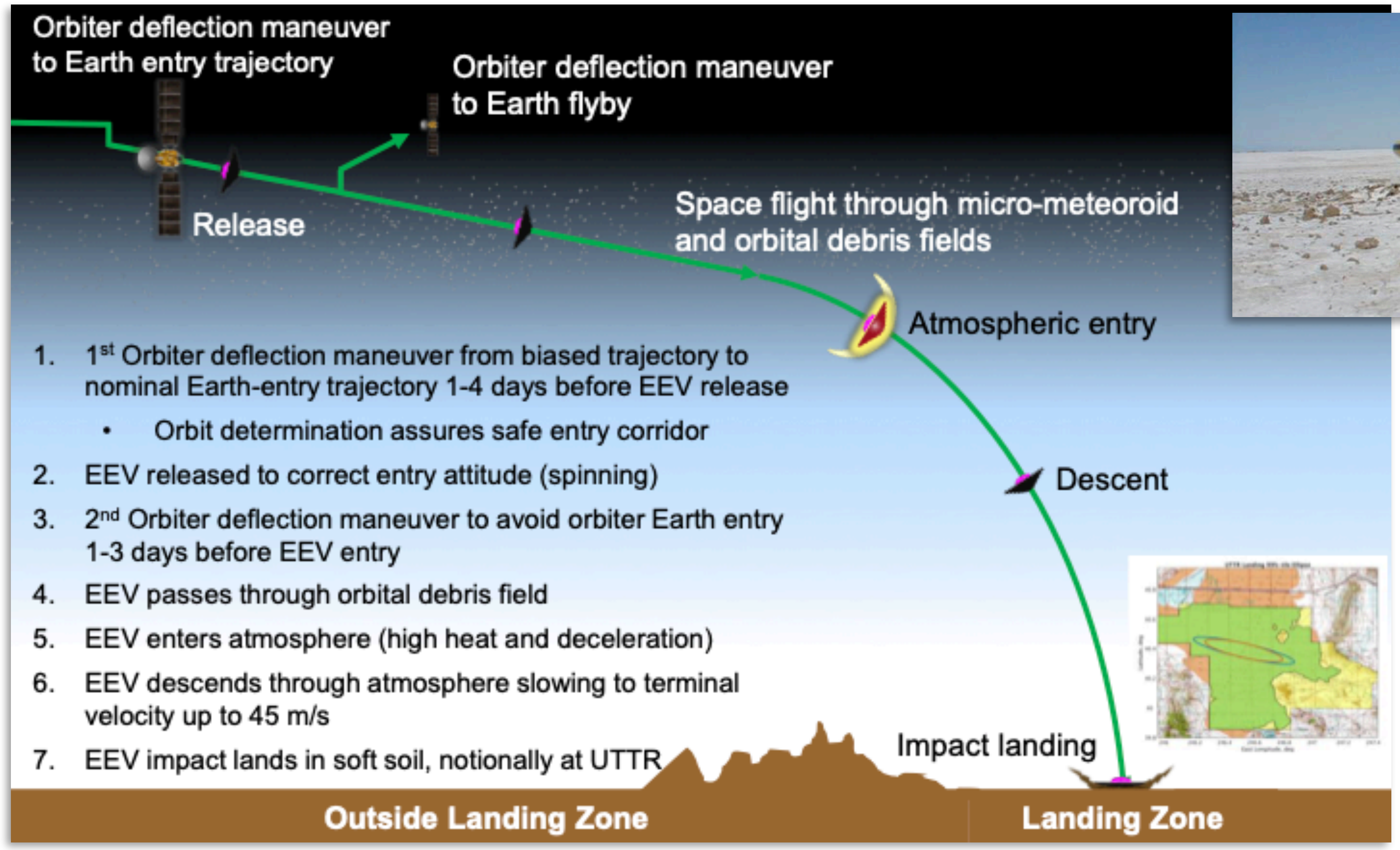

Characterization of Dynamic Stability

- Blunt-body capsules are subject to dynamic instabilities at low-supersonic and transonic Mach numbers
- Dynamic stability typically characterized exclusively via experiment: forced-, free-oscillation, and ballistic range
  - These methods have a long pedigree of producing dynamic aero for missions
  - However, each method has drawbacks resulting in uncertain predictions
- Current entry missions have dynamics challenges:
  - MSR EES: dynamics during terminal descent drive impact angle which is key for containment
  - Dragonfly: coupled capsule-chute dynamics drive Lander separation event
- Mission needs motivate improved capabilities beyond what standard methods can provide
- Renewed effort on various fronts to characterize dynamics via new testing and computational methods

Mars Phoenix Lander (Desai, 2011)

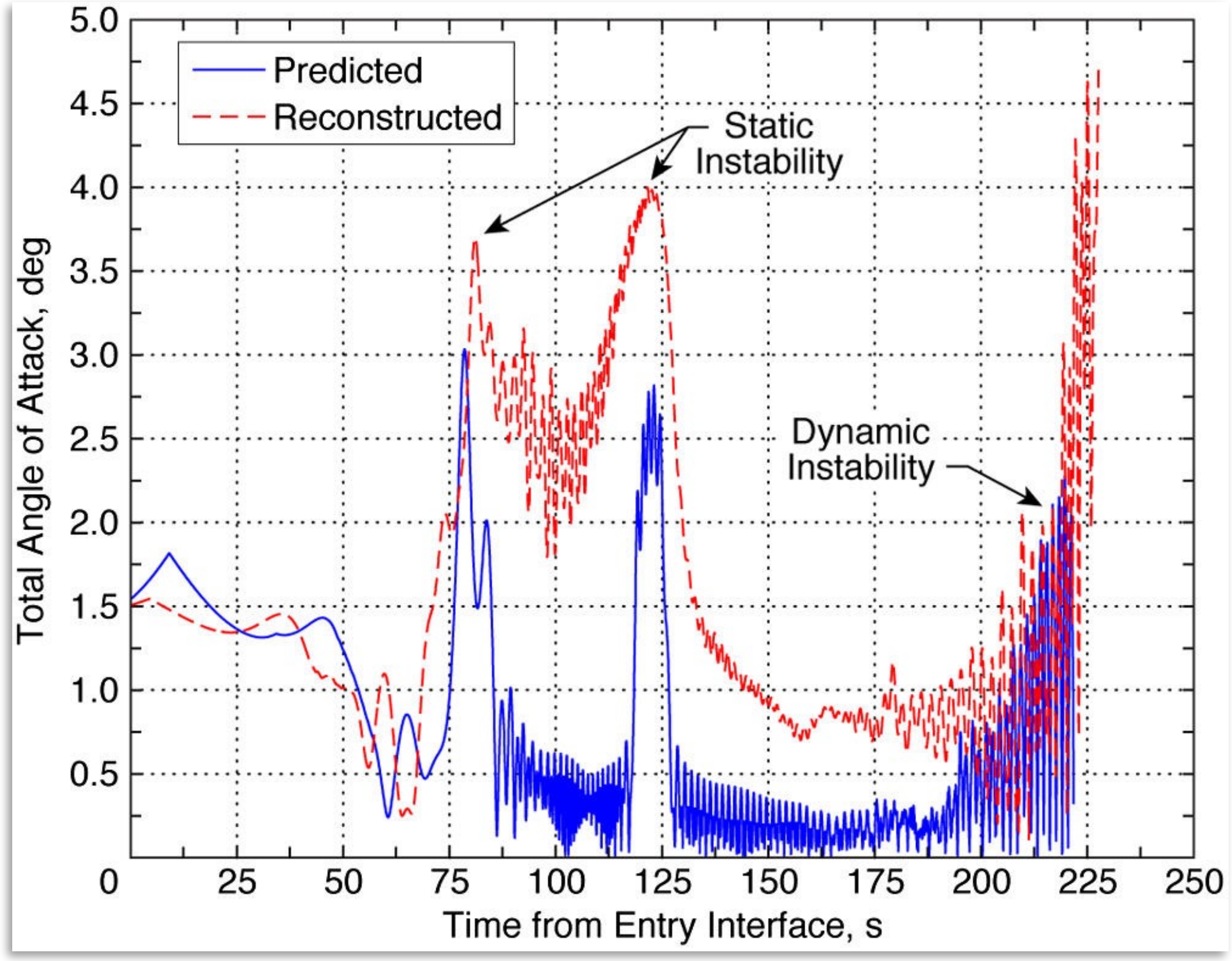

Dynamic instabilities of blunt bodies often arise at low-supersonic and transonic Mach numbers

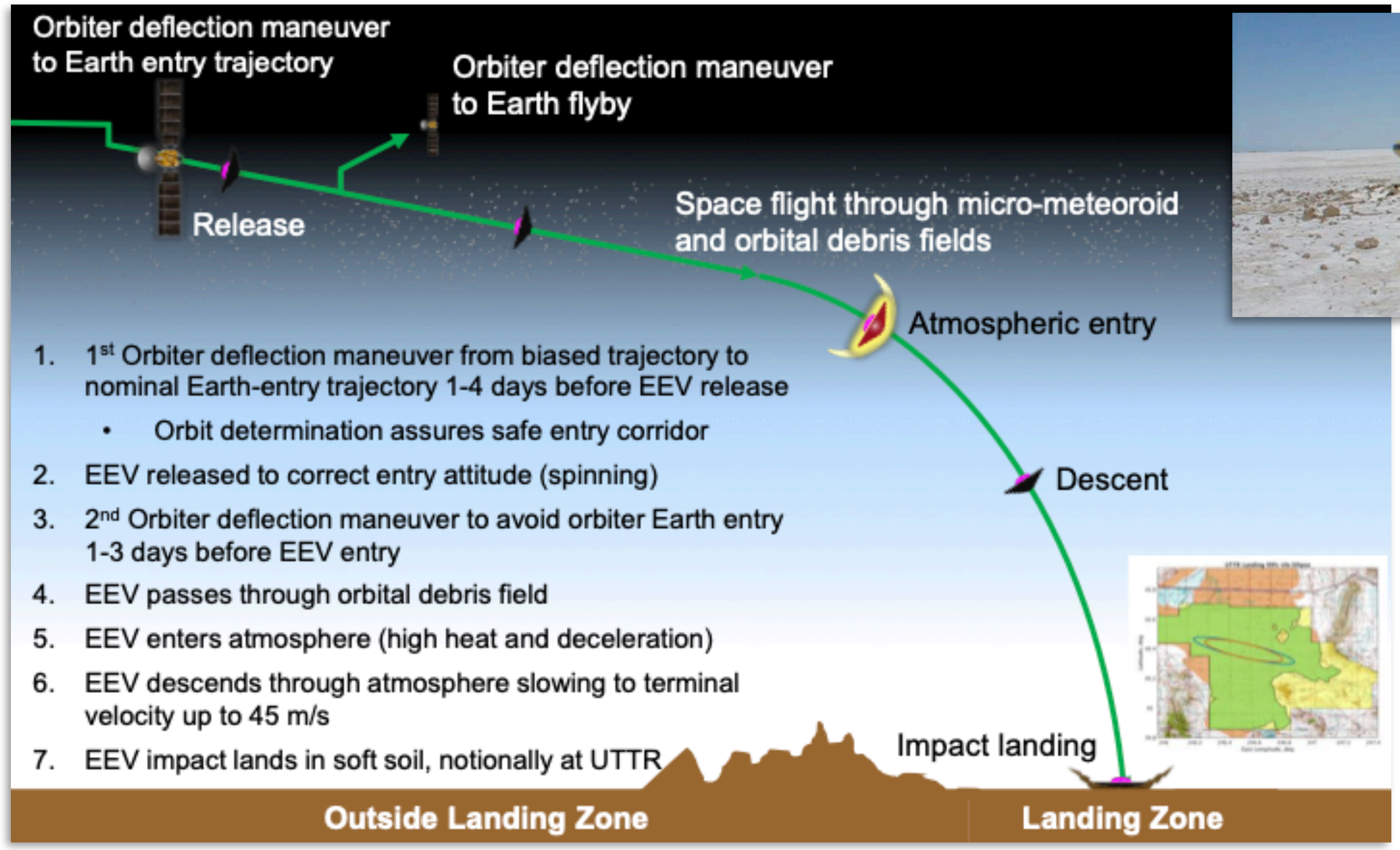

State of the Art: Experimental Facilities

- The current paradigm for dynamic stability testing relies on a piecemeal of different test methods:
  - Multiple test methods provides Mach coverage and helps to compensate for the deficiencies of each individual test method.
  - Flight testing requires typically occurs at lower speeds, sub-scale, or approximate Reynolds number due to gas composition differences
  - Sting mounted setups mirror classic wind-tunnel approaches to provide force and moment data directly
  - Each test methodology relies on a different data reduction approach, all of which differ from flight reconstruction methods
  - Little overlap between the attainable Mach numbers for the different methodologies.

- Each test approach has one or more key weaknesses:
  - Facility induced effects (e.g. stings)
  - Ability to match dynamic similitude and/or Reynolds Number
  - Richness of data for reconstruction and ADB development (e.g. loss of forces/moment data)

- Number of available test facilities is limited:
  - NASA Ames HFFAF and Aberdeen are the only available ballistic range facilities
  - NASA LaRC TDT facility is standard for free- and forced oscillation. Scheduling is difficult
  - Subsonic MWST is coming online to address some of the weakness above

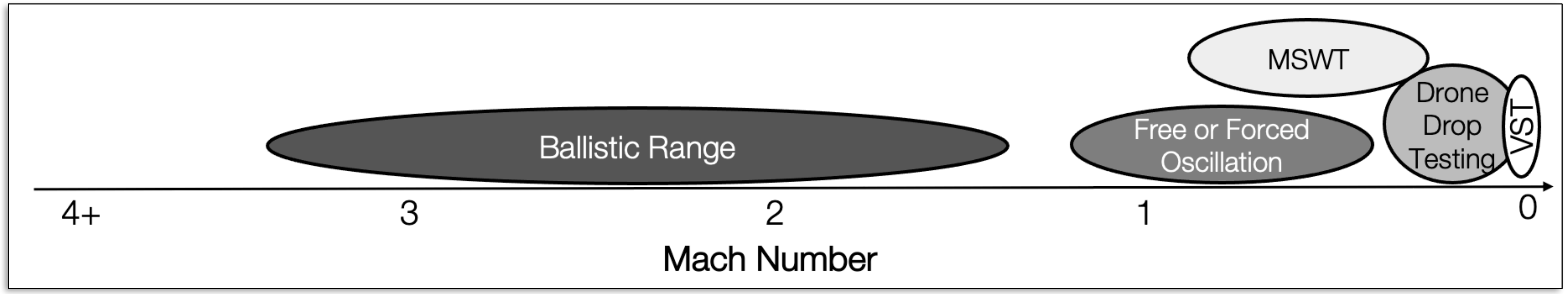

Vertical Spin Tunnel (VST)

Transonic Dynamics Tunnel (TDT)

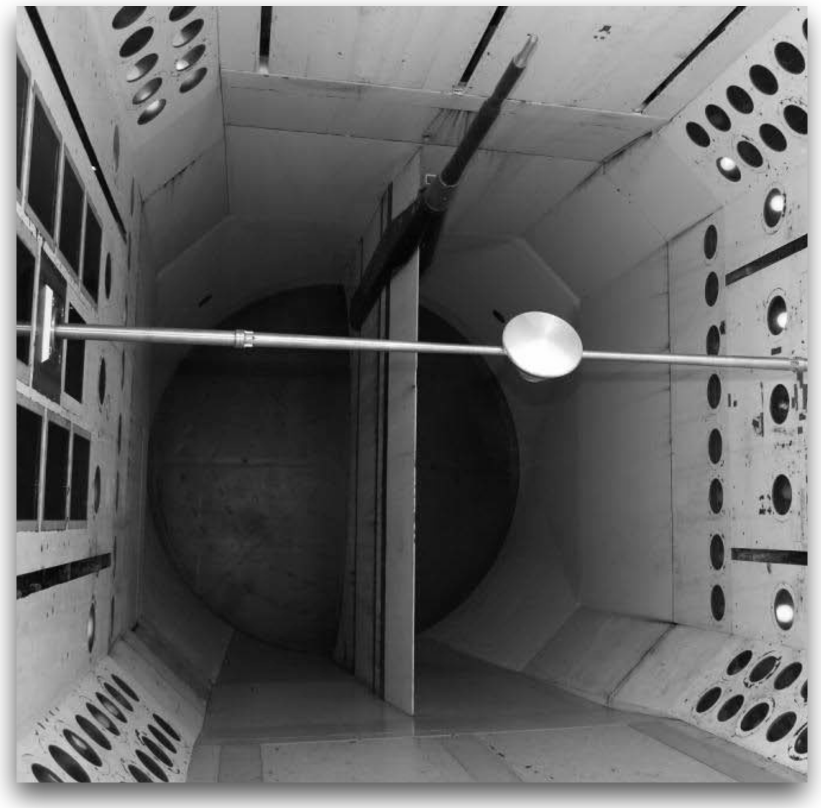

Indoor Ballistic Range

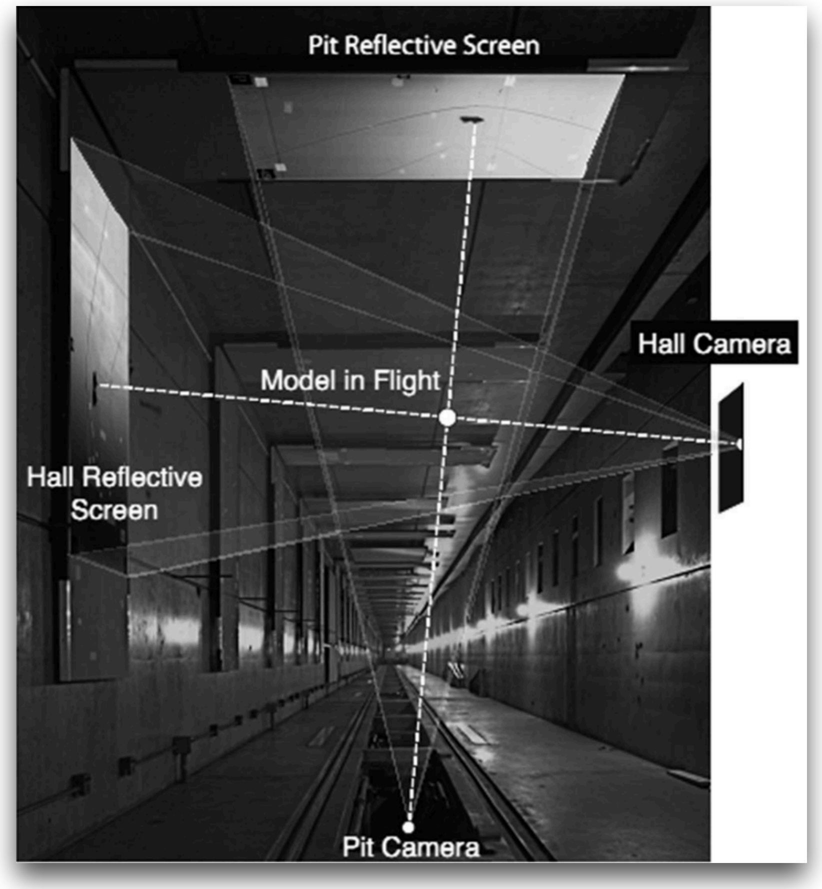

Magnetic Suspension Wind Tunnel

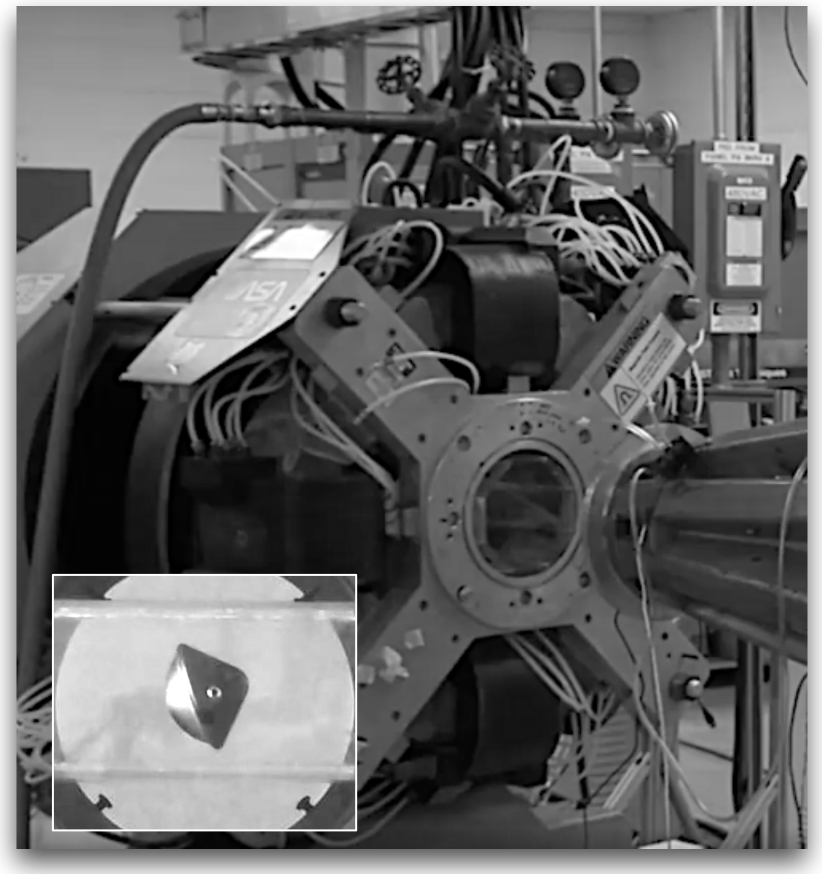

Hypervelocity Free Flight Aerodynamics Facility (HFFAF)

State of the Art: Experimental Facilities

- The current paradigm for dynamic stability testing relies on a piecemeal of different test methods:
  - Multiple test methods provides Mach coverage and helps to compensate for the deficiencies of each individual test method.
  - Flight testing requires typically occurs at lower speeds, sub-scale, or approximate Reynolds number due to gas composition differences
  - Sting mounted setups mirror classic wind-tunnel approaches to provide force and moment data directly
  - Each test meth
    reconstruction
  - Little overlap b

- Each test approach
  - Facility induce
  - Ability to matc
  - Richness of da

- Number of availabl
  - NASA Ames H
  - NASA LaRC T
  - Subsonic MWS

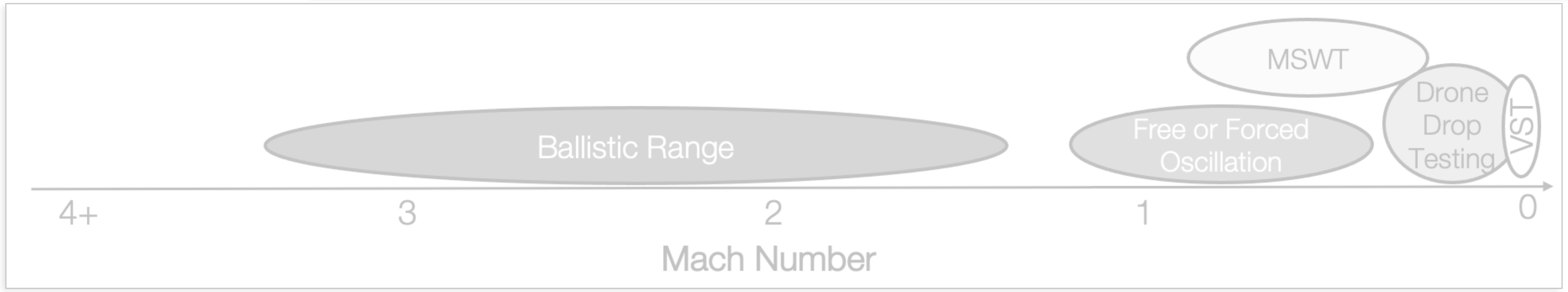

Vertical Spin Tunnel (VST)

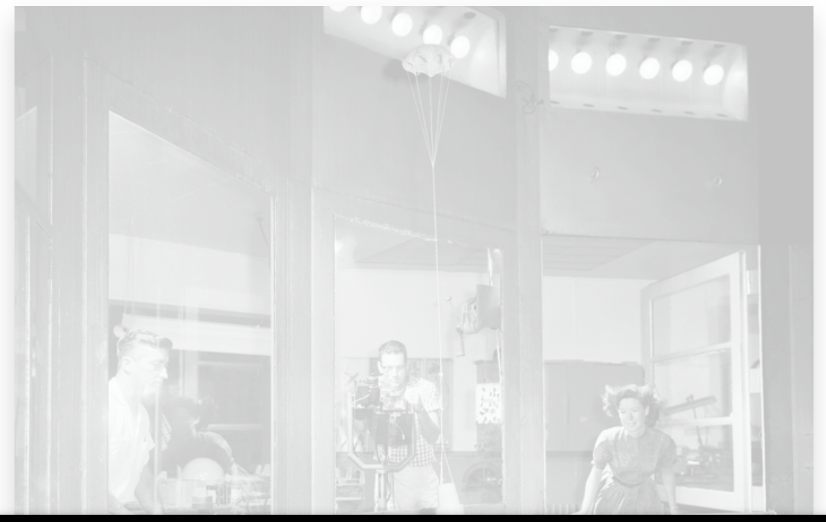

Transonic Dynamics Tunnel (TDT)

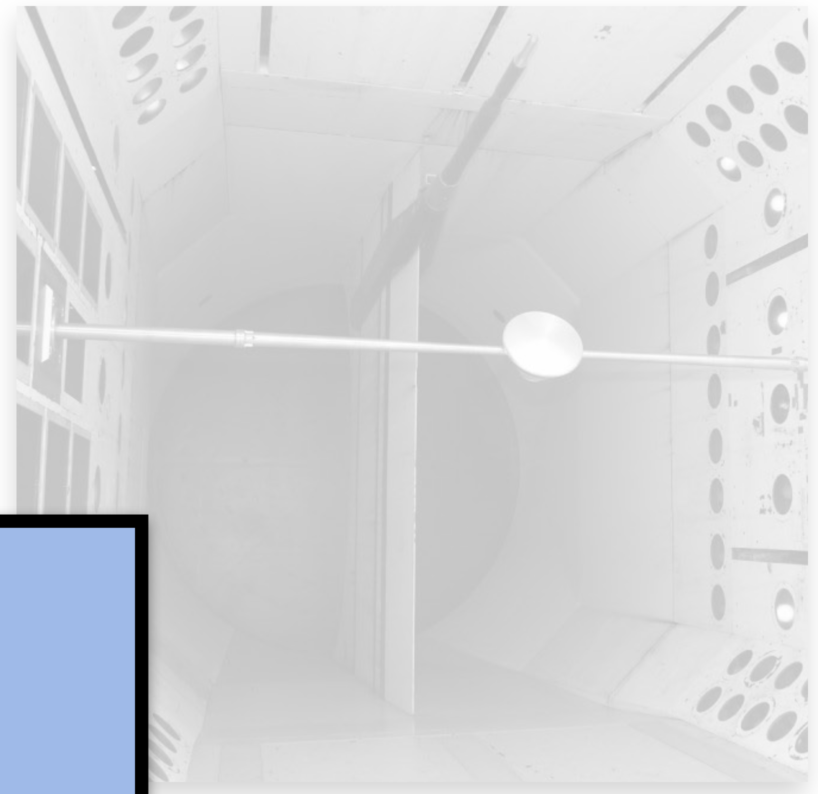

etic Suspension Wind Tunnel

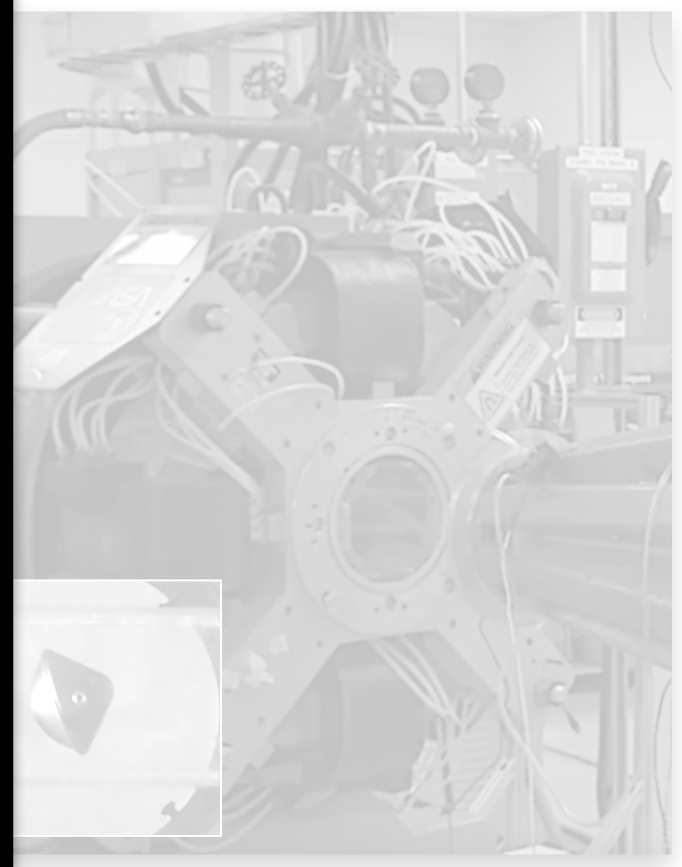

Hypervelocity Free Flight Aerodynamics Facility (HFFAF)

<u>There is no test capability that can simultaneously:</u>

- Replicate a flight-like environment across Mach regime of interest
  - Mach, Re, Degrees of Freedom, Free from interference
  - Free-Flight testing in transonic regime is not possible in current ground facilities
- Provide controlled and understood initial conditions
- Provide a detailed history of the vehicle state
  - Forces and moments, vehicle orientation and rotation rates, surface pressure
- Allow for enough test repeats to generate statistically significant set of observations
  - Oscillatory behavior is driven by interaction with the wake, making it inherently stochastic
  - Each shot in a ballistic range produces few oscillations in α_T

Computational Capabilities

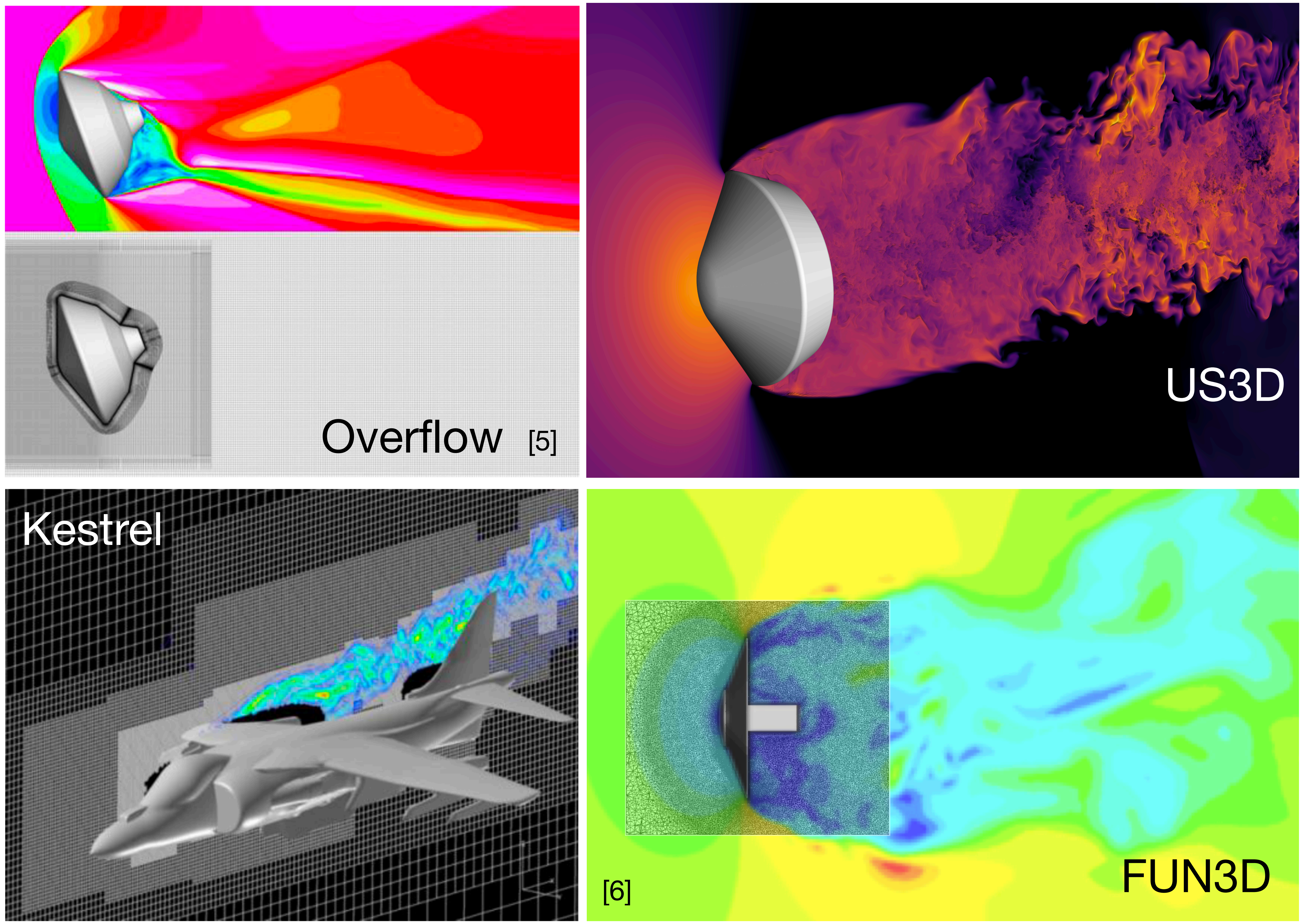

- Inherent constraints in test facilities motivate the development of complementary computational tools
- Several computational codes capable of 6DoF motion are emerging
  - Dynamic motion allows for simulations of forced and free-flying behavior of entry vehicles
- Simulation software verified with experiments will be used to generate dynamic databases anchored with experimental results
- Multiple tool sets provide wide range of Mach numbers and flow regimes to be analyzed

Computational Capabilities

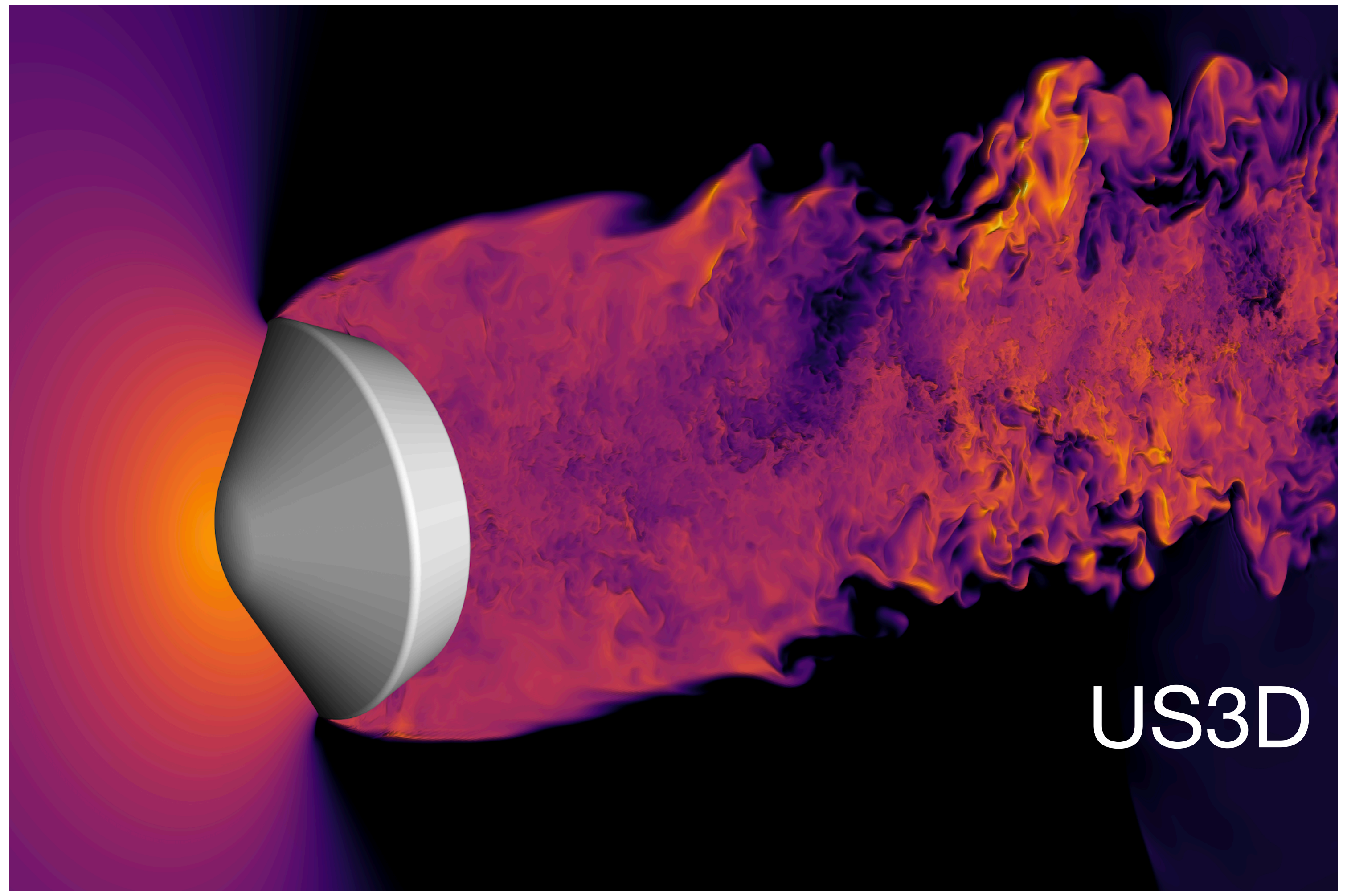

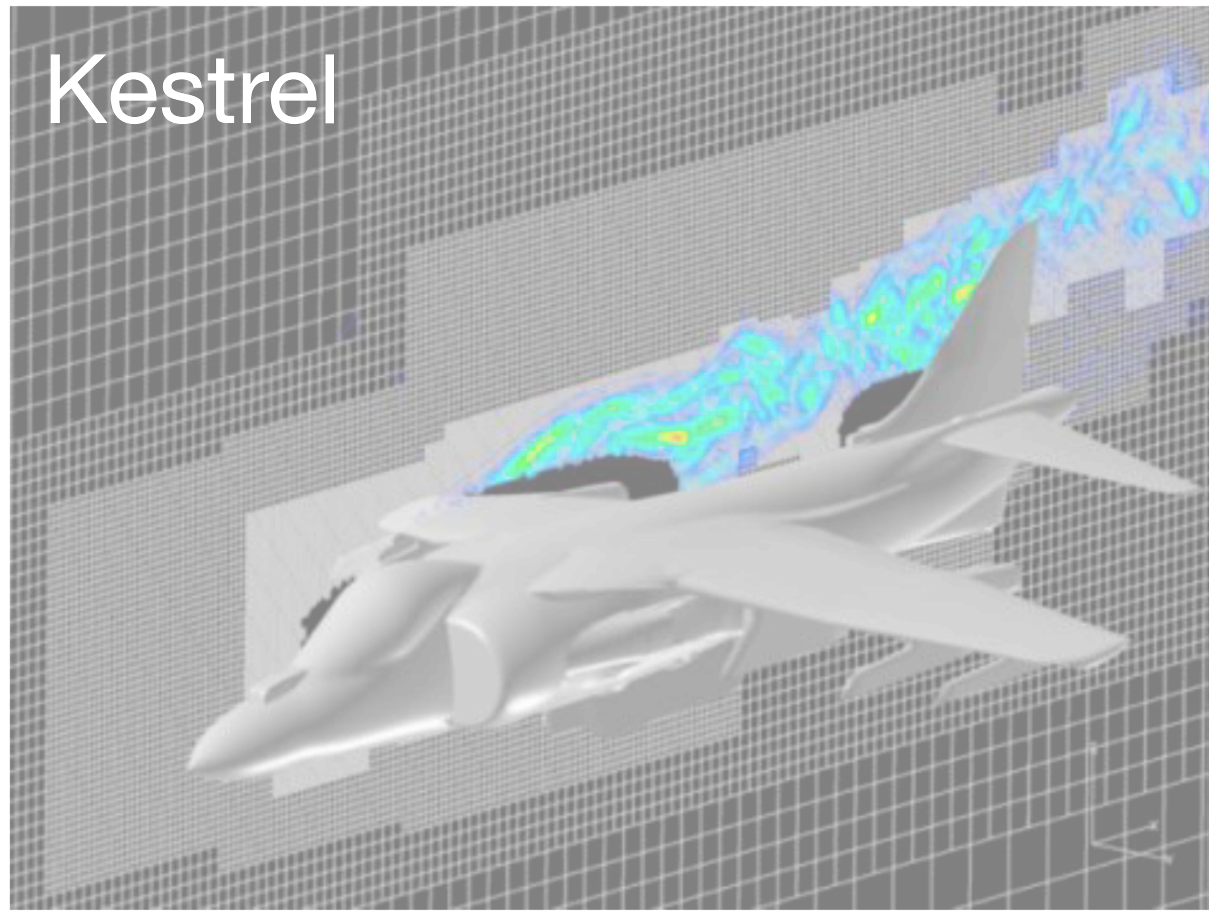

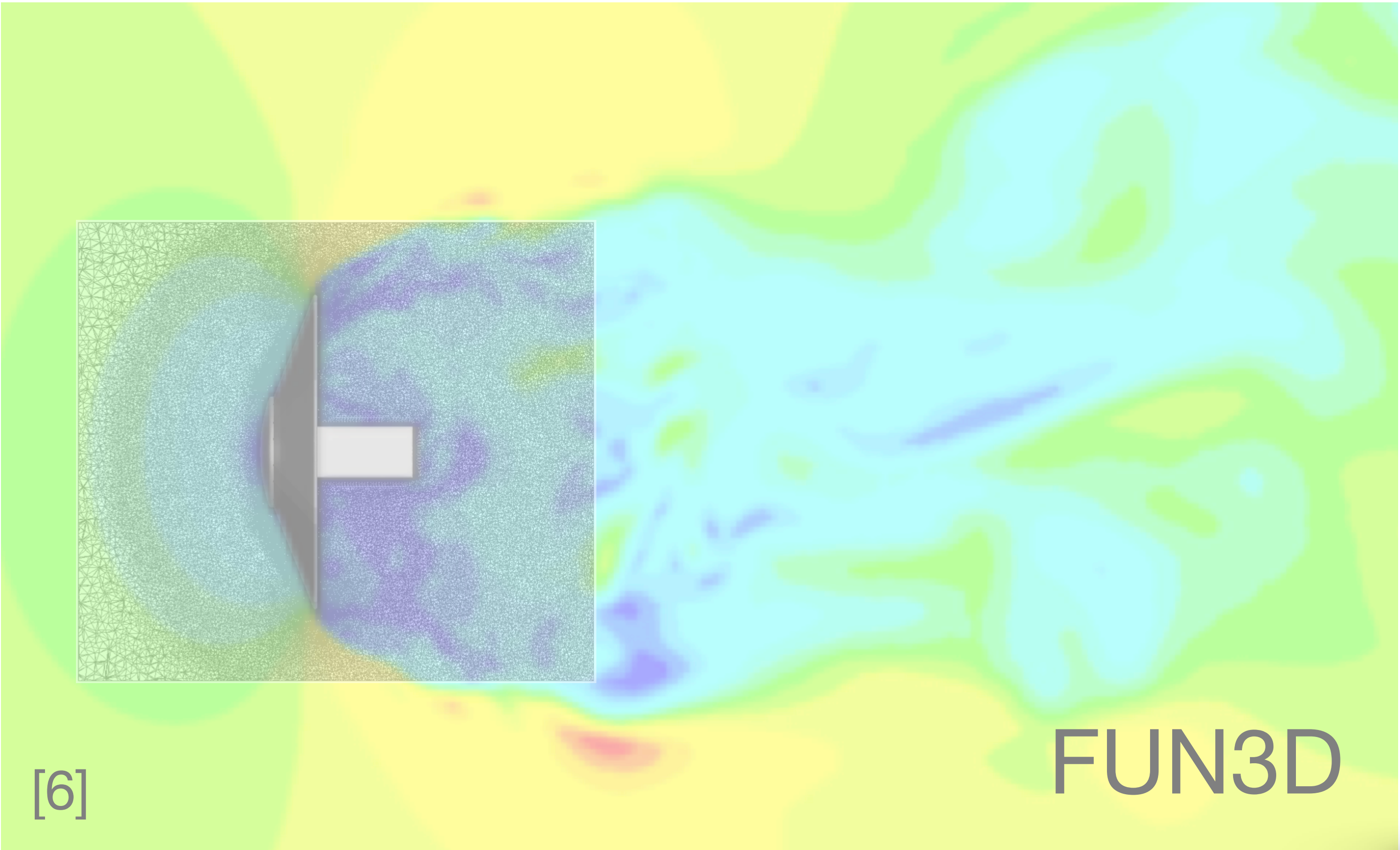

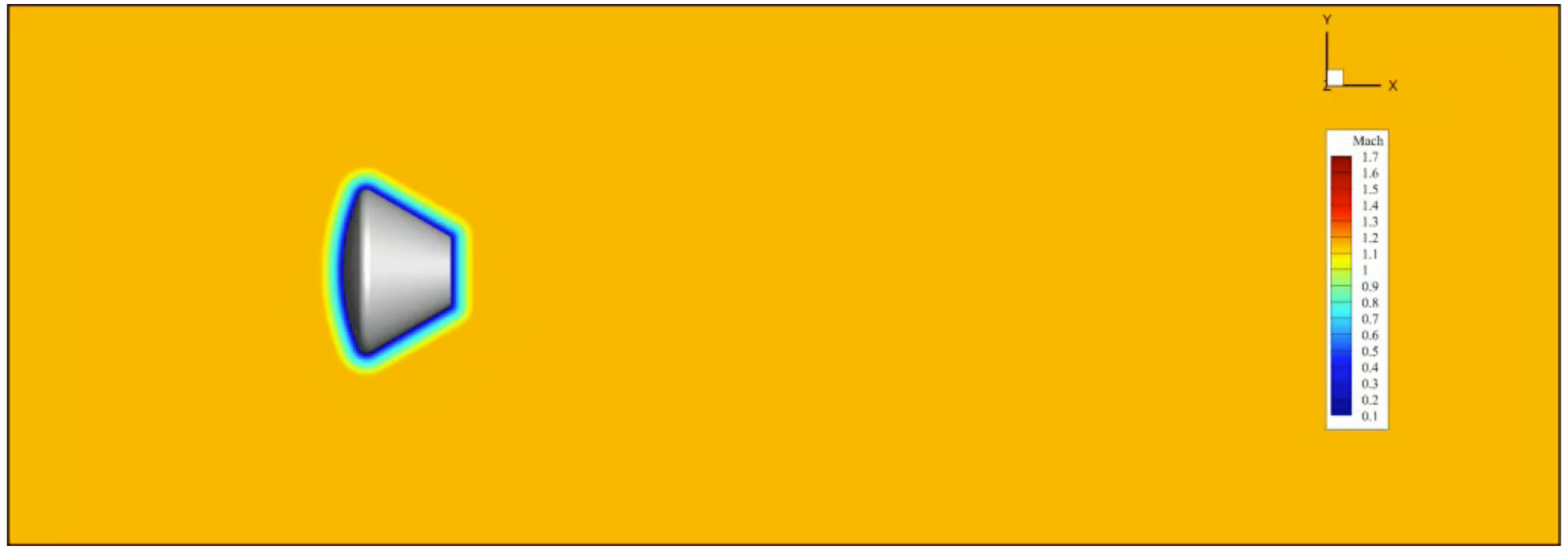

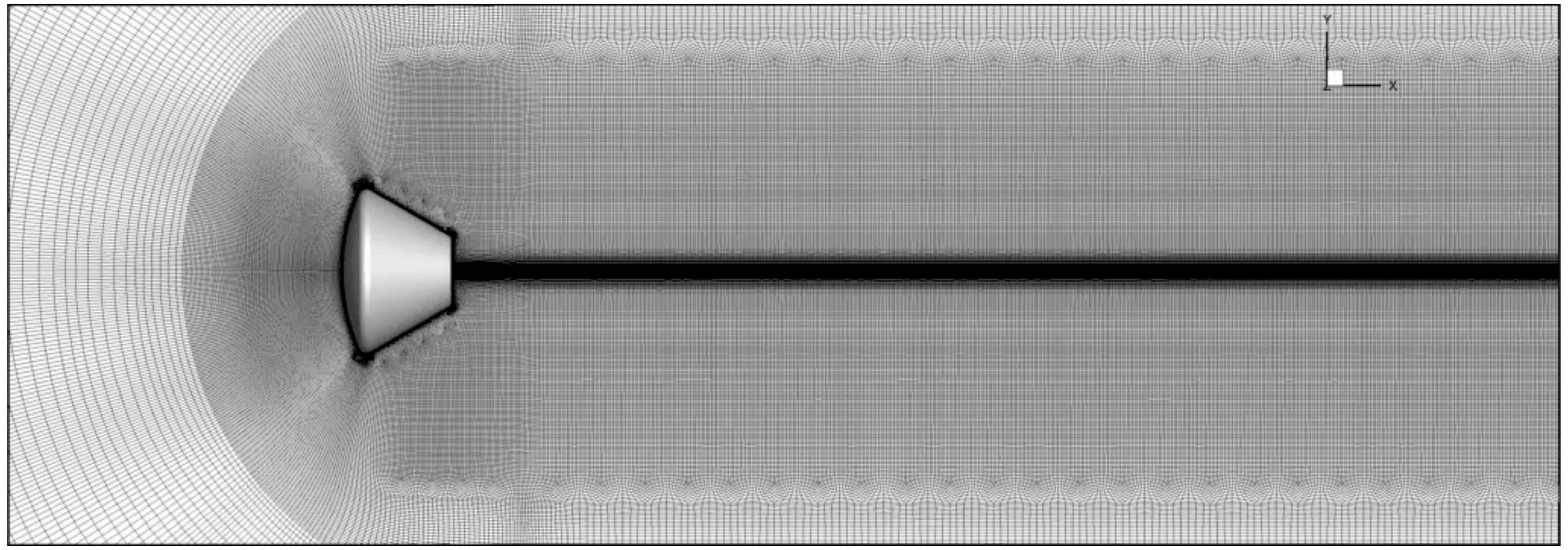

Free-Flight CFD (FF-CFD) combines a mesh deformation capability into an existing CFD solver (US3D) to allow an object to rigidly rotate about a center-of-gravity in response to aerodynamic forces. Translational velocities, which are accounted for in the discrete equations, allow a full six degrees of freedom simulation of free-flying objects.

Computational Capabilities

CFD is an integral part of *static* aerodynamic characterization and design.
It would be desirable to have similar capability for *dynamic* aerodynamics.

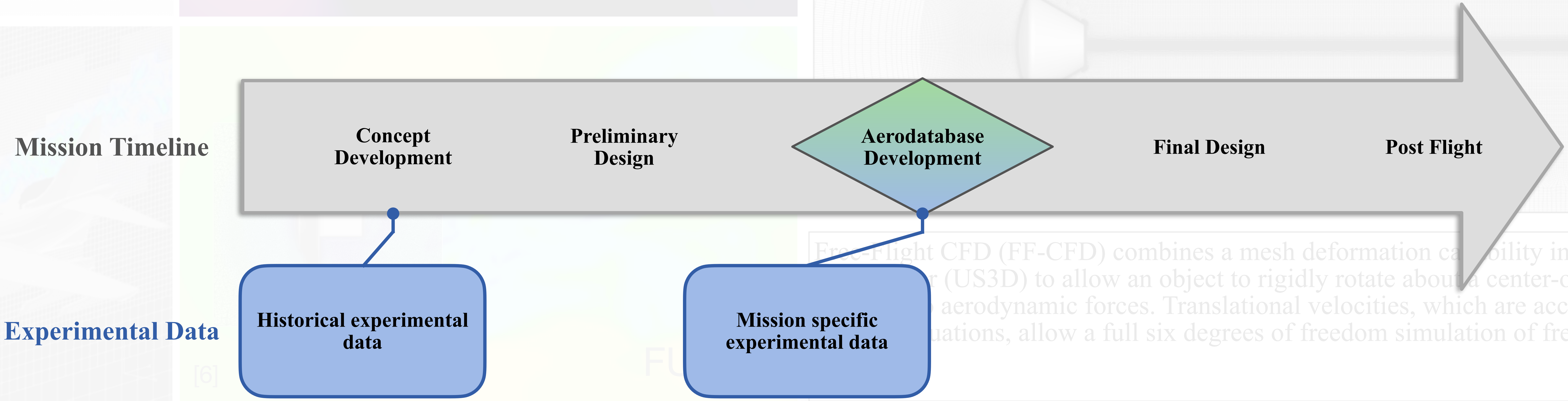

Computational Capabilities

CFD is an integral part of *static* aerodynamic characterization and design.
It would be desirable to have similar capability for *dynamic* aerodynamics.

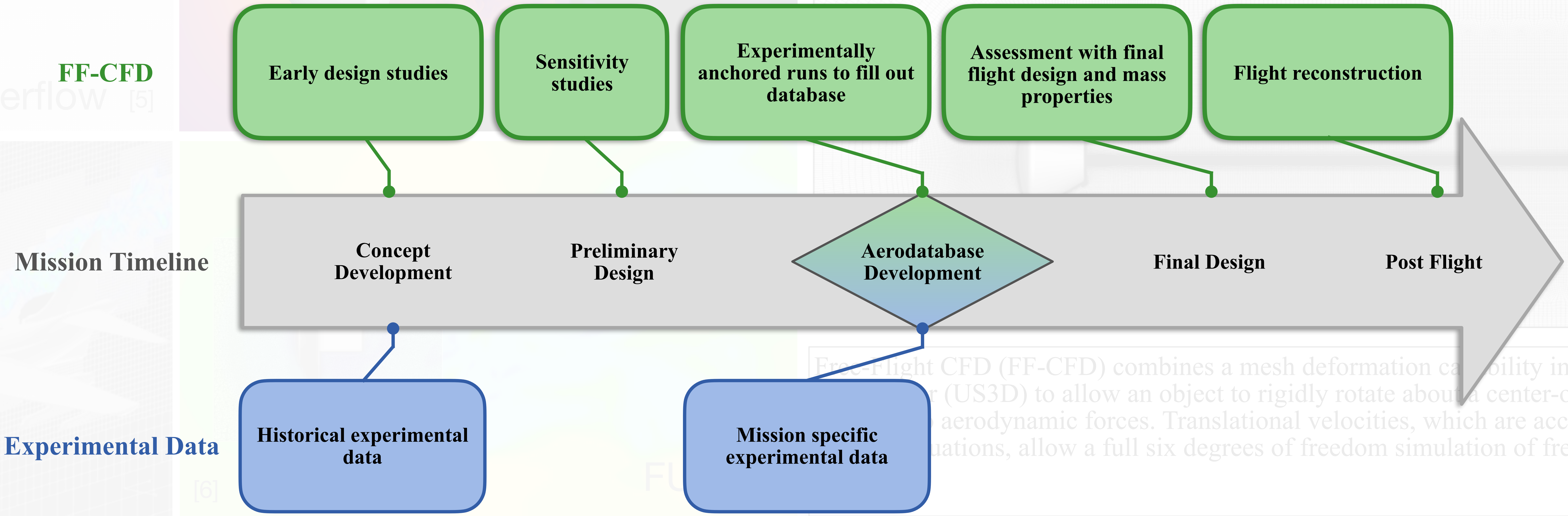

Current State of the Art

Single/Multi-body Dynamics

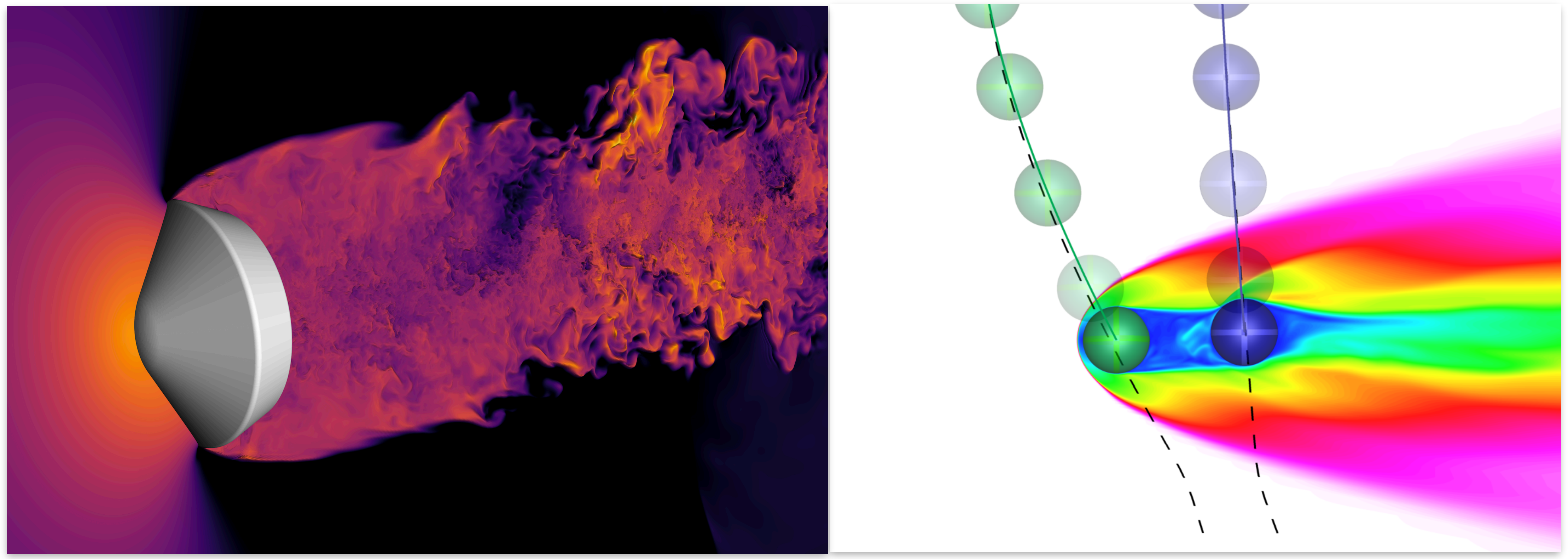

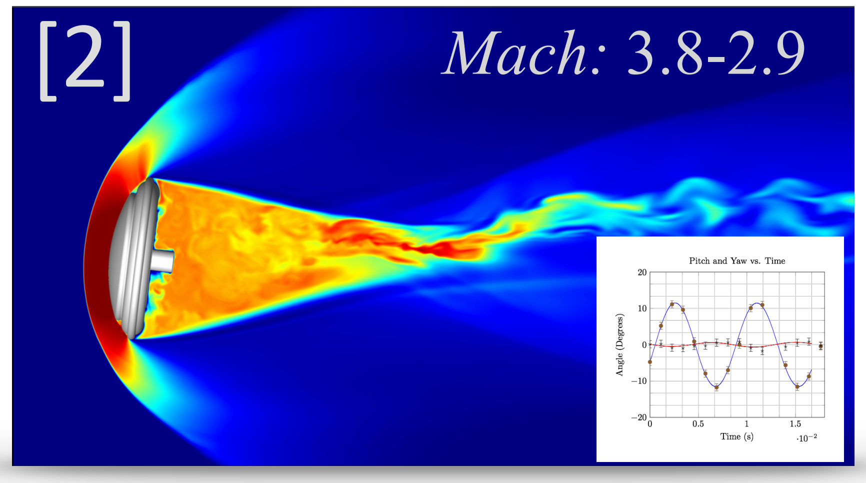

Validated against Experiment

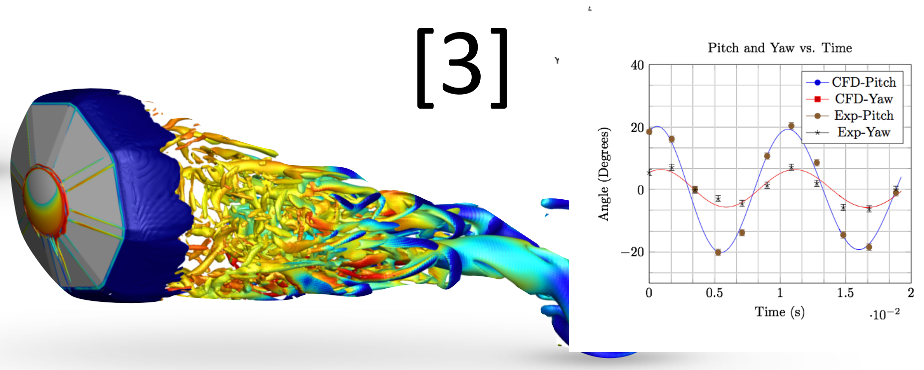

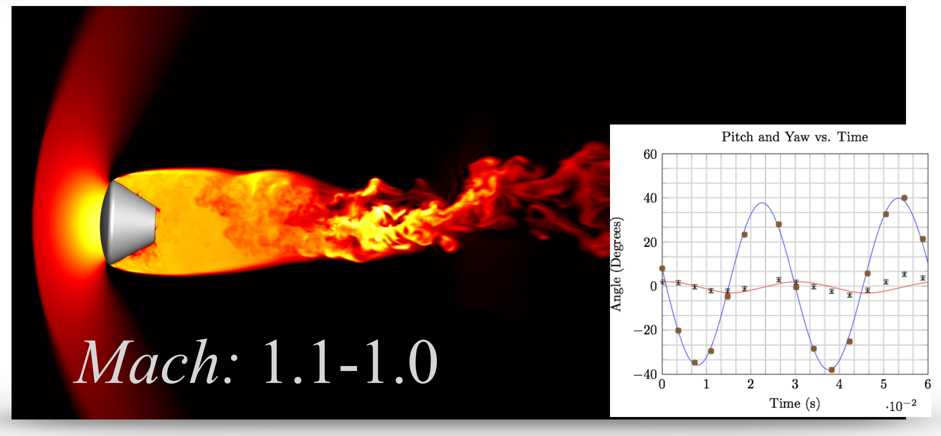

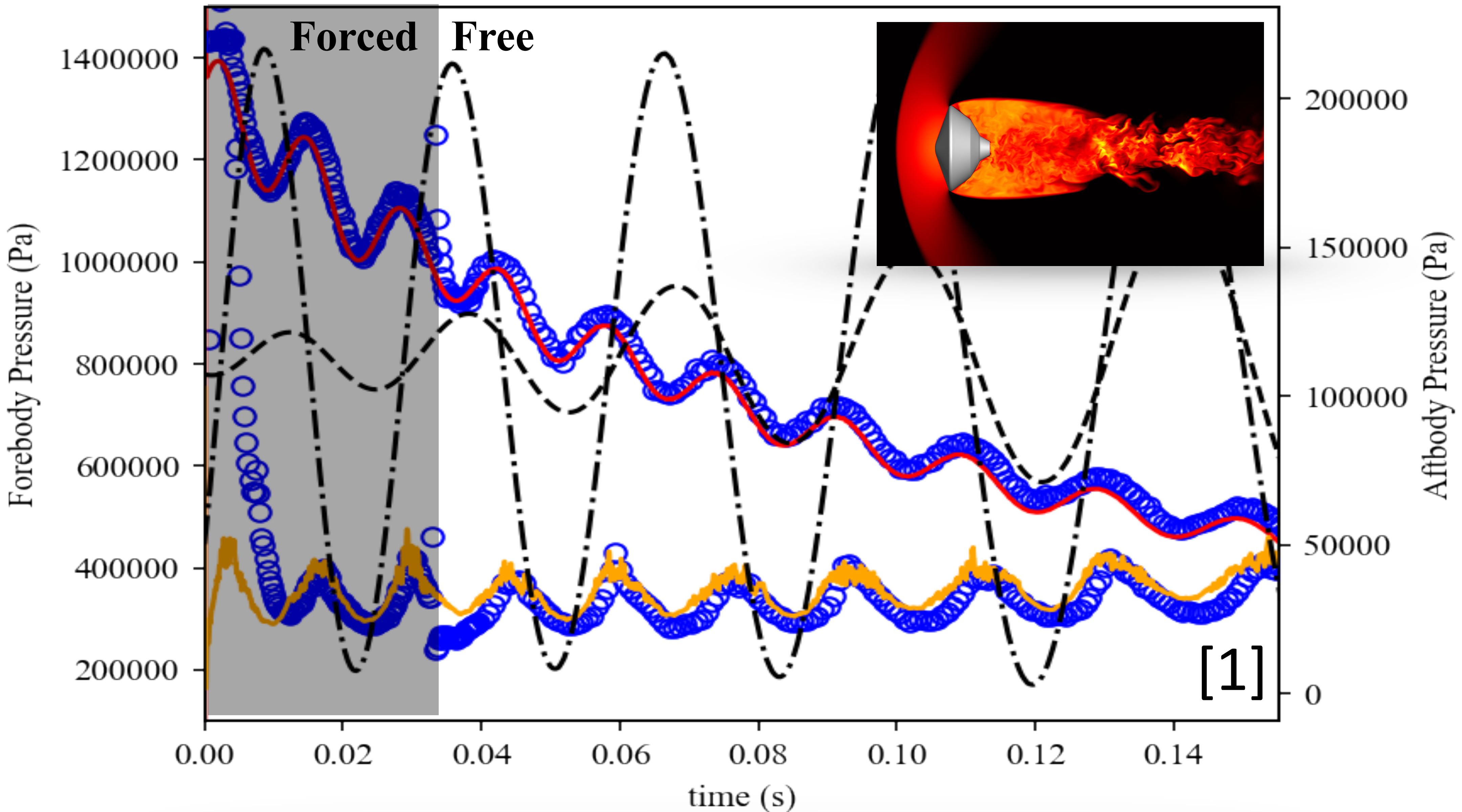

Atmospheric Flight with EarthGRAM

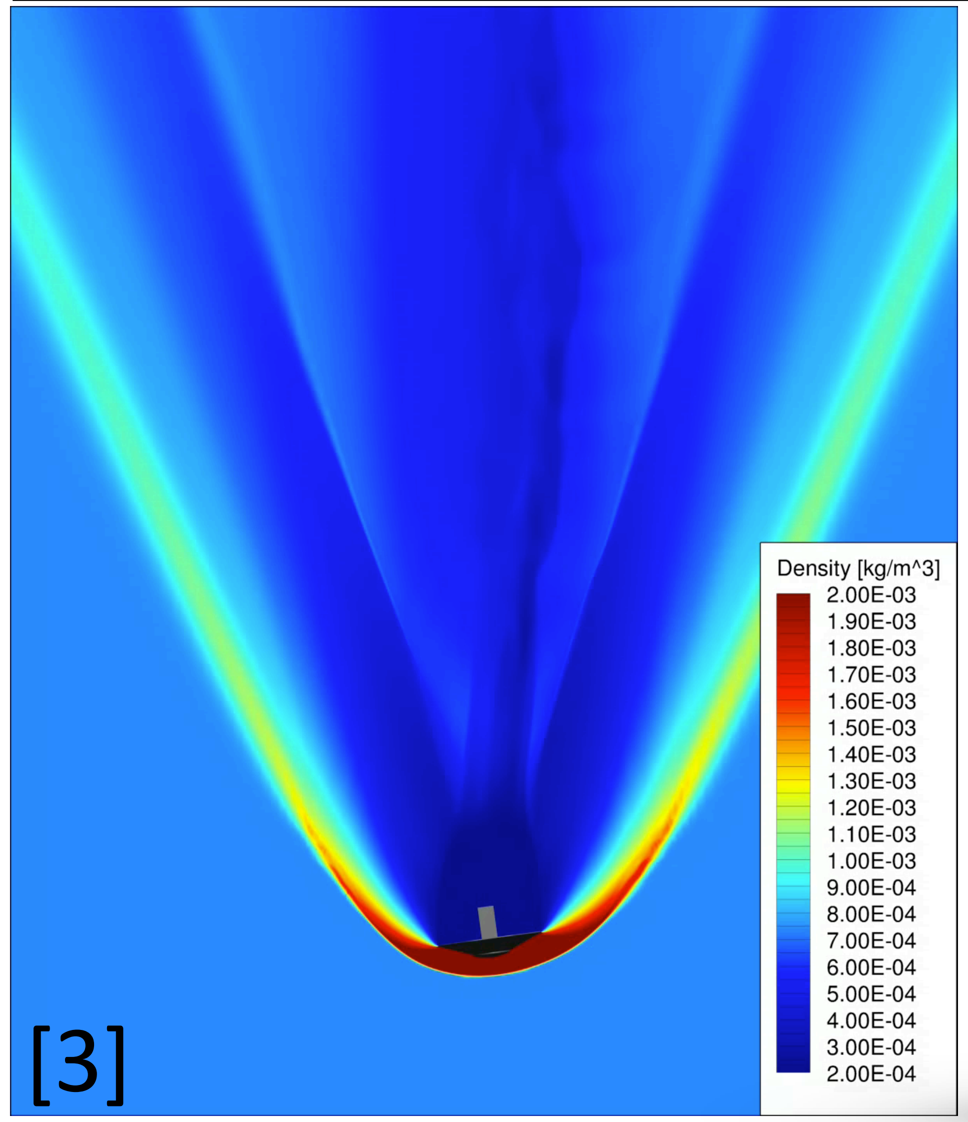

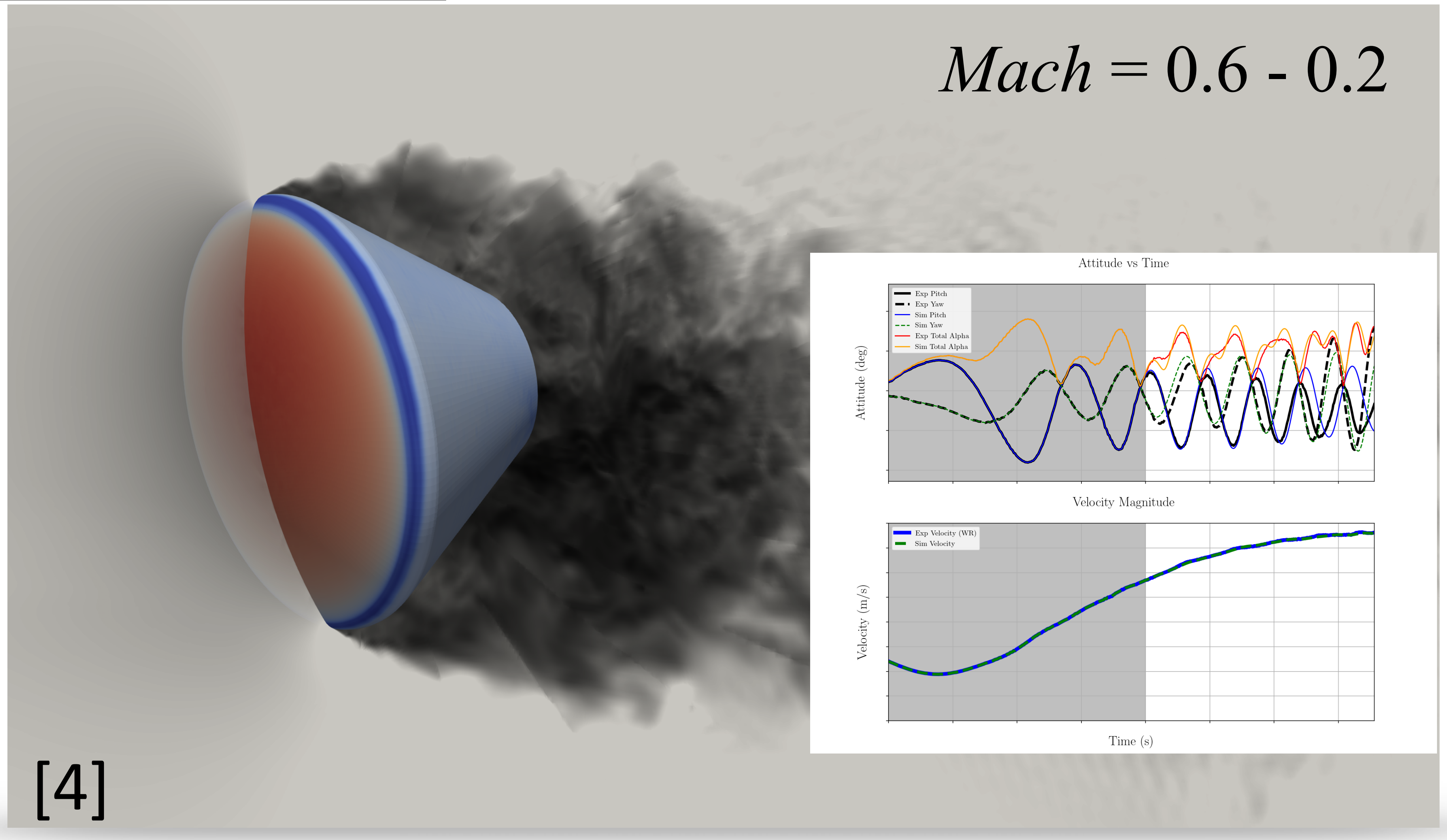

Current State of the Art

Single/Multi-body Dynamics

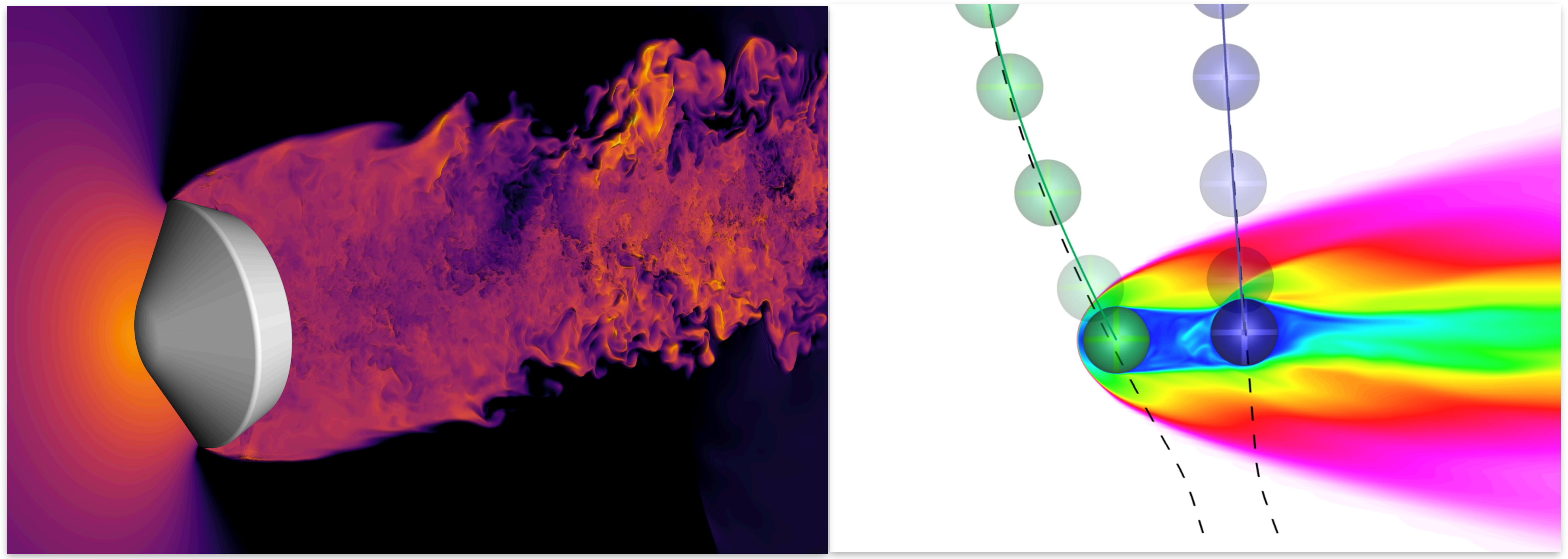

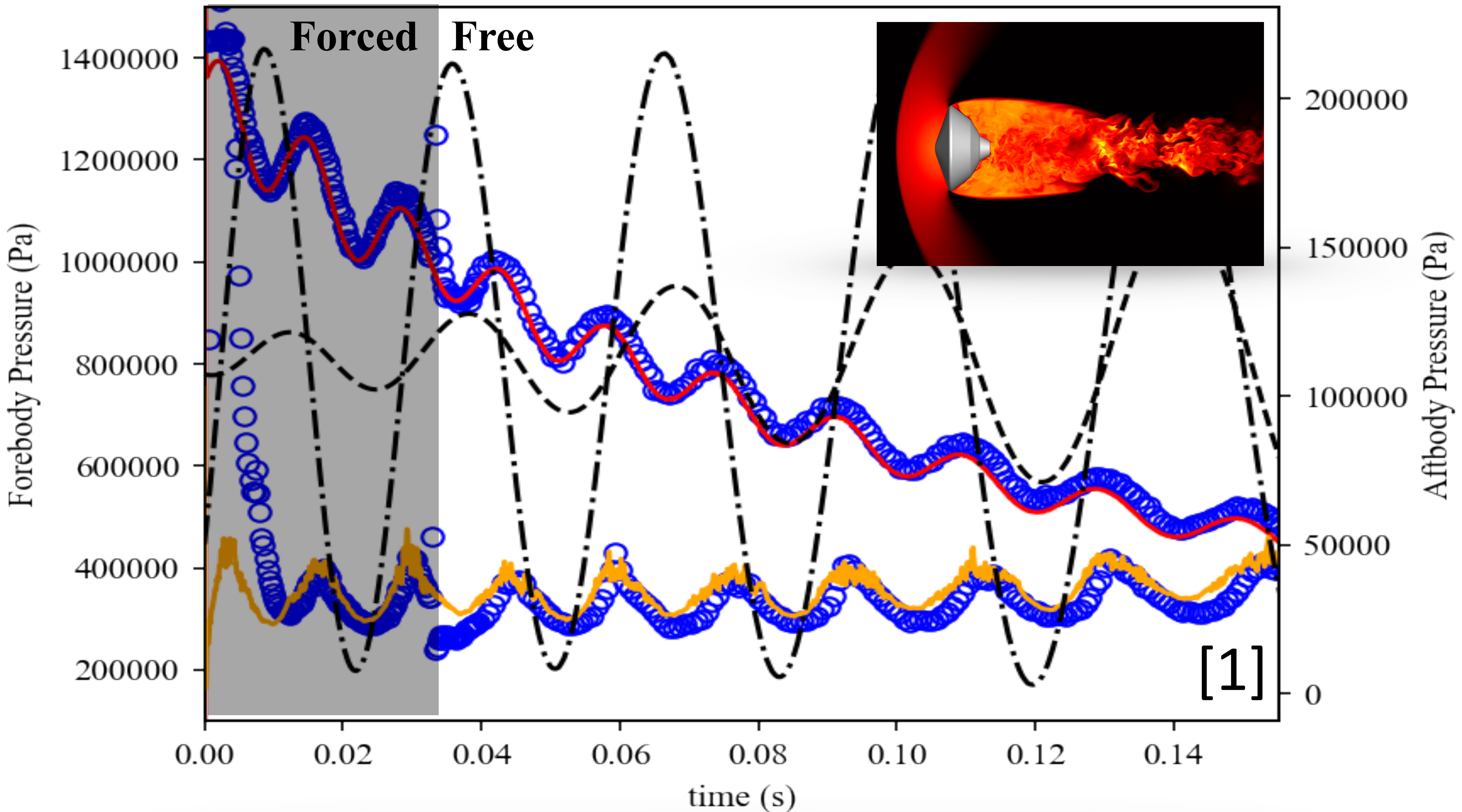

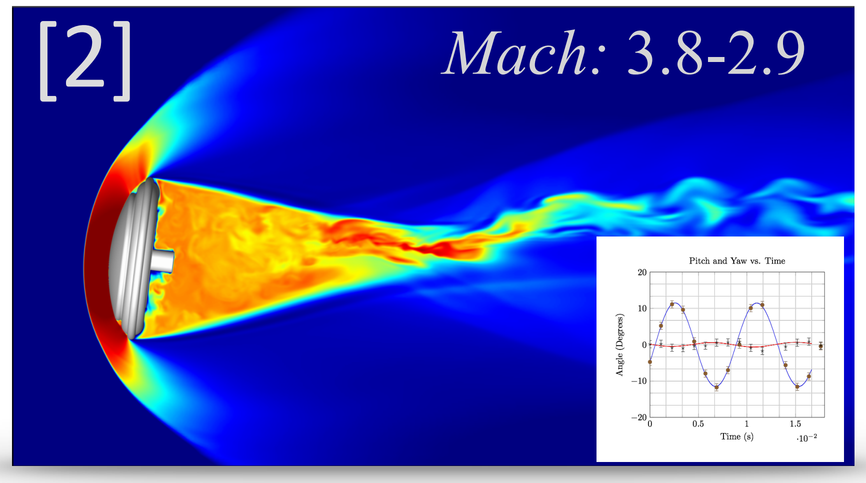

Validated against Experiment

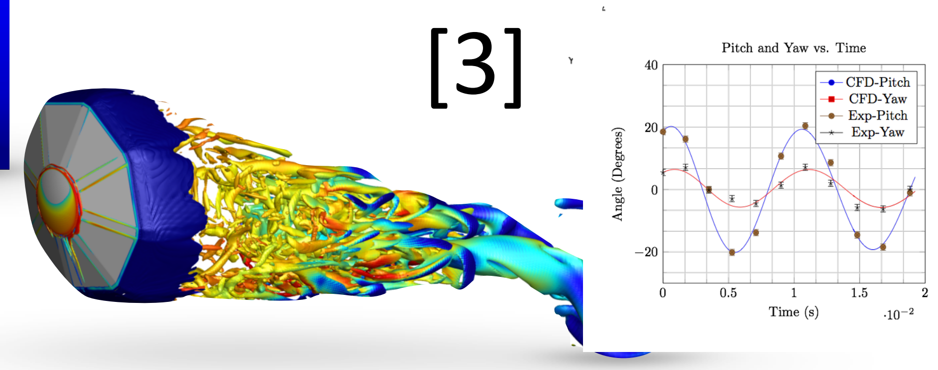

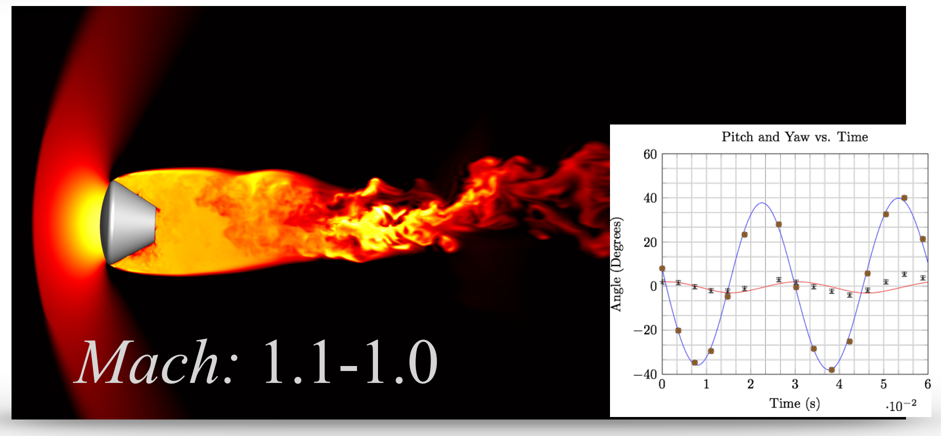

Atmospheric Flight with EarthGRAM

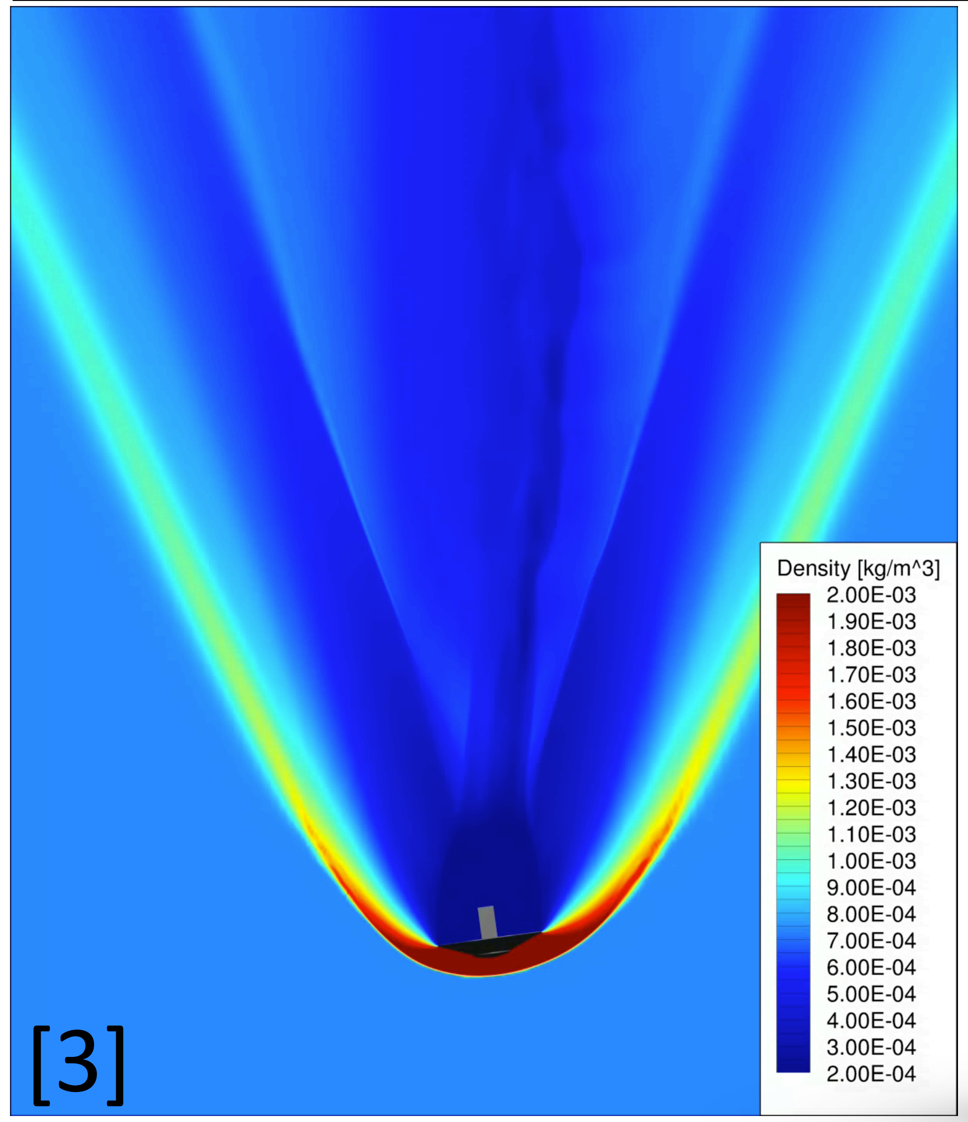

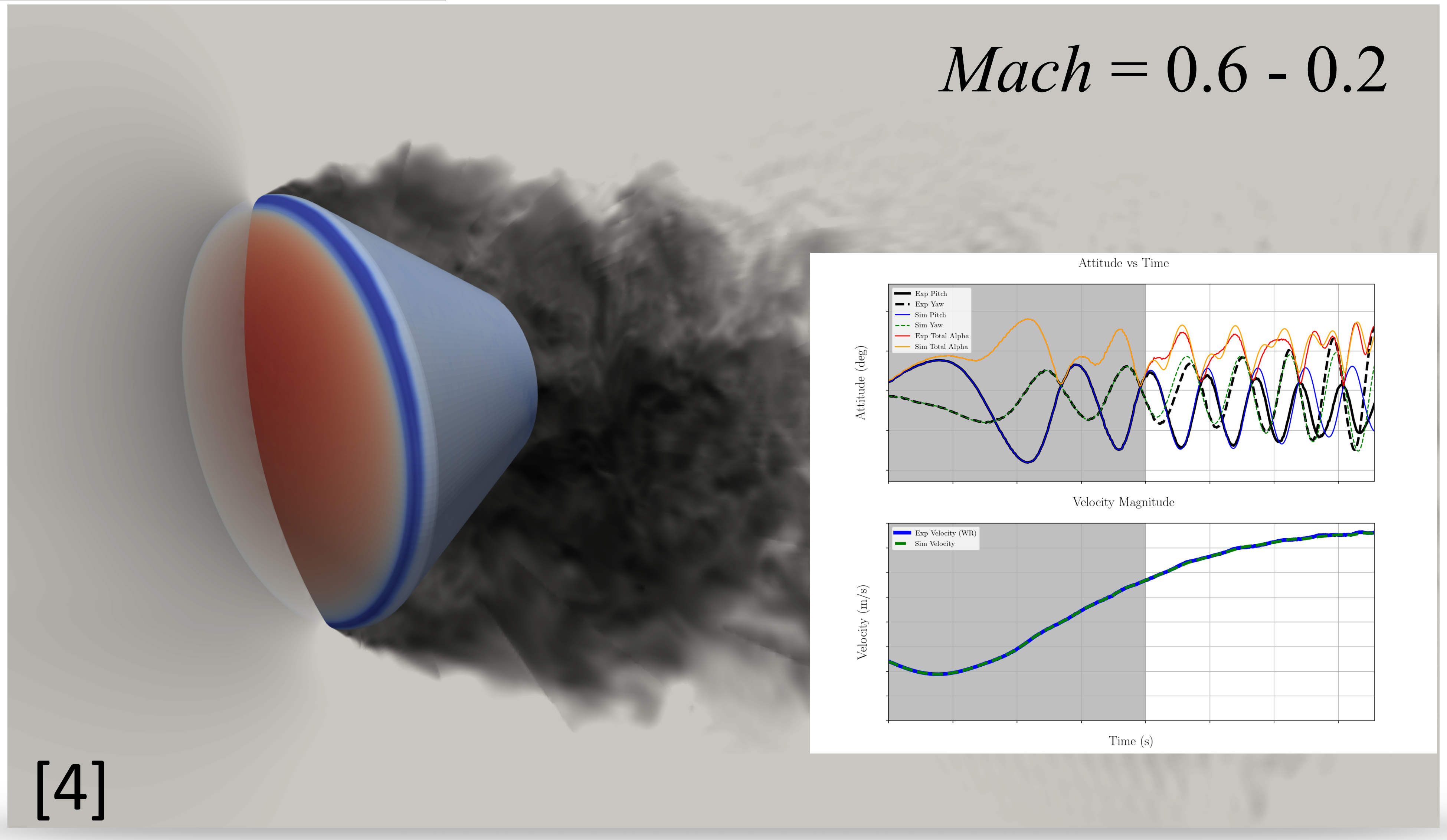

Free-Flight CFD Data as Input to Heritage Methods

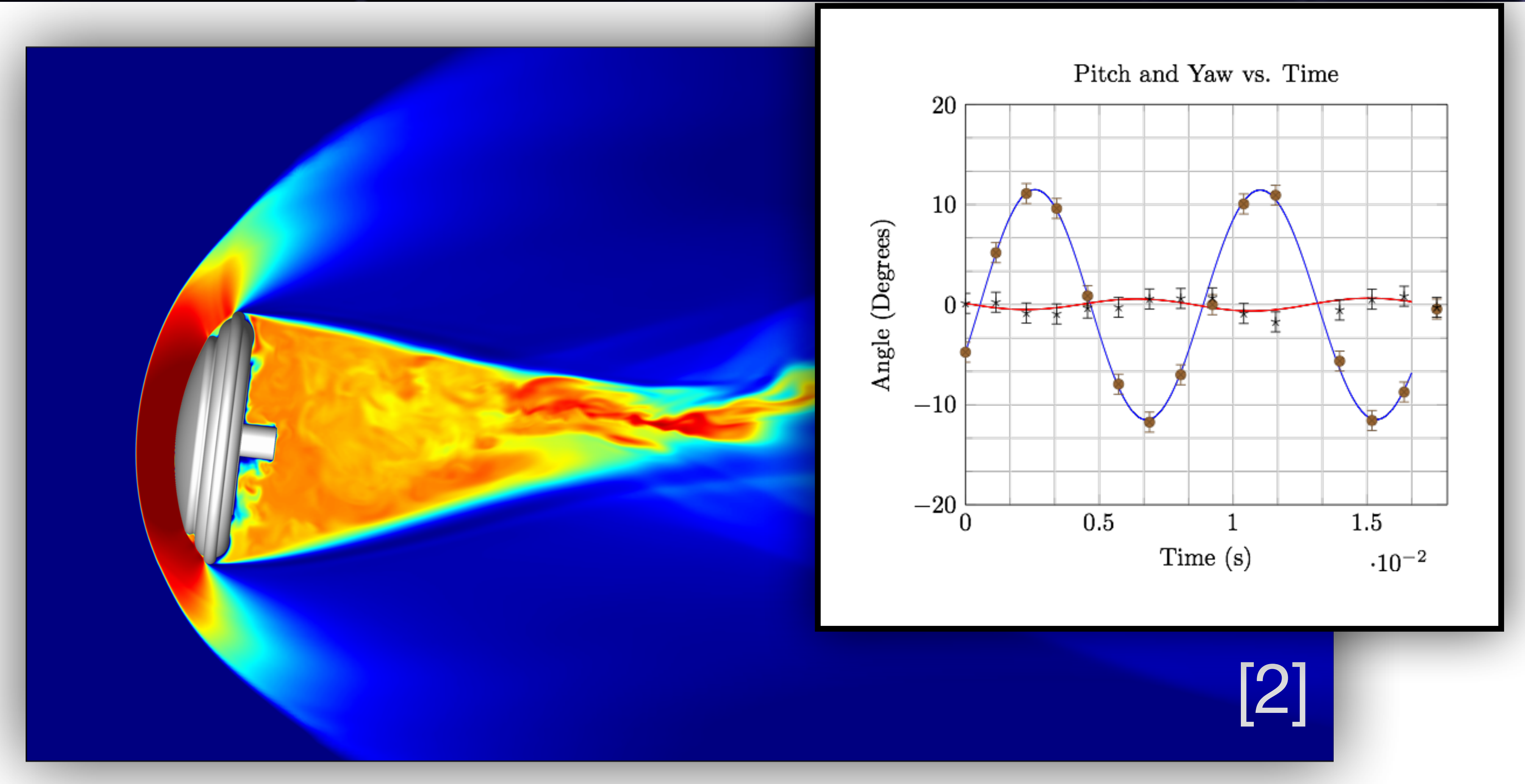

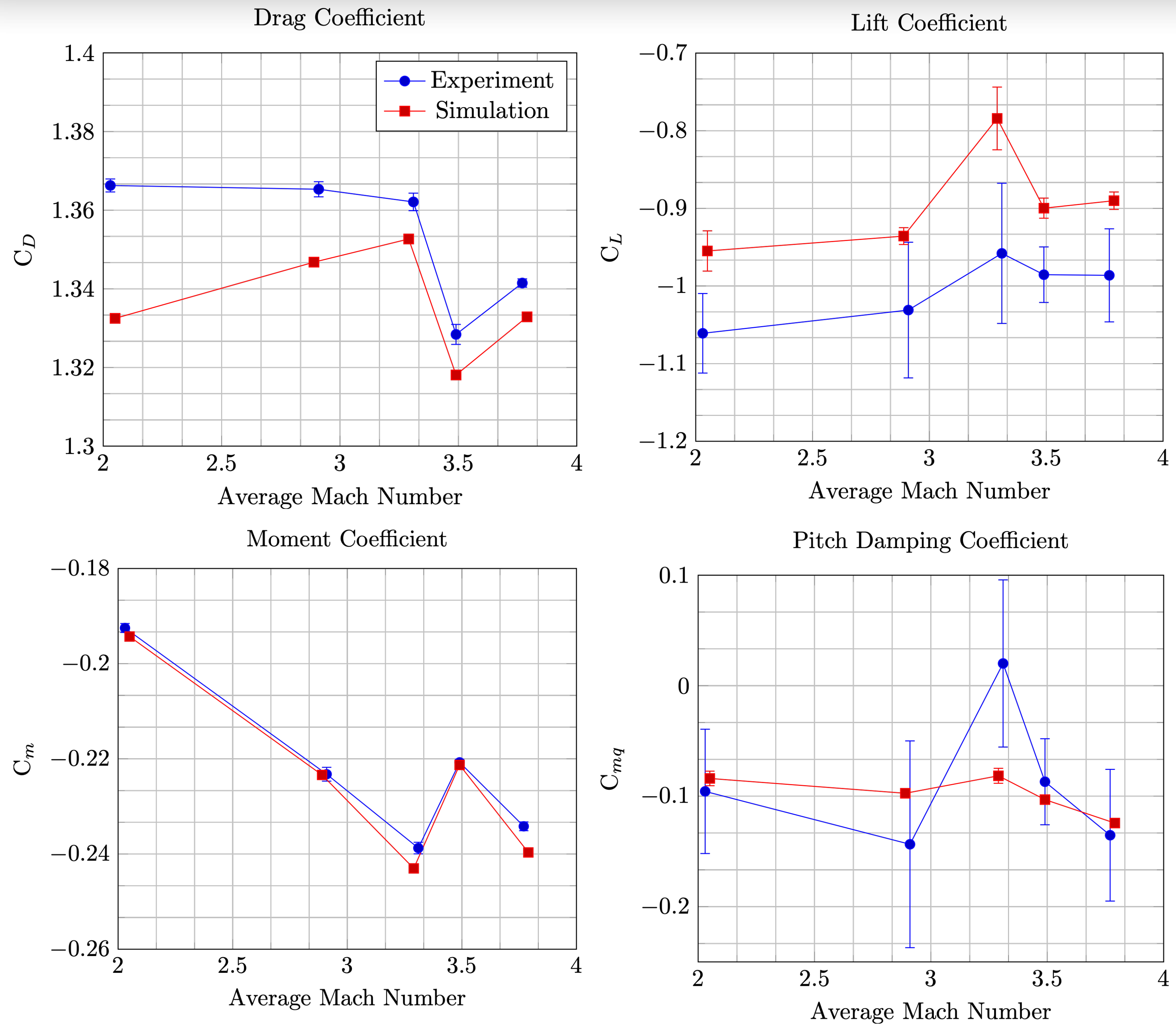

- Dynamic stability is often characterized by the pitch damping coefficient (C_{m_q})
- Derivations of pitch damping coefficient in previous studies were obtained using the aerodynamic software CADRA
  - Results shows good comparison between simulation and ballistic range results
  - Required significant coarsening from order 100,000 time steps of CFD data down to 16 data points to obtain 1-to-1 comparison with BR data
- Rich datasets from FF-CFD simulations present an opportunity to apply new data reduction approaches

Data Reduction for Free-Flight CFD

- PYnamics software suite to process FF-CFD output
  - A python suite of tools available to post-process FFCFD data and generate static and dynamic aero-coefficients
- Schoenenberger [5] states that (within assumptions of derived models) an equivalent $\boldsymbol{C_{m_q}}$ can be derived from 1- 2- or 3-DoF simulations

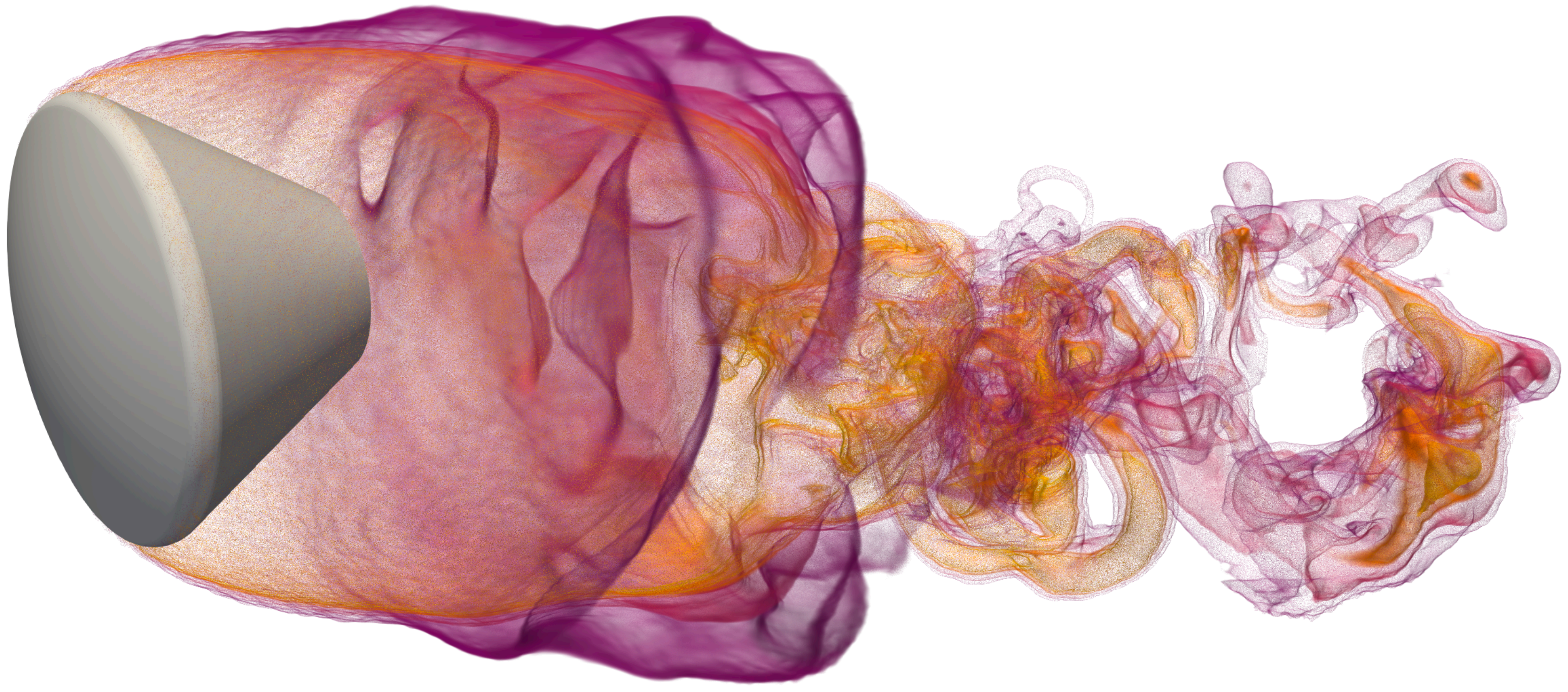

- Two methods developed for using FF-CFD 1-DoF analysis to computing dynamic coefficients
  1. Run reduced 1DoF FF-CFD simulations and then:

  2a. Use analytical forms of equations to generate non-linear fits to C_{m_q} as a function of oscillation amplitude

  2b. Use inverse estimation and 1-DoF EOMs to identify optimal C_{m_q} curve as a function of instantaneous angle of attack.

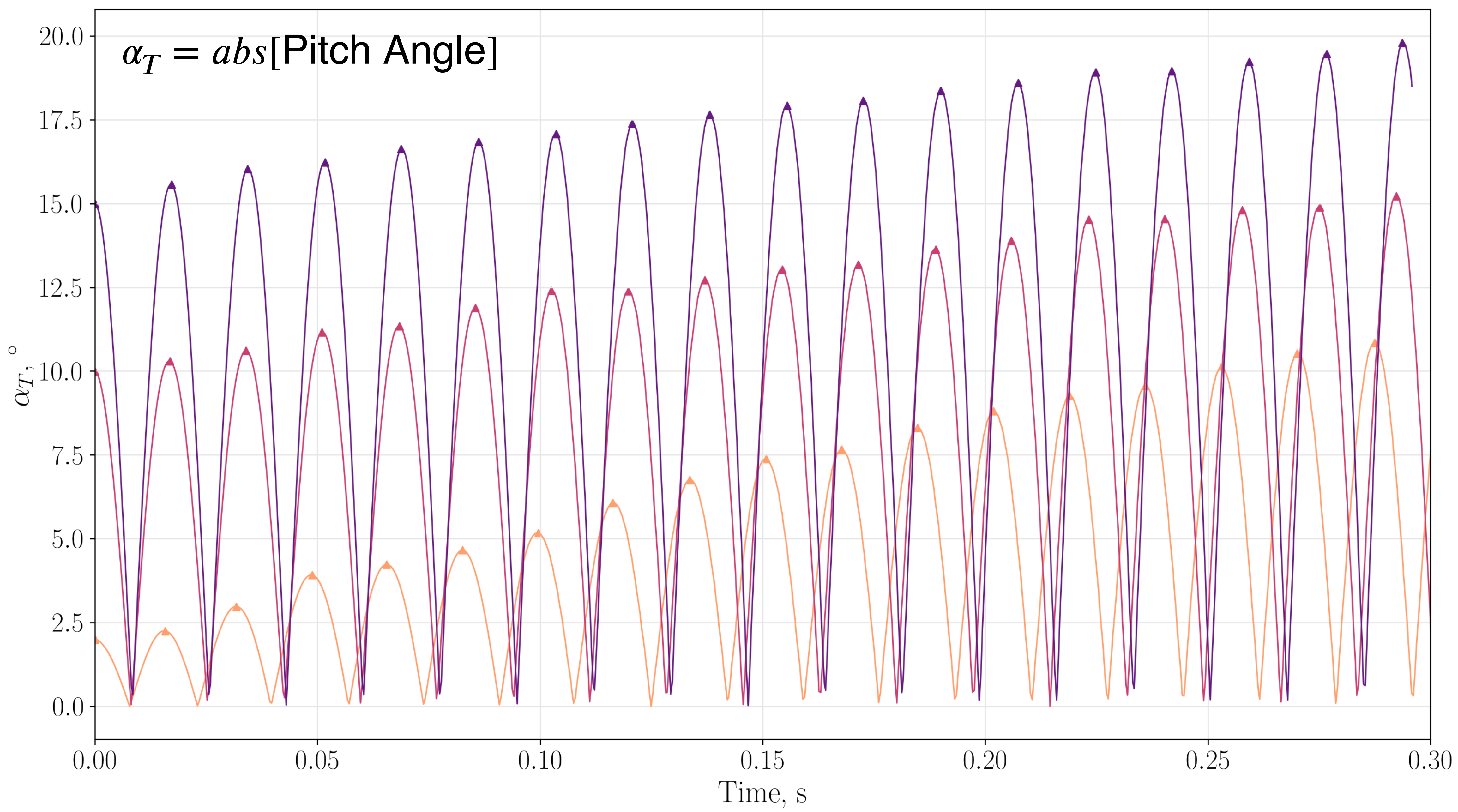

Data Reduction for Free-Flight CFD

- PYnamics software suite to process FF-CFD output
  - A python suite of tools available to post-process FFCFD data and generate static and dynamic aero-coefficients
- Schoenenberger [5] states that (within assumptions of derived models) an equivalent $\boldsymbol{C_{m_q}}$ can be derived from 1- 2- or 3-DoF simulations

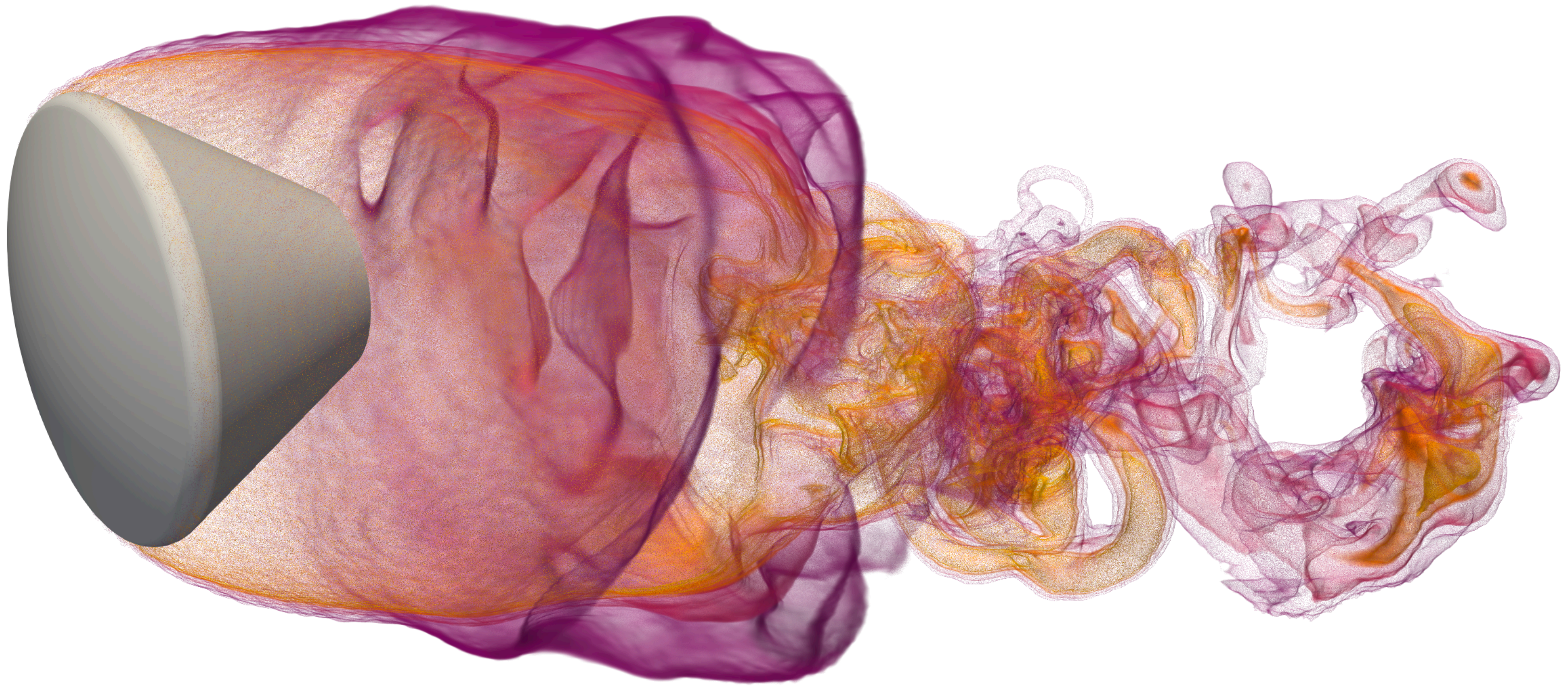

- Two methods developed for using FF-CFD 1-DoF analysis to computing dynamic coefficients
  1. Run reduced 1DoF FF-CFD simulations and then:

  2a. Use analytical forms of equations to generate non-linear fits to C_{m_q} as a function of oscillation amplitude

  2b. Use inverse estimation and 1-DoF EOMs to identify optimal C_{m_q} curve as a function of instantaneous angle of attack.

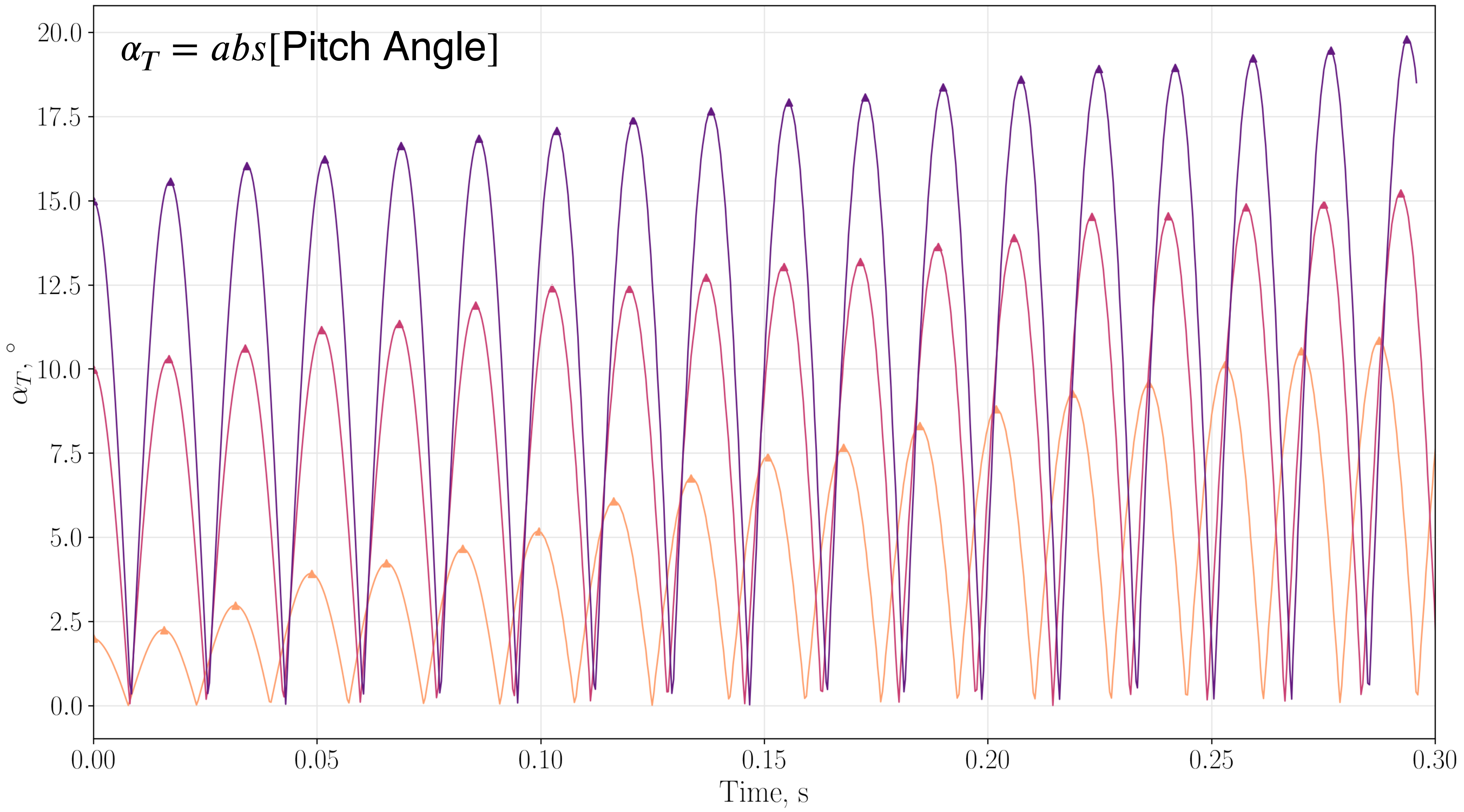

Use of Analytical Solutions To Compute Pitch Damping

- Methodology for using FF-CFD 1-DoF analysis to compute dynamic coefficients [6]

1-DoF Analytical Solution

$$\ddot{\alpha} - \frac{\rho V_\infty S d^2}{4I}\left(C_{m_q} + C_{m_{\dot{\alpha}}}\right)\dot{\alpha} - \frac{\rho V_\infty^2 S d}{2I} C_{m_\alpha}\alpha = 0$$

$$\alpha = A e^{\xi_1 t}\cos(\omega t + \delta) \quad \longrightarrow \quad \xi_1 = \frac{\rho V S d^2}{8I}\left(C_{m_q} + C_{m_{\dot{\alpha}}}\right)$$

- Algorithm:
  - ➢ For each α_0:
    - Using a stencil of 3-5 peaks, fit analytical expression for $\bar{C}_{m_q}$ to segments of the trajectory to capture local amplitude growth (or decay)
    - Add this $\bar{C}_{m_q}$ value to our larger $\bar{C}_{m_q}$ vs a space at the average total angle of attack for the peaks within that stencil
    - Move to next set of stenciled peaks and repeat
  - ➢ Combine all individual stencil fits into amplitude bins
  - ➢ Curve fit bins to get $\bar{C}_{m_q}$ as a function of amplitude

Results in a mapping across all *amplitudes*

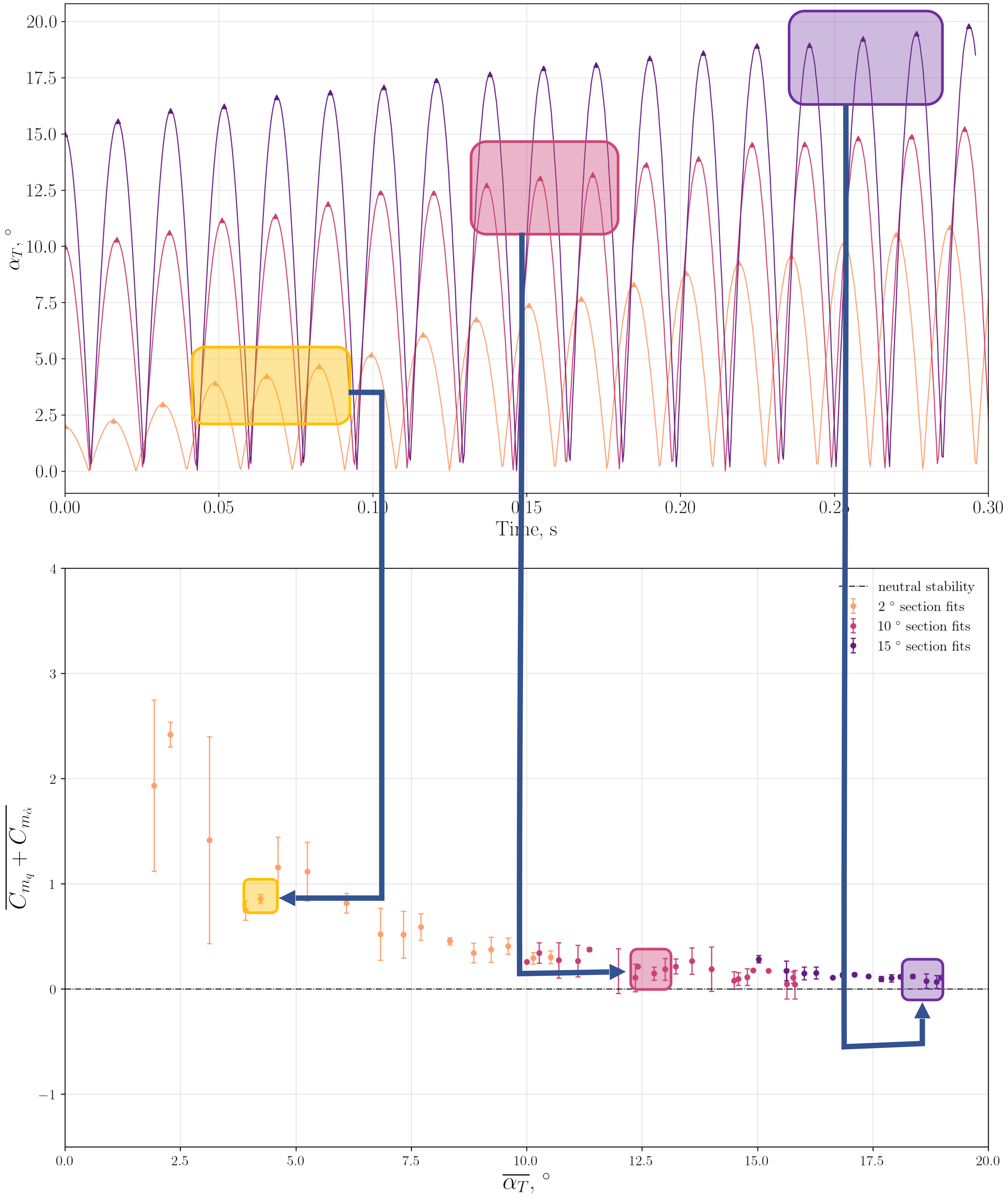

Comparison to Crew Module

- 1-DoF FF-CFD dynamic analysis applied to Orion CM
  - Constant Mach=1.07 corresponding to mid Mach condition of HFFAF BR Shot 2366
- All initial amplitudes grow with no observable stable limit cycle
- Comparison of derived distribution of C_{m_q} section fits from 1-DoF trajectories agree well with experimental data obtained at a separate facility
  - Results suggest dynamic behavior is consistent between facility and simulation
- Static coefficients can be obtained from collection 1-DoF trajectories

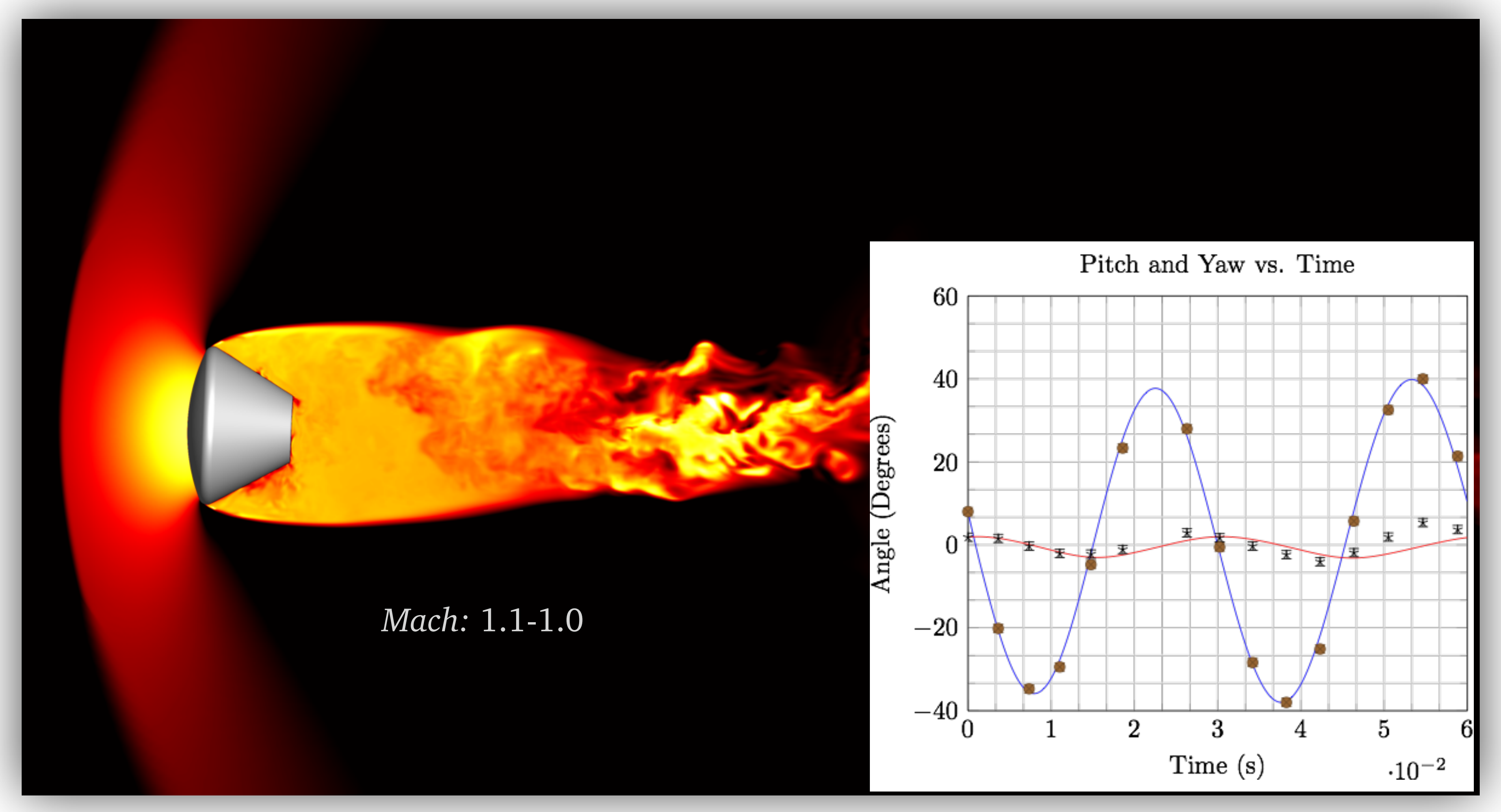

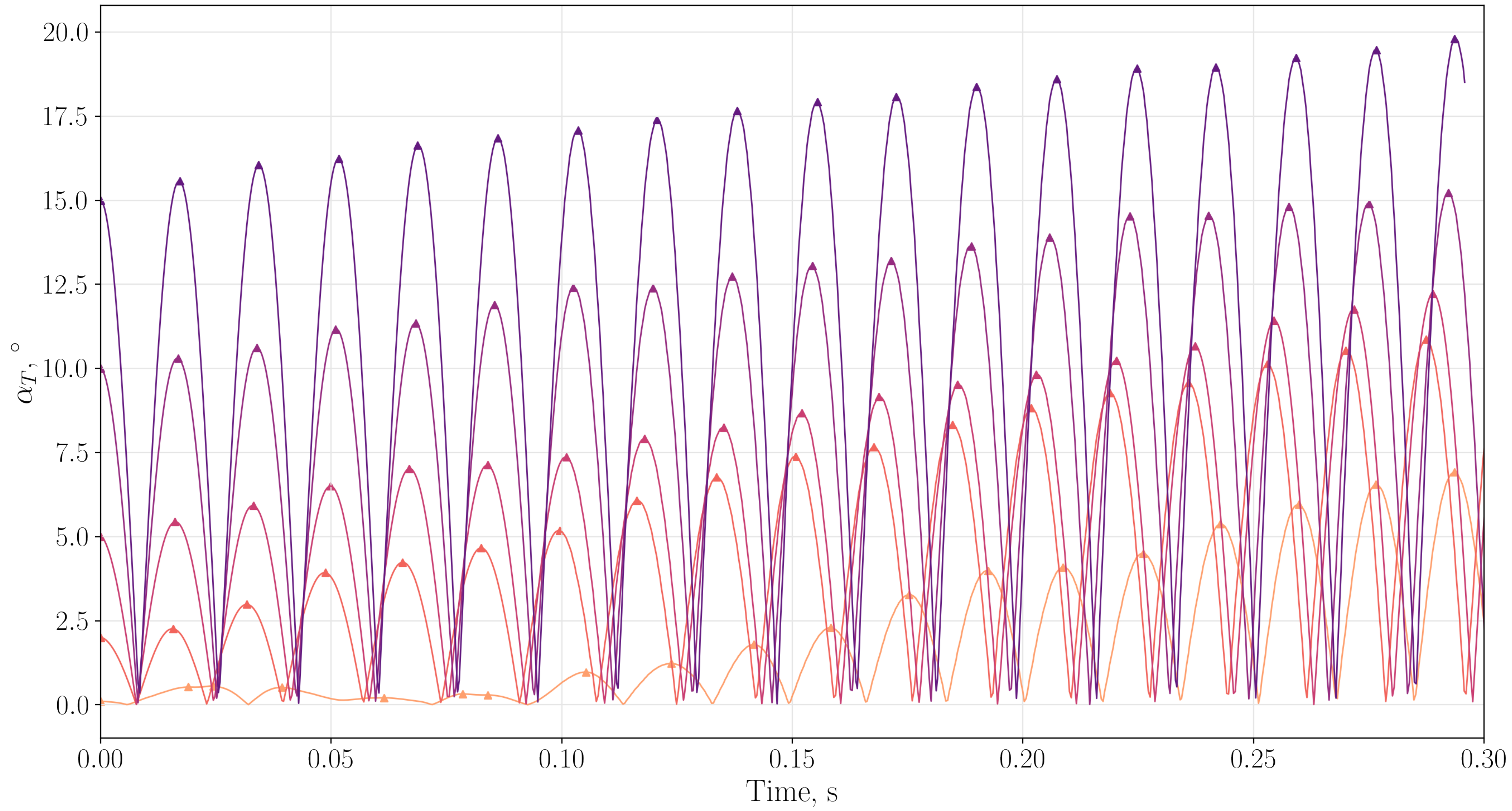

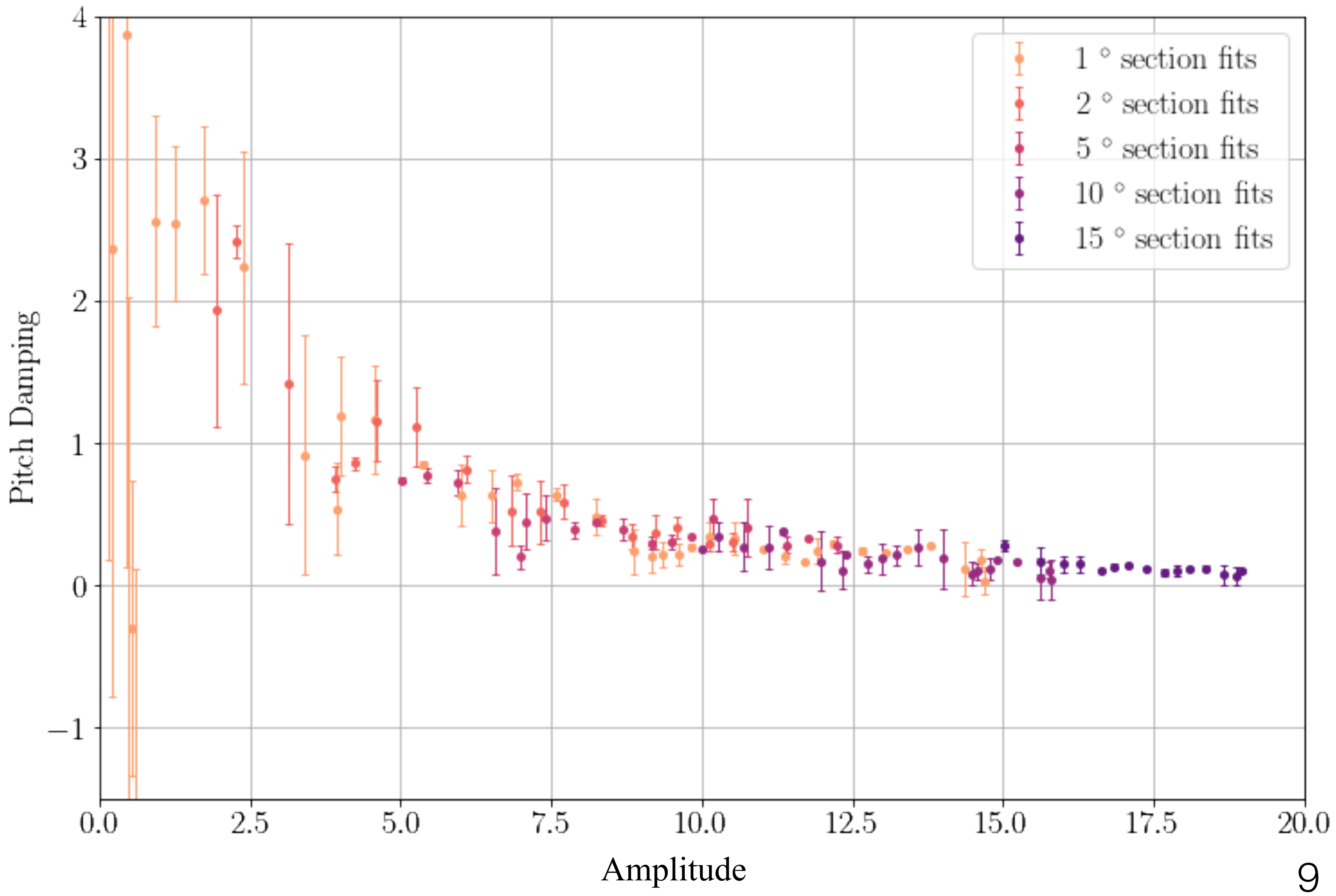

Comparison to Crew Module

- 1-DoF FF-CFD dynamic analysis applied to Orion CM
  - Constant Mach=1.07 corresponding to mid Mach condition of HFFAF BR Shot 2366
- All initial amplitudes grow with no observable stable limit cycle
- Comparison of derived distribution of C_{m_q} section fits from 1-DoF trajectories agree well with experimental data obtained at a separate facility
  - Results suggest dynamic behavior is consistent between facility and simulation
- Static coefficients can be obtained from collection 1-DoF trajectories

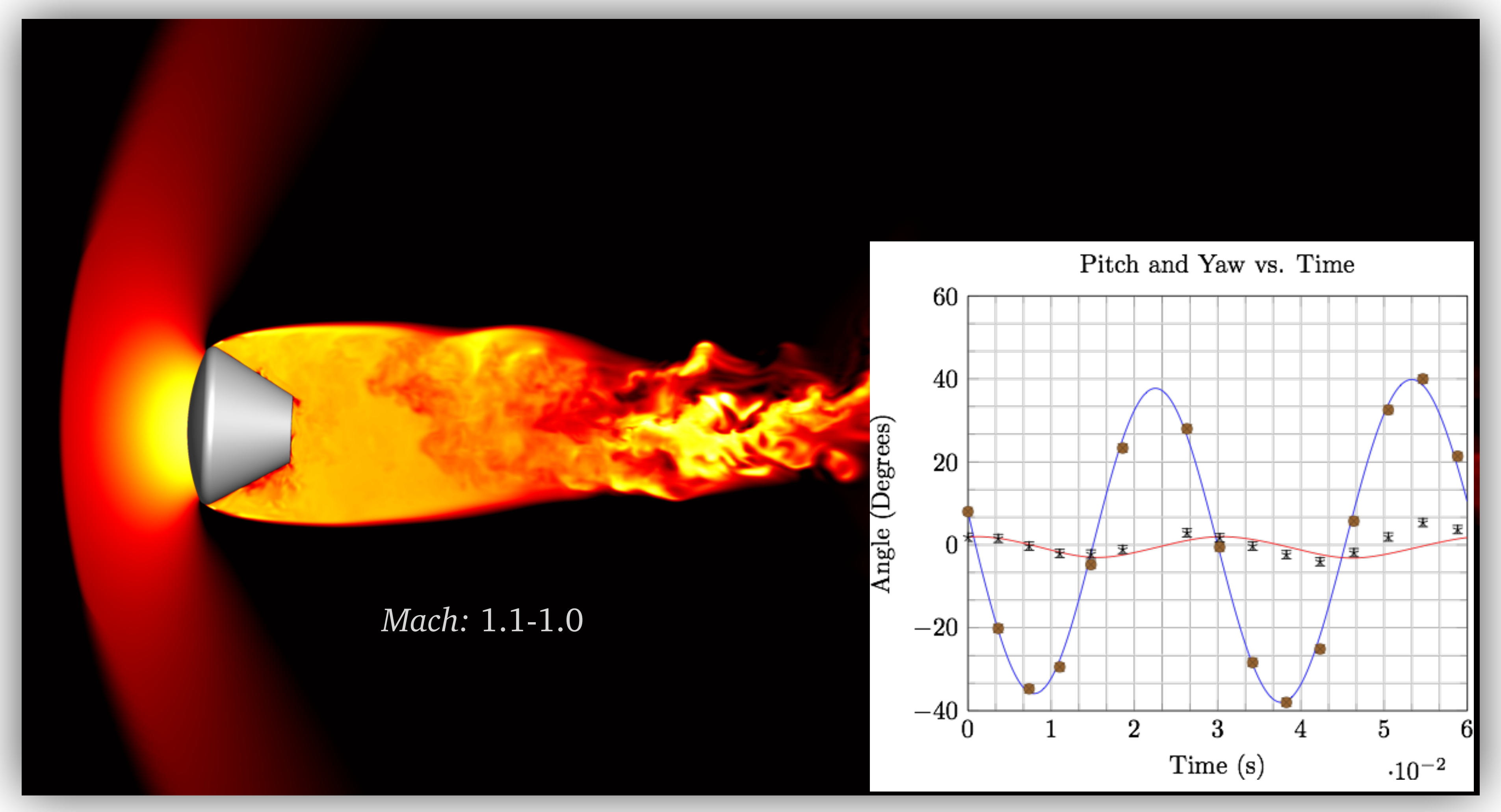

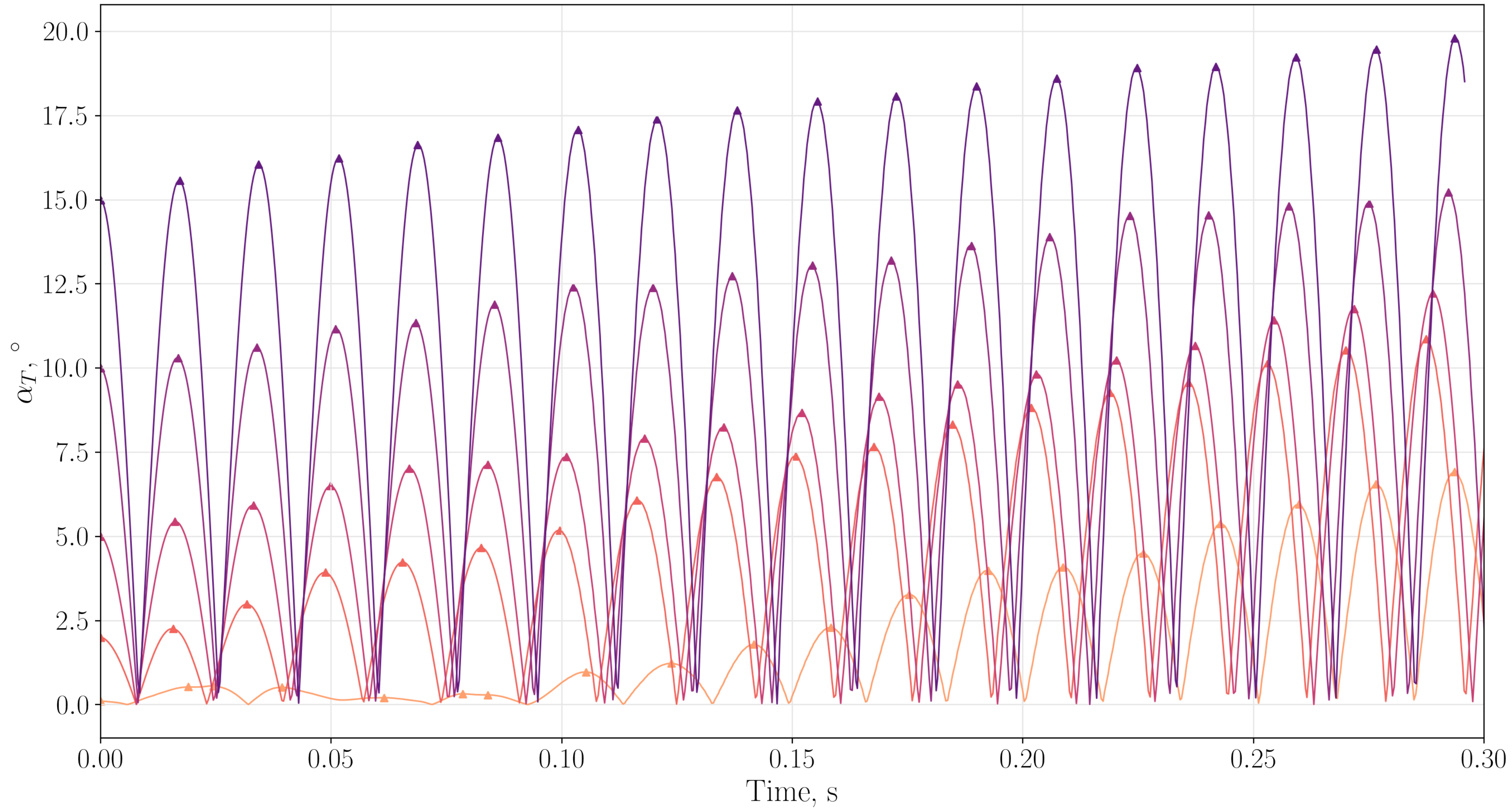

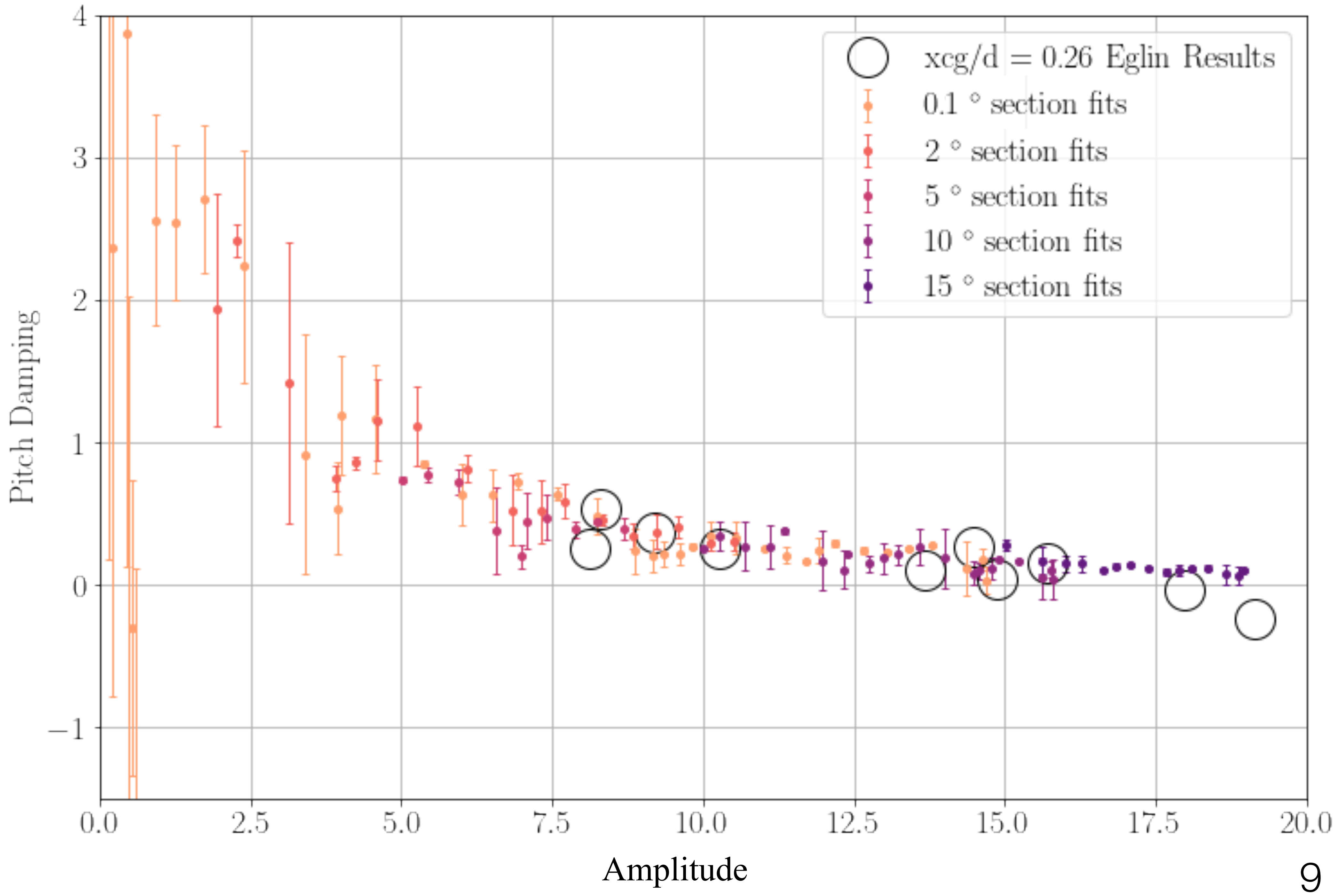

Comparison to Crew Module

- 1-DoF FF-CFD dynamic analysis applied to Orion CM
  - Constant Mach=1.07 corresponding to mid Mach condition of HFFAF BR Shot 2366
- All initial amplitudes grow with no observable stable limit cycle
- Comparison of derived distribution of C_{m_q} section fits from 1-DoF trajectories agree well with experimental data obtained at a separate facility
  - Results suggest dynamic behavior is consistent between facility and simulation
- Static coefficients can be obtained from collection 1-DoF trajectories

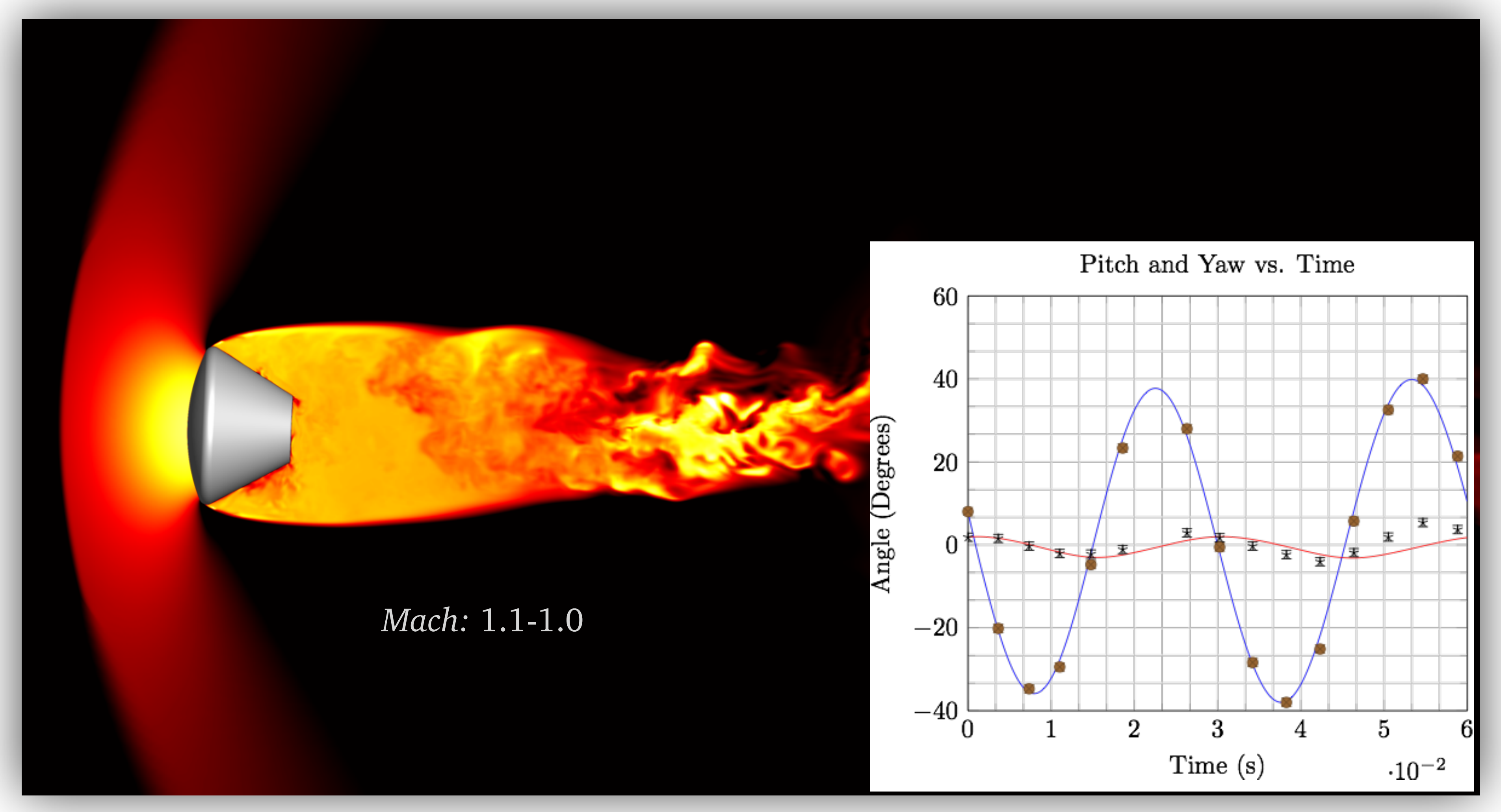

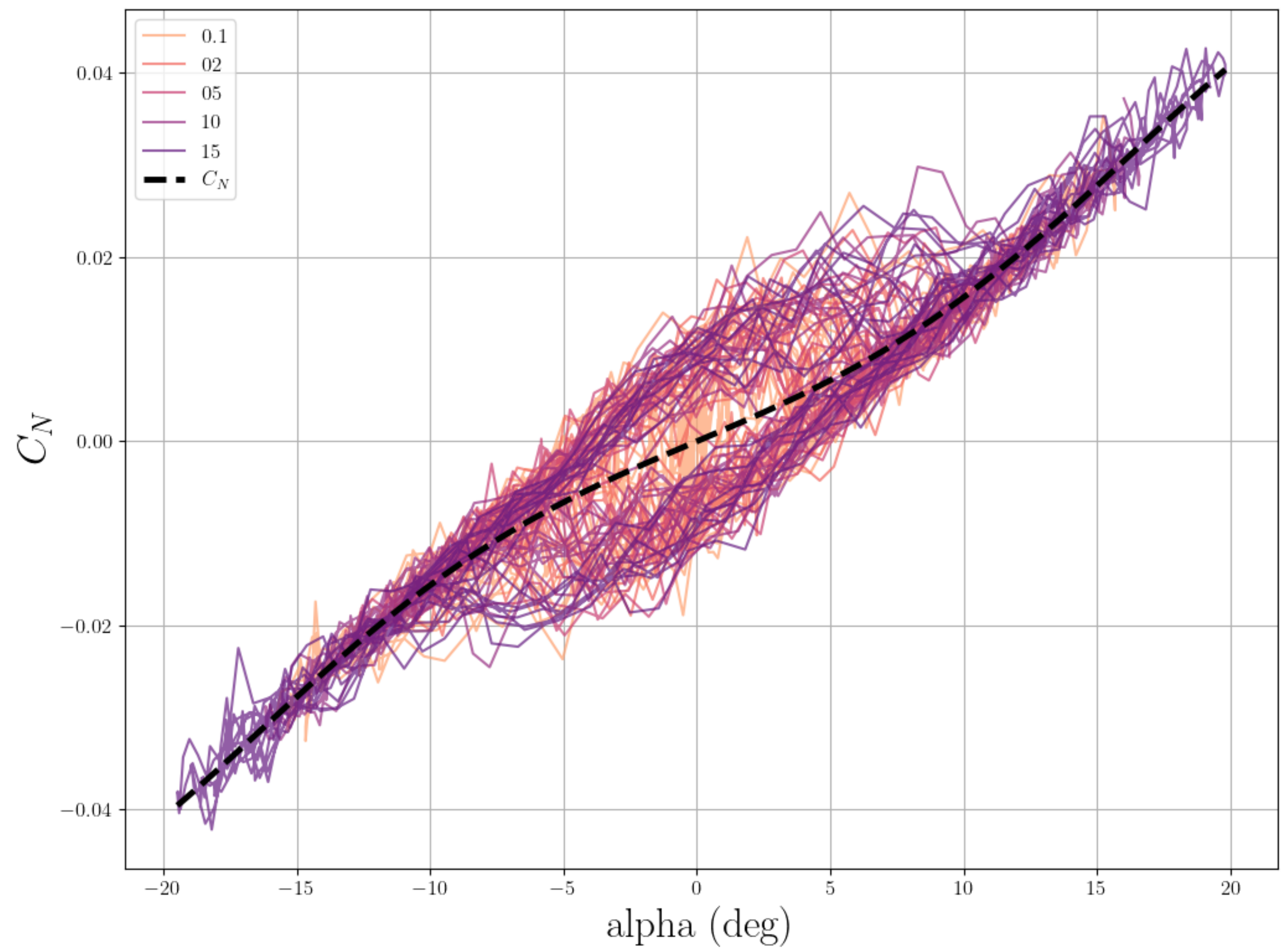

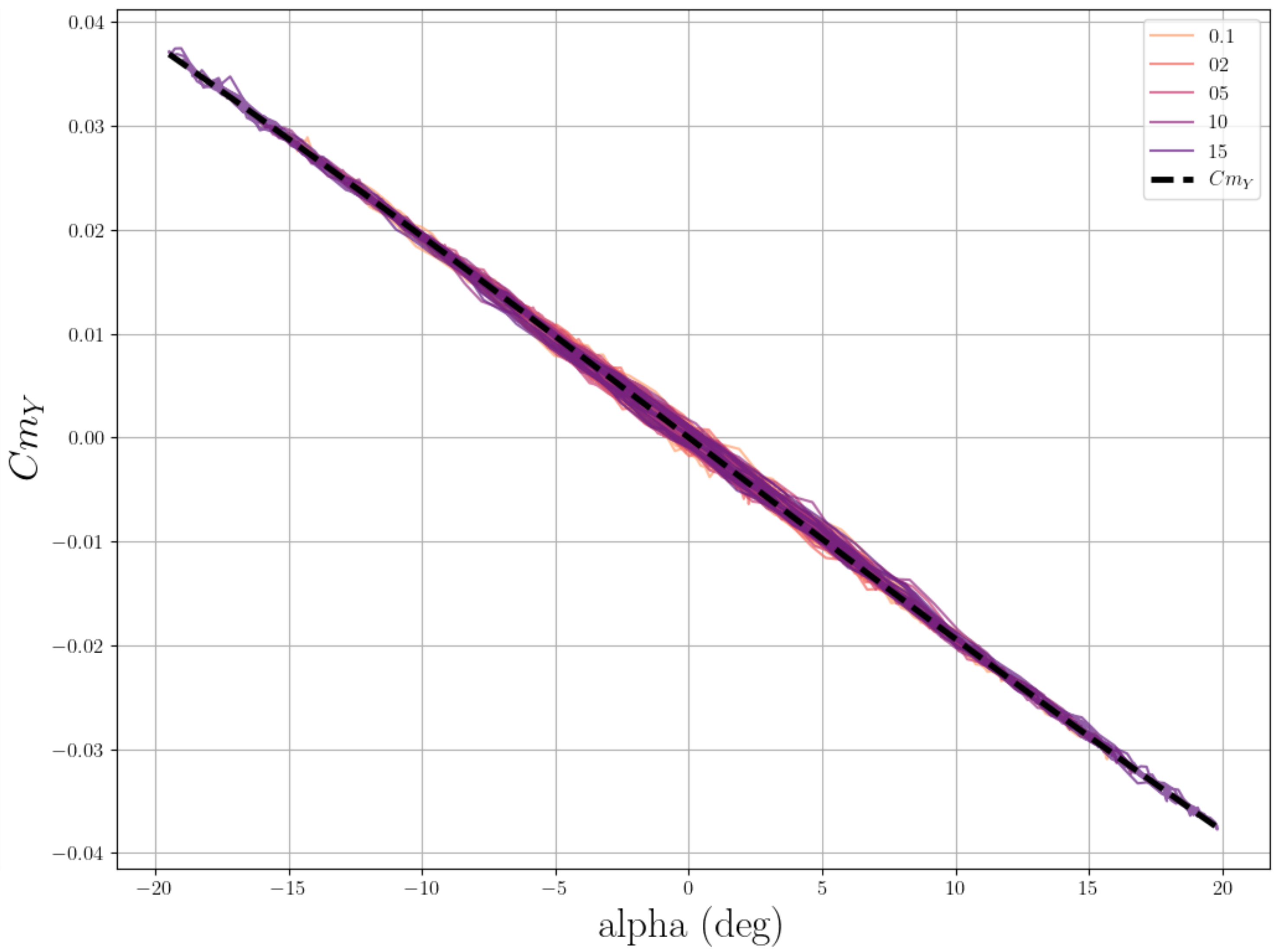

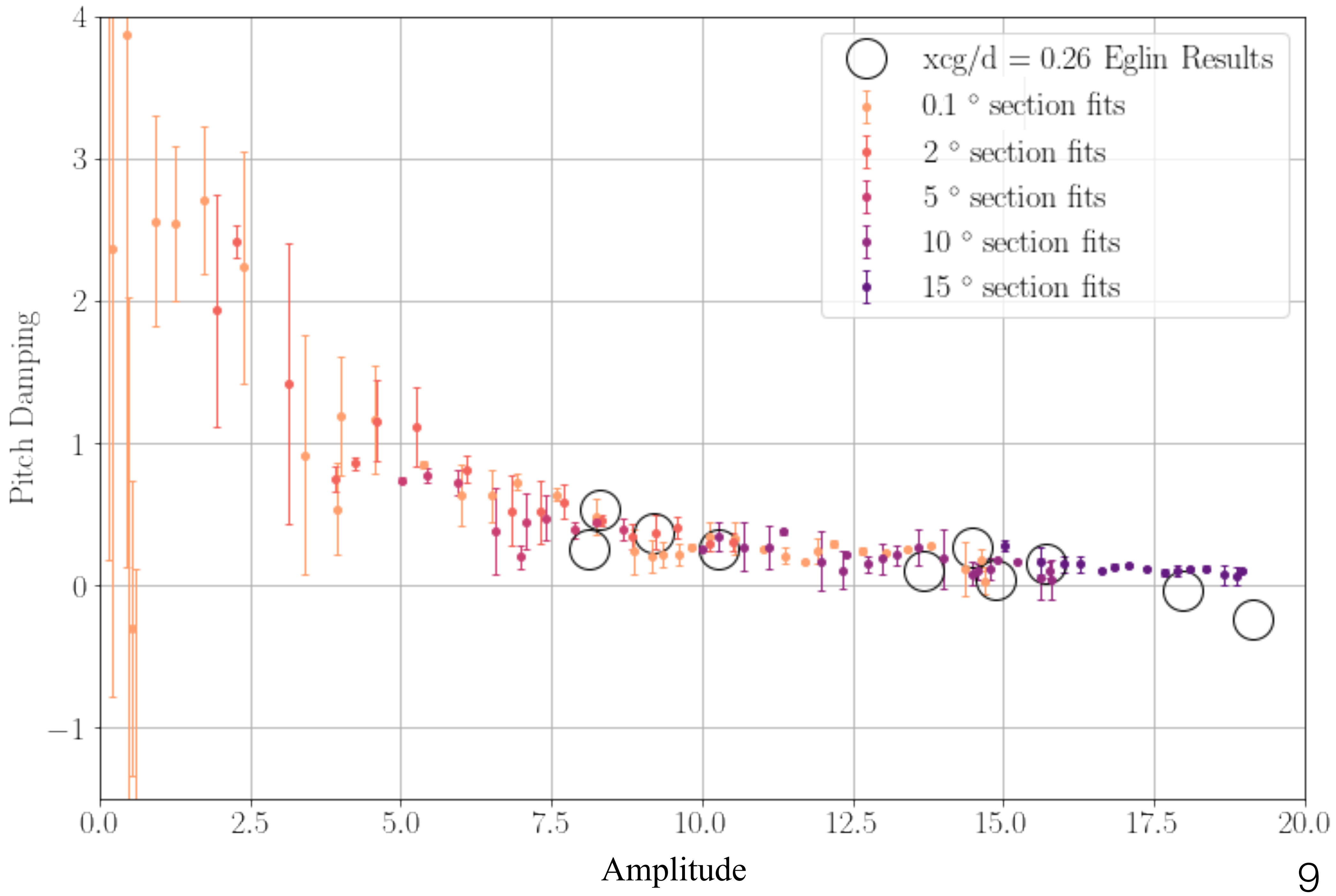

Data Reduction for Free-Flight CFD

- PYnamics software suite to process FF-CFD output
  – A python suite of tools available to post-process FFCFD data and generate static and dynamic aero-coefficients

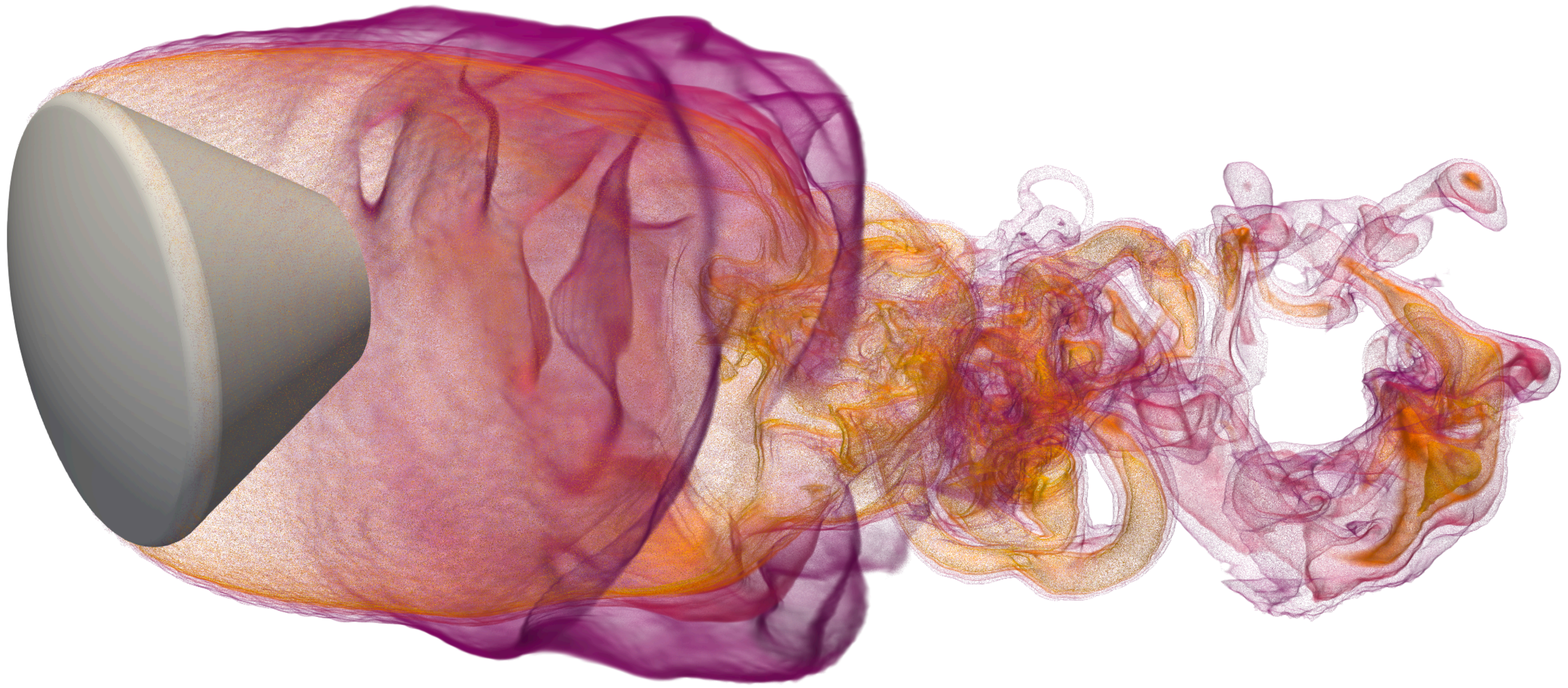

- Schoenenberger [5] states that (within assumptions of derived models) an equivalent $\boldsymbol{C_{m_q}}$ can be derived from 1- 2- or 3-DoF simulations

- Two methods developed for using FF-CFD 1-DoF analysis to computing dynamic coefficients
  1. Run reduced 1DoF FF-CFD simulations and then:

  2a. Use analytical forms of equations to generate non-linear fits to C_{m_q} as a function of oscillation amplitude

  2b. Use inverse estimation and 1-DoF EOMs to identify optimal C_{m_q} curve as a function of instantaneous angle of attack.

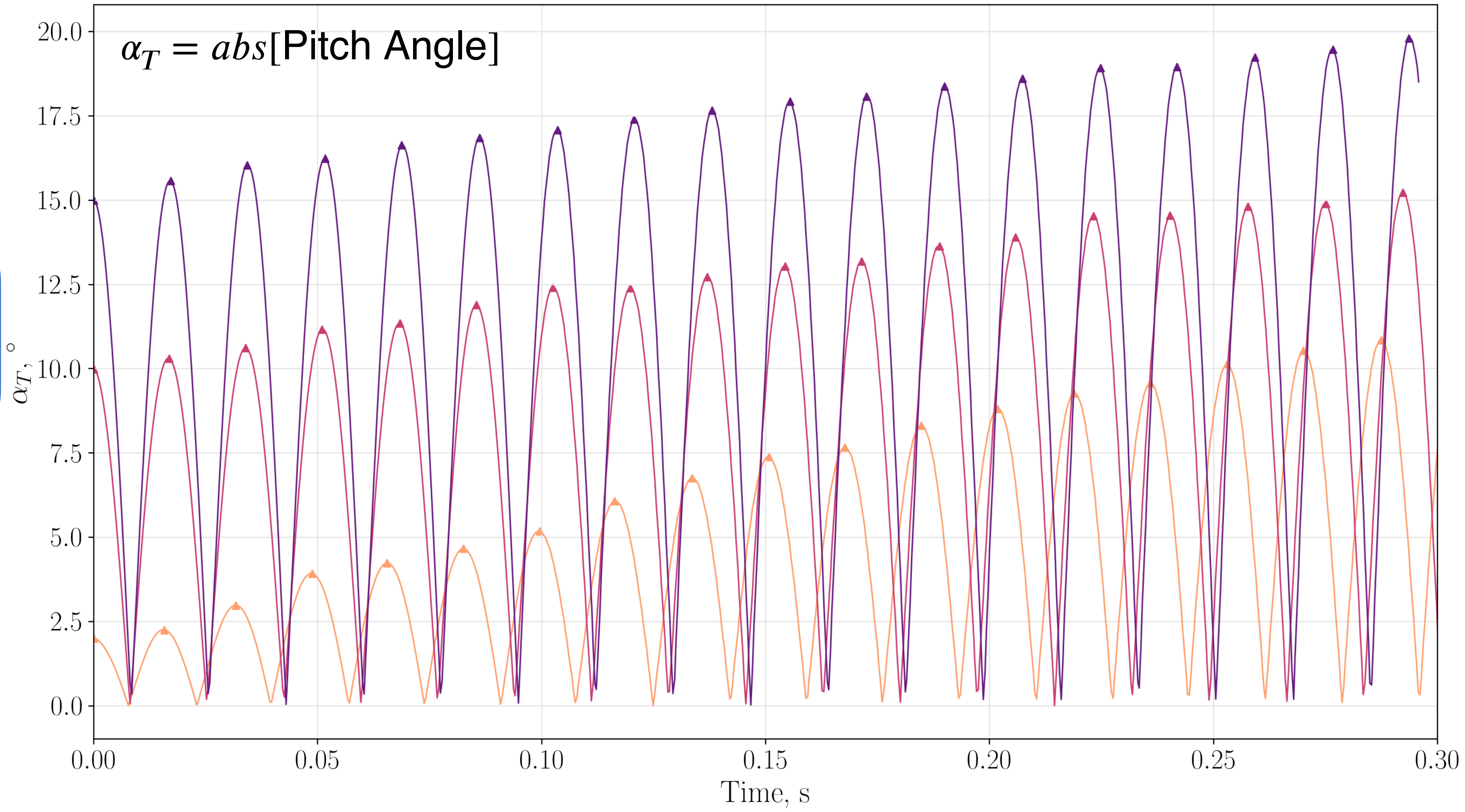

Data Reduction for Free-Flight CFD

- PYnamics software suite to process FF-CFD output
  - A python suite of tools available to post-process FFCFD data and generate static and dynamic aero-coefficients
- Schoenenberger [5] states that (within assumptions of derived models) an equivalent $\boldsymbol{C_{m_q}}$ can be derived from 1- 2- or 3-DoF simulations

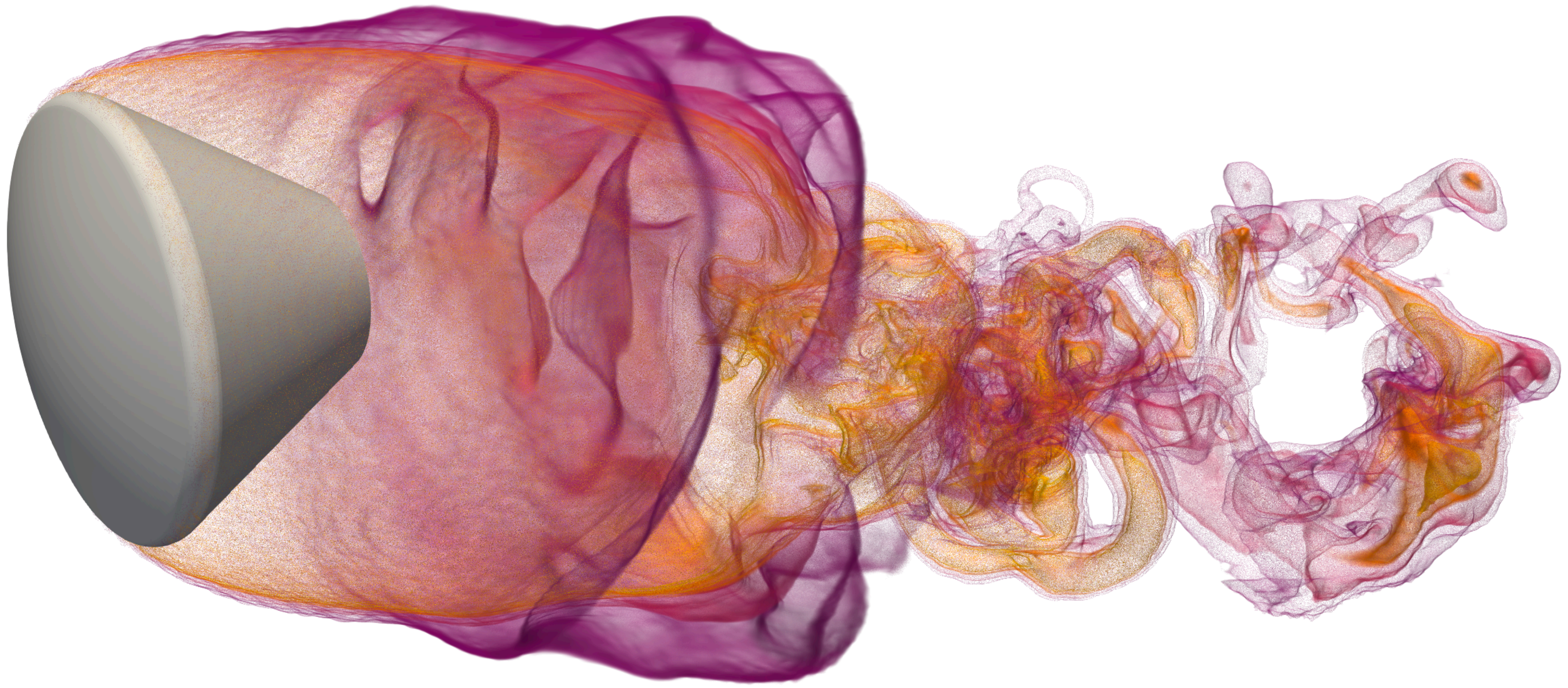

- Two methods developed for using FF-CFD 1-DoF analysis to computing dynamic coefficients
  1. Run reduced 1DoF FF-CFD simulations and then:

  2a. Use analytical forms of equations to generate non-linear fits to C_{m_q} as a function of oscillation amplitude

  2b. Use inverse estimation and 1-DoF EOMs to identify optimal C_{m_q} curve as a function of instantaneous angle of attack.

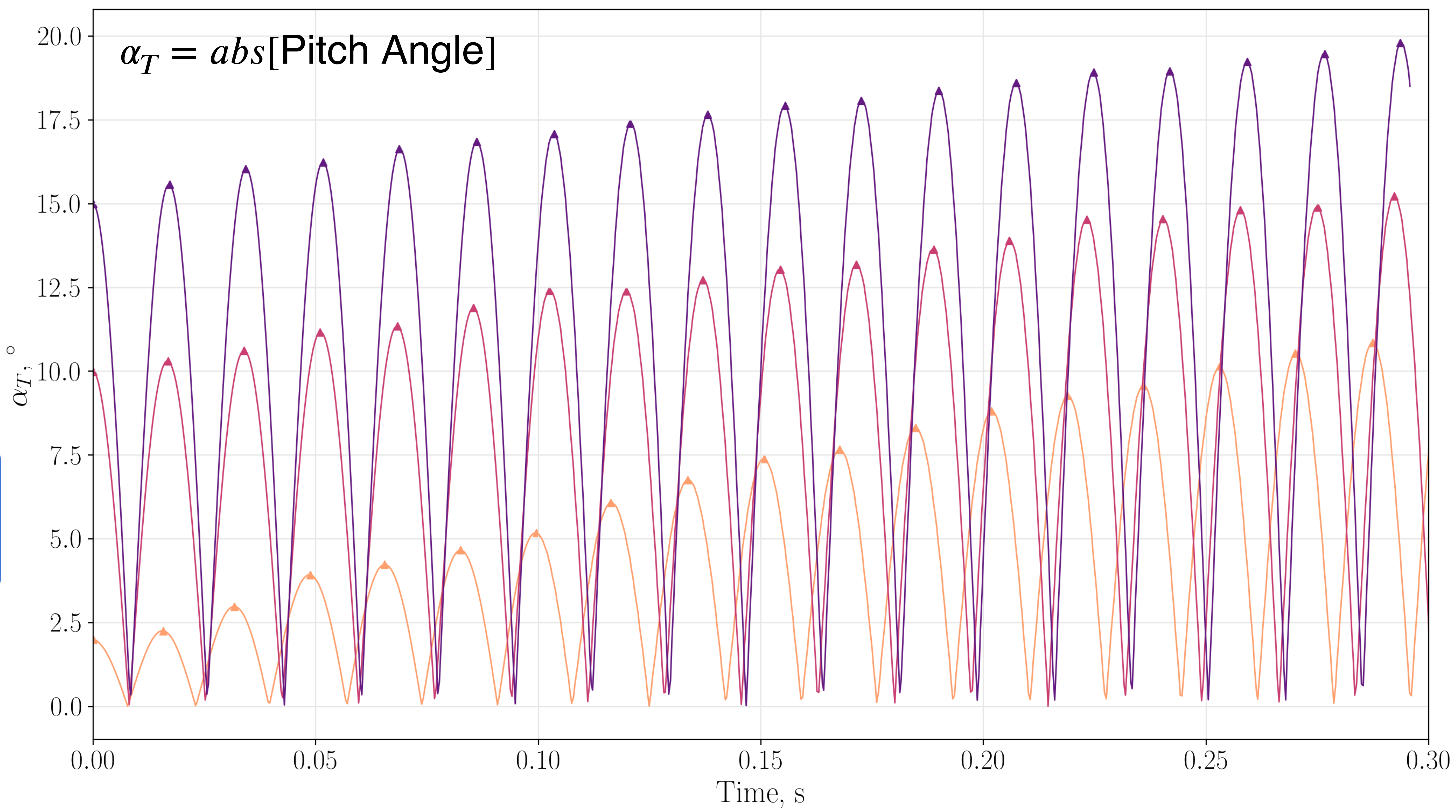

Inverse Estimation of Pitch Damping at Constant Mach (1-DoF)

End-to-End pipeline has been created for extracting static and dynamic aero coefficients from 1-DoF (free-to-pitch) FF-CFD simulations

- Theory suggests and previous work has shown that pitch damping coefficient derived from 1-DoF is equivalent to that from higher DoF simulations
- Reconstruction: Using the ODE derived by Schoenenberger, Queen: $\ddot{\alpha} - \frac{\rho V S}{2m}\left(-C_{L_\alpha} + \frac{md^2}{2I}\left(C_{m_q} + C_{m_{\dot{\alpha}}}\right)\right)\dot{\alpha} - \frac{\rho V^2 S d}{2I} C_{m_\alpha}\alpha = 0$ integrate forwards in time using Python's **solve_ivp** to generate a trajectory history
  - Requires: dof simplifications, geometric constants, static aero coefficients, α_0 (initial amplitude), $\dot{\alpha}_0$ (local maxima), and $C_{m_q} + C_{m_{\dot{\alpha}}}$ as a function of α
- Optimization: Send Python's **scipy.optimize.minimize** a functional form of the pitch damping curve with an initial guess, wrap the reconstruction (**solve_ivp**) scheme in the optimizer, and iterate on input curve coefficients to minimize the normalized L_2 residual between peak amplitudes
  - Optional inclusion of peak times in the objective function allows for co-optimization of C_{m_α} (shown below). Otherwise, compute in static aero routine.

Inverse Estimation of Pitch Damping at Constant Mach (1-DoF)

End-to-End pipeline has been created for extracting static and dynamic aero coefficients from 1-DoF (free-to-pitch) FF-CFD simulations

- Theory suggests and previous work has shown that pitch damping coefficient derived from 1-DoF is equivalent to that from higher DoF simulations
- Reconstruction: Using the ODE derived by Schoenenberger, Queen: $\ddot{\alpha} - \frac{\rho V S}{2m}\left(-C_{L_\alpha} + \frac{md^2}{2I}\left(C_{m_q} + C_{m_{\dot{\alpha}}}\right)\right)\dot{\alpha} - \frac{\rho V^2 S d}{2I} C_{m_\alpha}\alpha = 0$ integrate forwards in time using Python's **solve_ivp** to generate a trajectory history
  - Requires: dof simplifications, geometric constants, static aero coefficients, α_0 (initial amplitude), $\dot{\alpha}_0$ (local maxima), and $C_{m_q} + C_{m_{\dot{\alpha}}}$ as a function of α
- Optimization: Send Python's **scipy.optimize.minimize** a functional form of the pitch damping curve with an initial guess, wrap the reconstruction (**solve_ivp**) scheme in the optimizer, and iterate on input curve coefficients to minimize the normalized L_2 residual between peak amplitudes
  - Optional inclusion of peak times in the objective function allows for co-optimization of C_{m_α} (shown below). Otherwise, compute in static aero routine.

End-to-End Example

End-to-End Example

Complete FFCFD Data Set

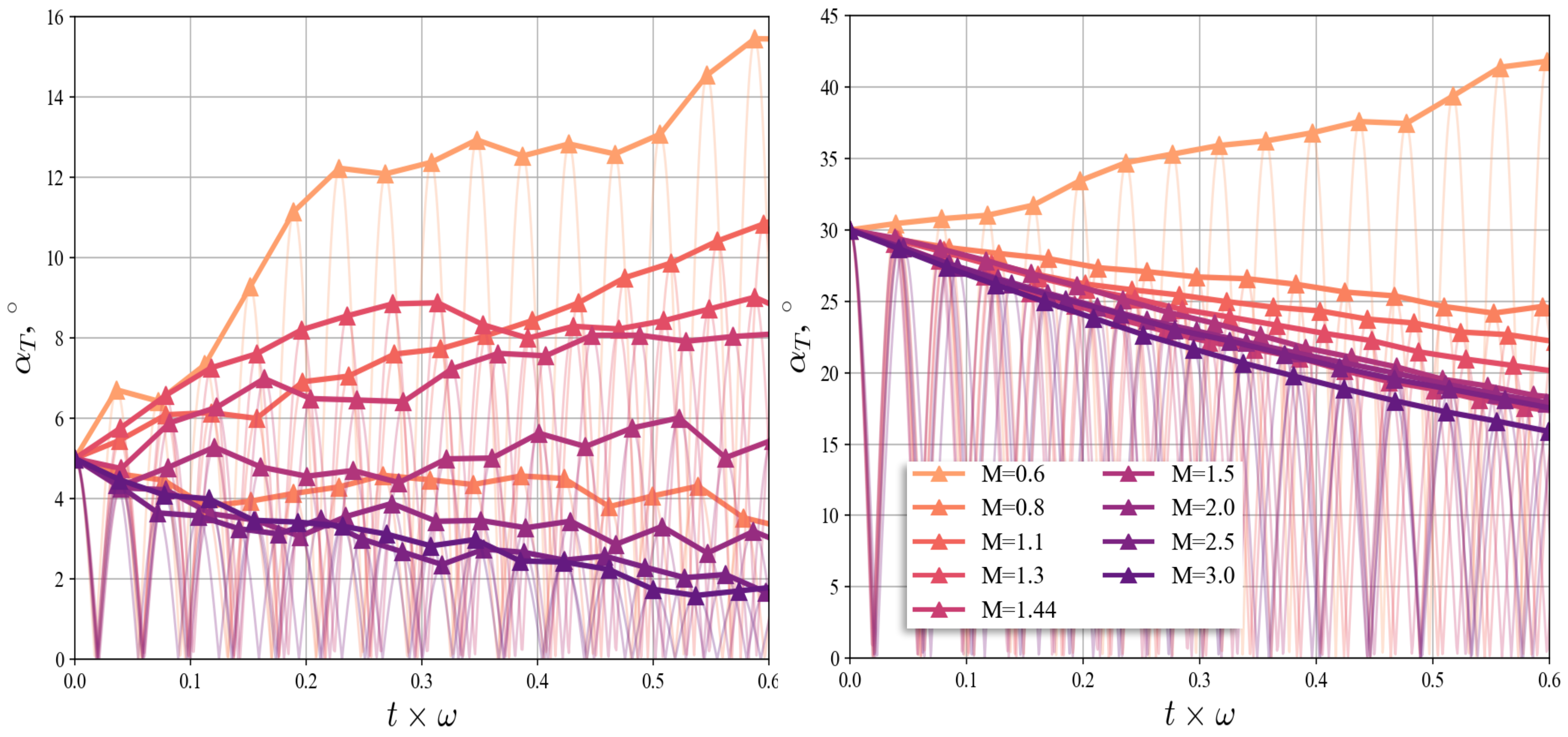

End-to-End Example

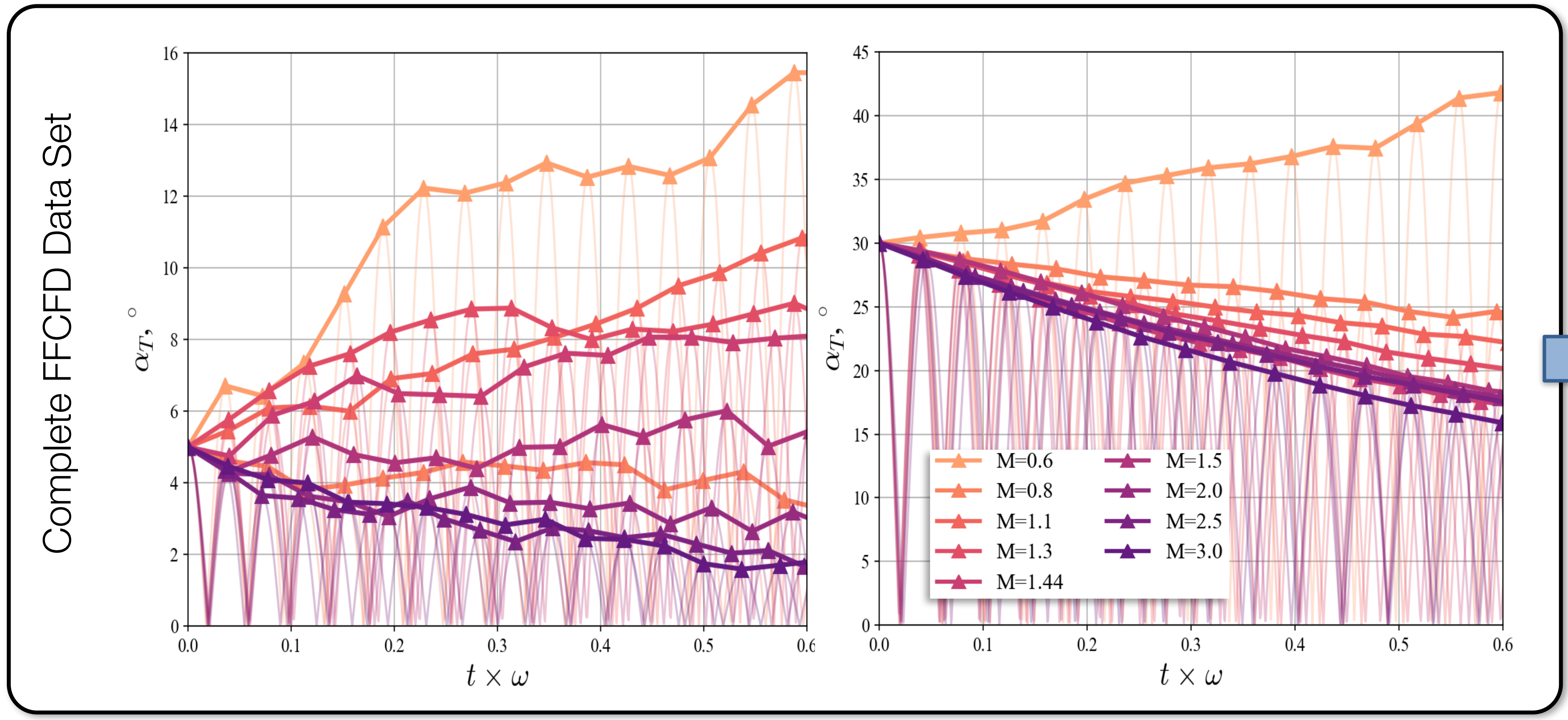

Train

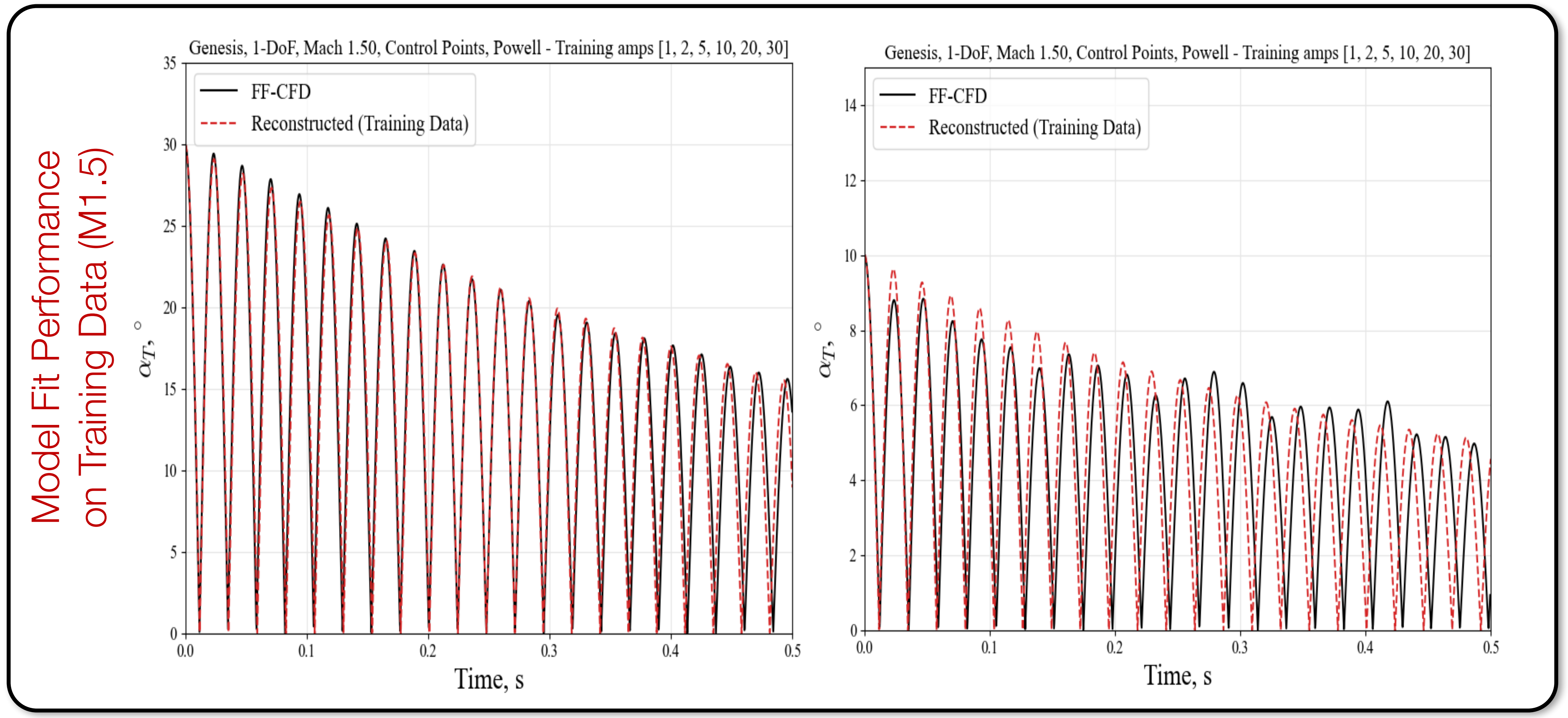

End-to-End Example

Complete FFCFD Data Set

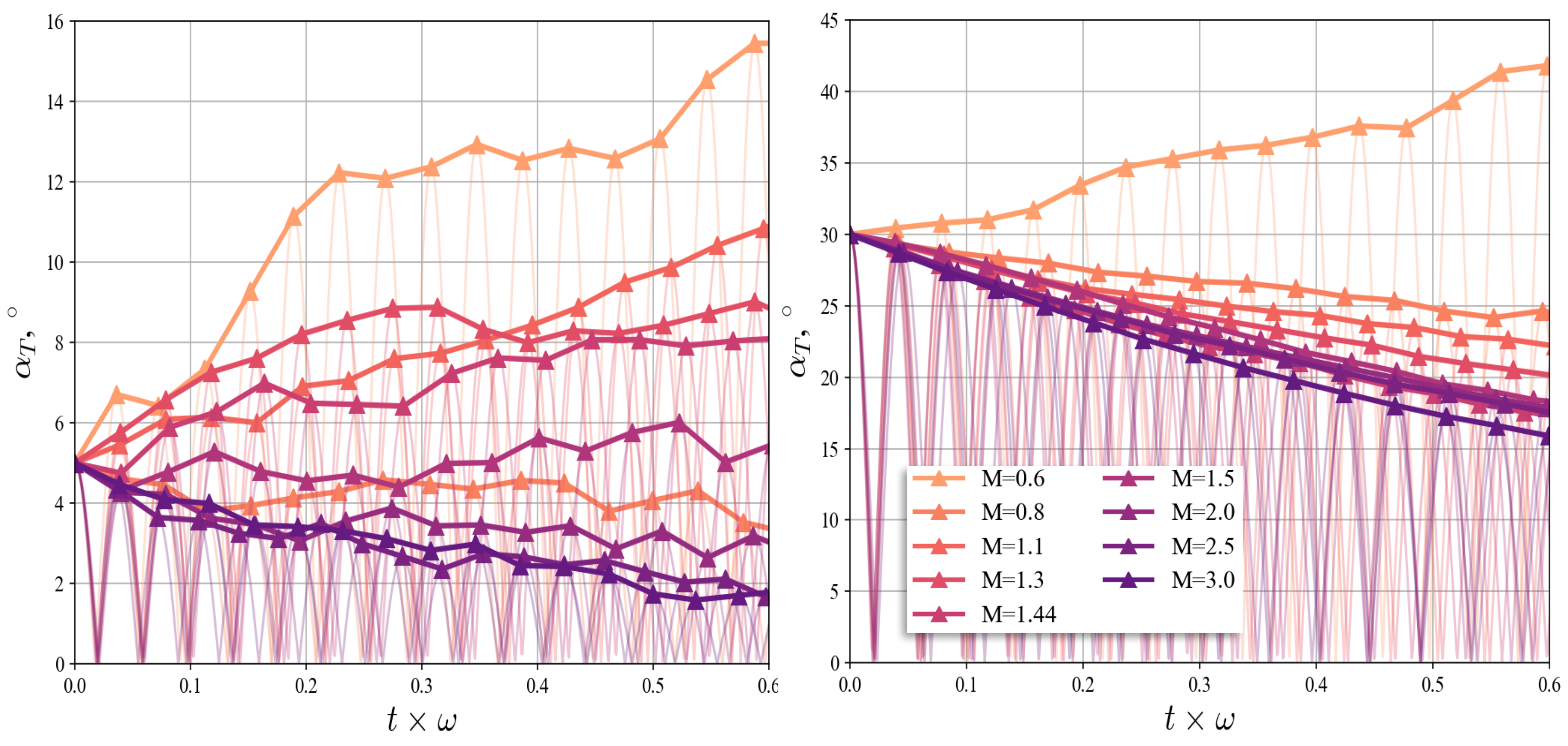

Train

Model Fit Performance on Training Data (M1.5)

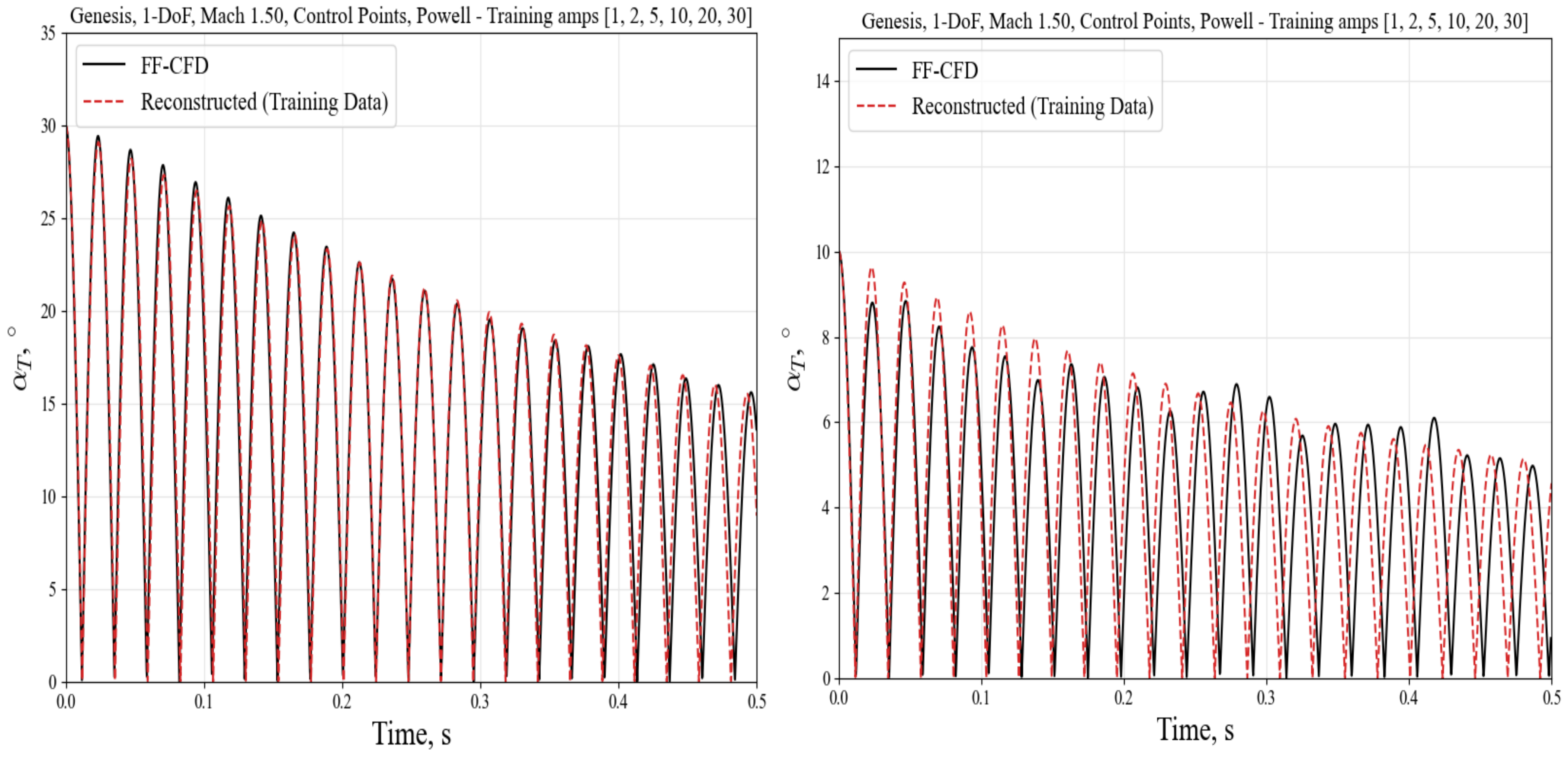

$C_{m_q}(M, \alpha)$

Static and Dynamic Aerodatabase as f(M,α)

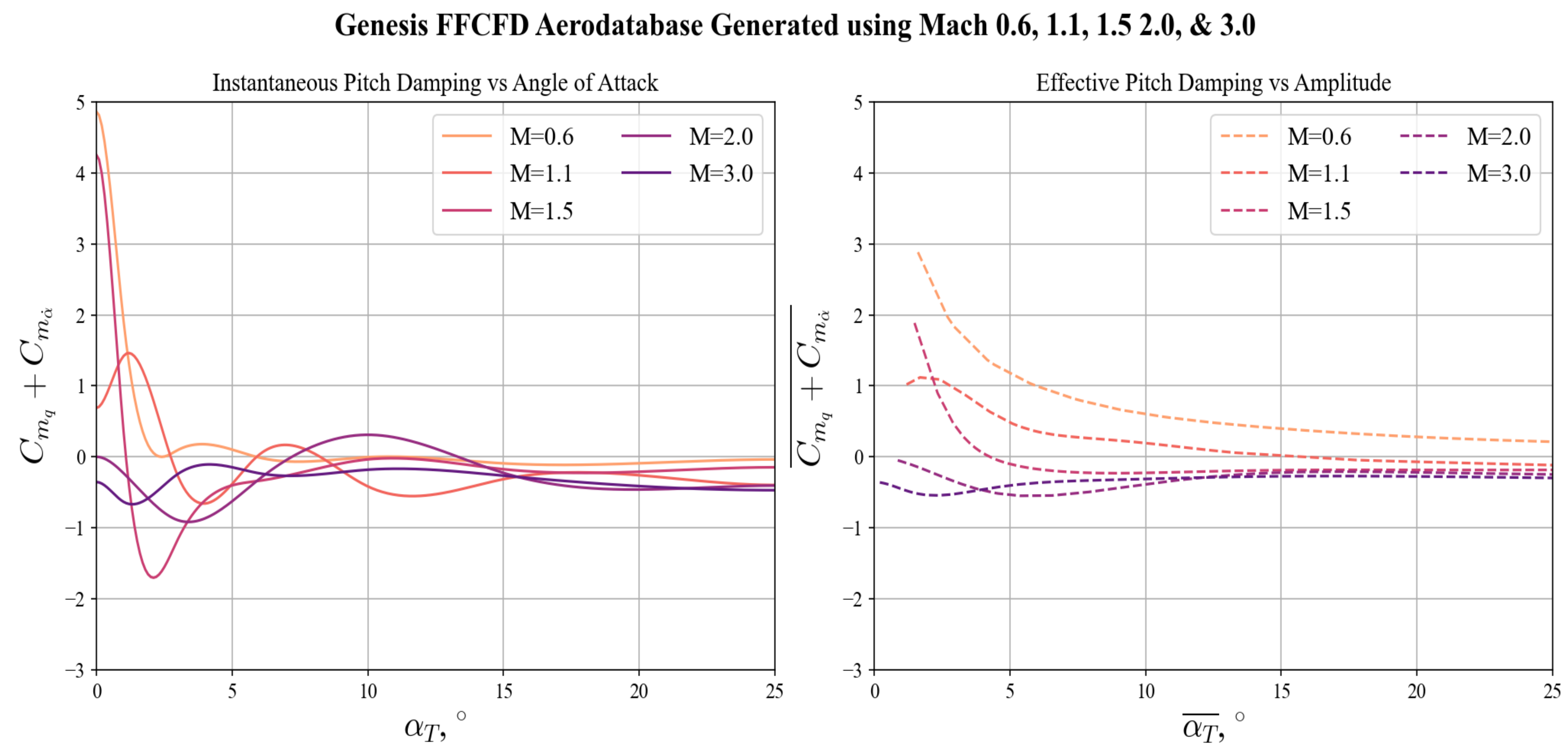

End-to-End Example

Complete FFCFD Data Set

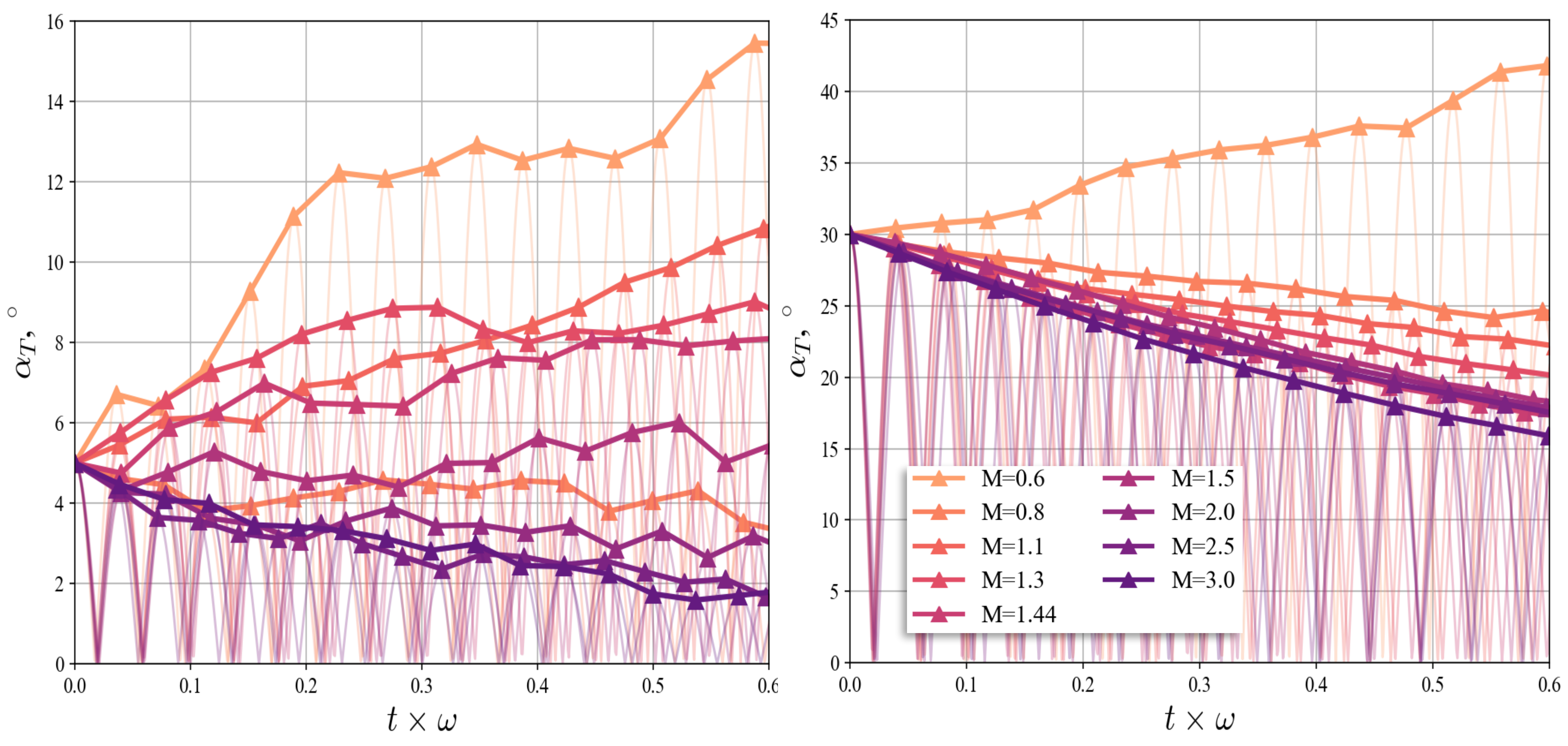

Train

Model Fit Performance on Training Data (M1.5)

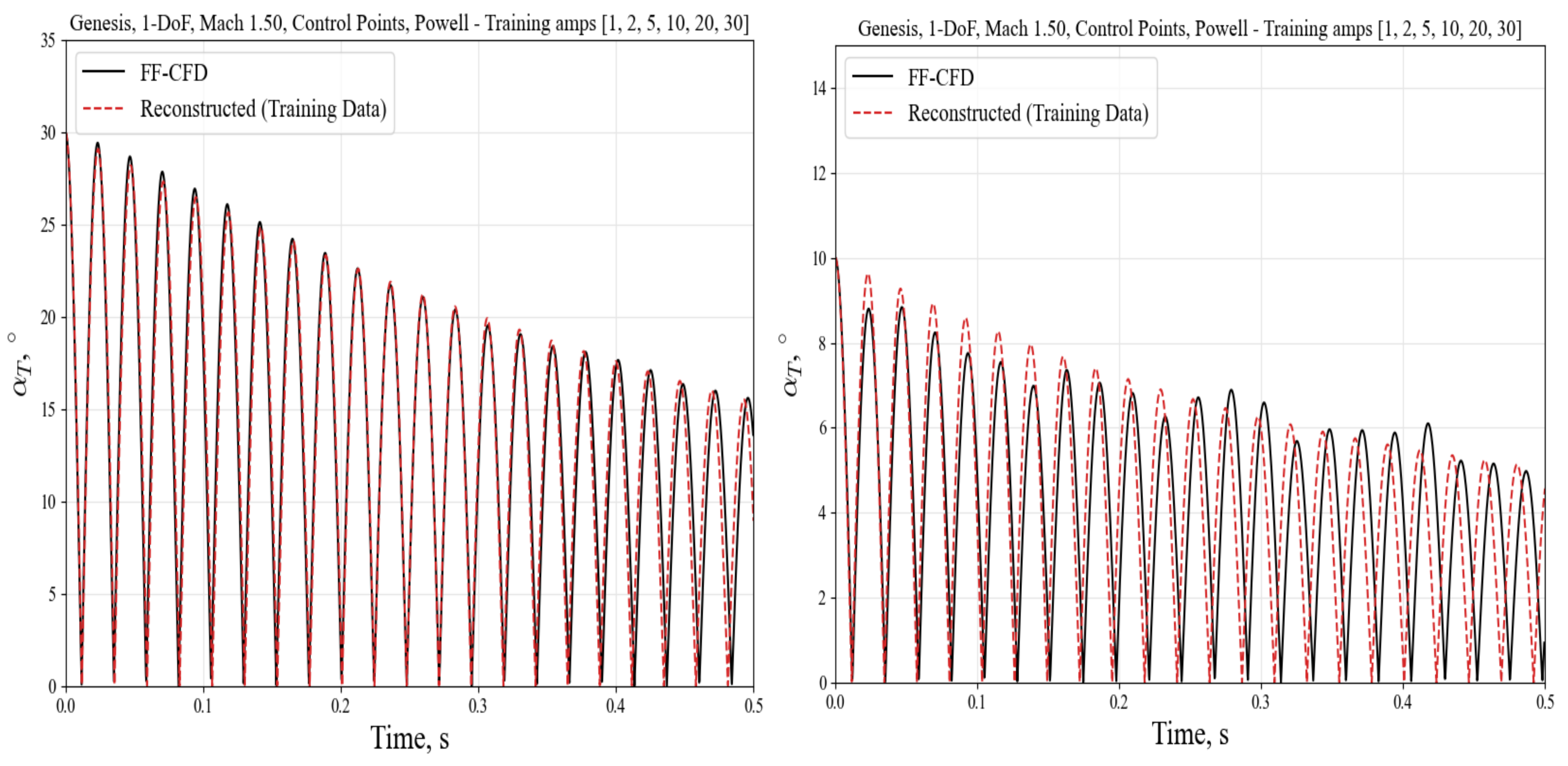

$C_{m_q}(M, \alpha)$

Static and Dynamic Aerodatabase as f(M,α)

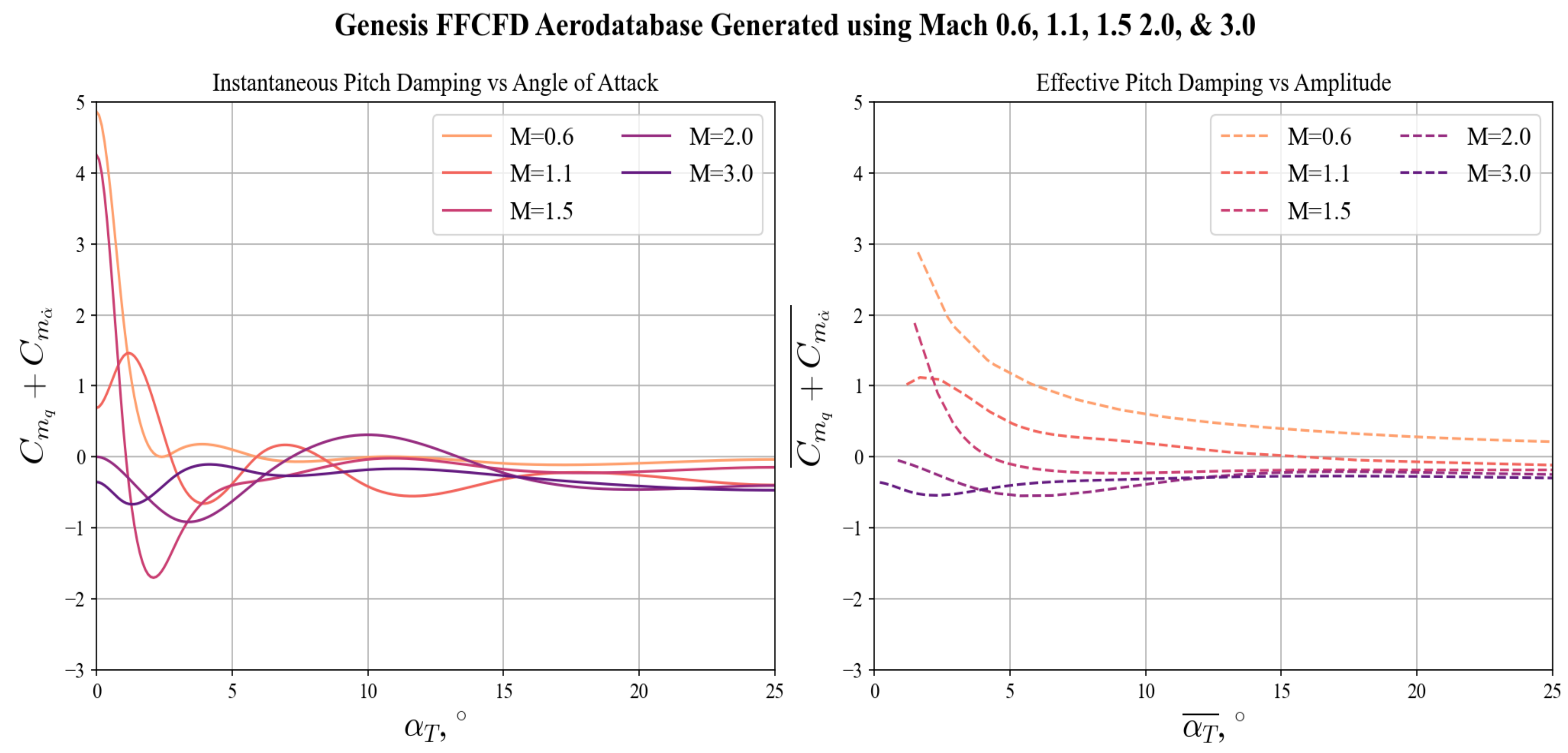

Validate

Model Validation on previously unseen Data (M1.3 and 2.5)

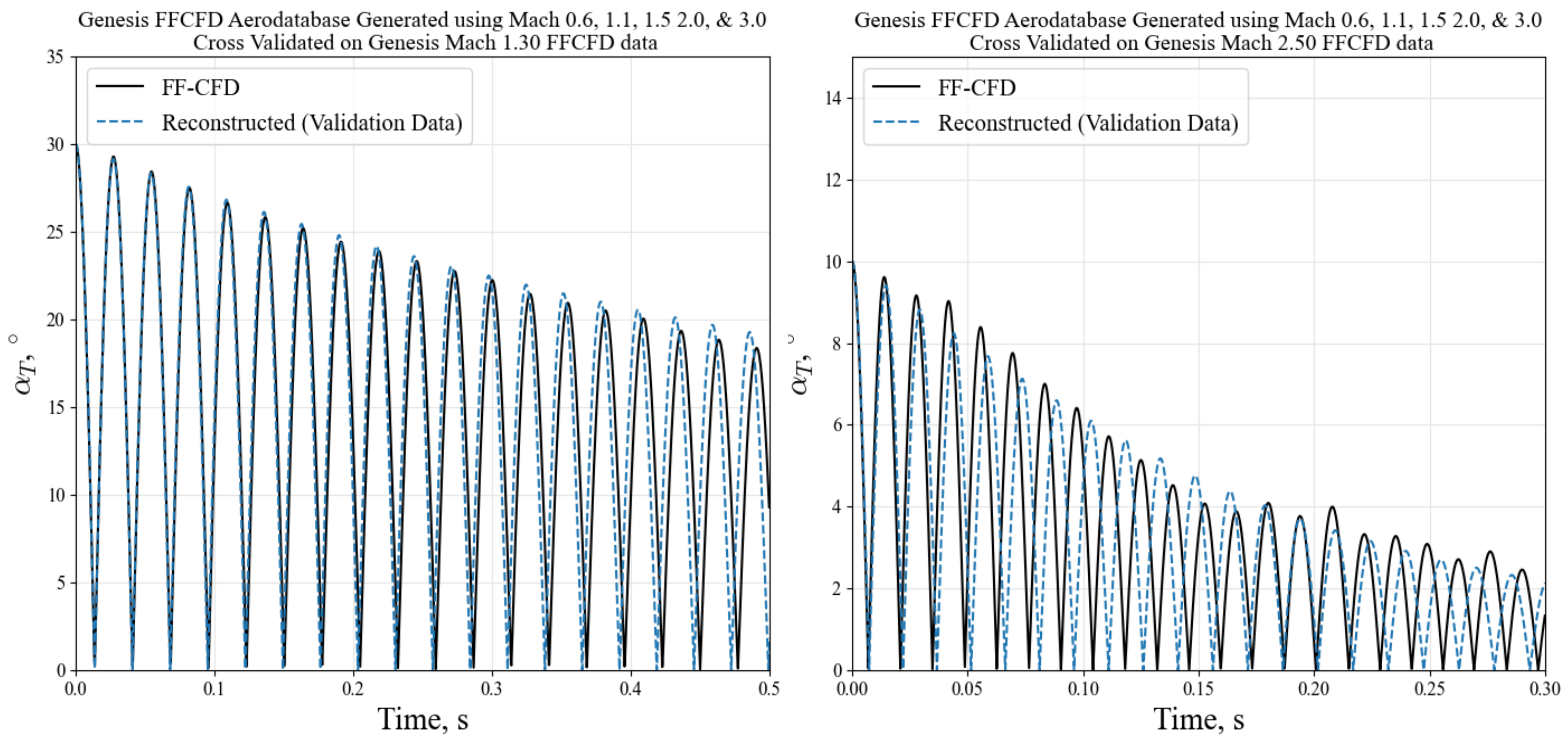

Utilities: Effective CMq curves, section fits

- Effective pitch damping integrated over one cycle
  - Map $C_{M_q}(\alpha) \rightarrow \bar{C}_{M_q}(amplitude)$
  - C_{M_q} as a function of instantaneous α is required for integration into flight dynamics simulations
  - Effective C_{M_q} as a function of oscillation amplitude provides more intuitive insights about where the vehicle is stable and permits more readily digested comparisons between data-sets
  - With effective curve, limit cycle can be predicted for 1dof (simulation or experiment) and 3dof (flight-like) configurations
- Sectional fitting of effective CMq using analytical solutions
  - Shows good agreement with effective CMq curve computed above
  - Provides means to quantify scatter in curve

$$\bar{C}_{mq} = \frac{\int_0^{\frac{2\pi}{\omega}} \left(C_{mq} + C_{m\dot{\alpha}}\right)\dot{\alpha}^2\, dt}{\int_0^{\frac{2\pi}{\omega}} \dot{\alpha}^2\, dt}$$

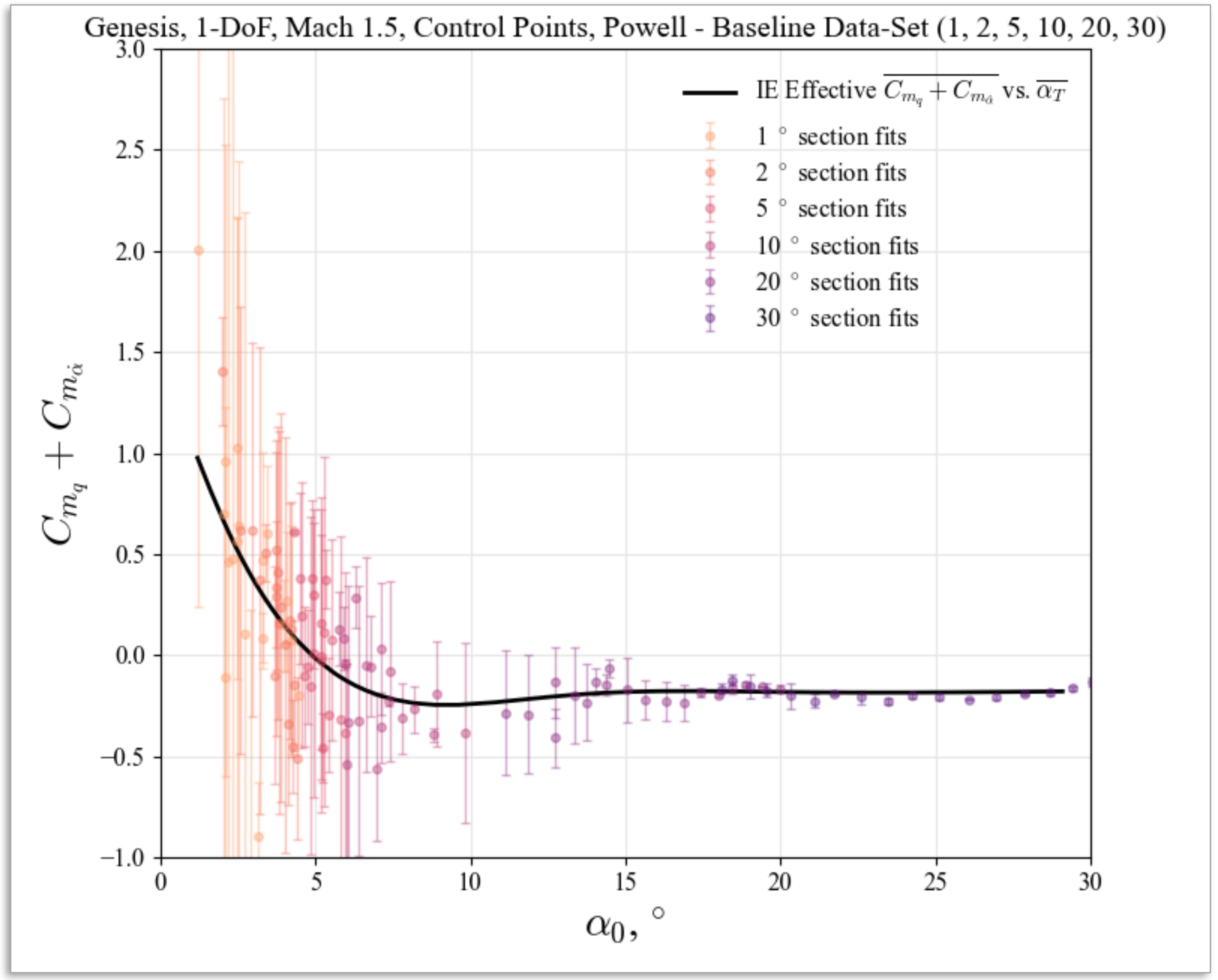

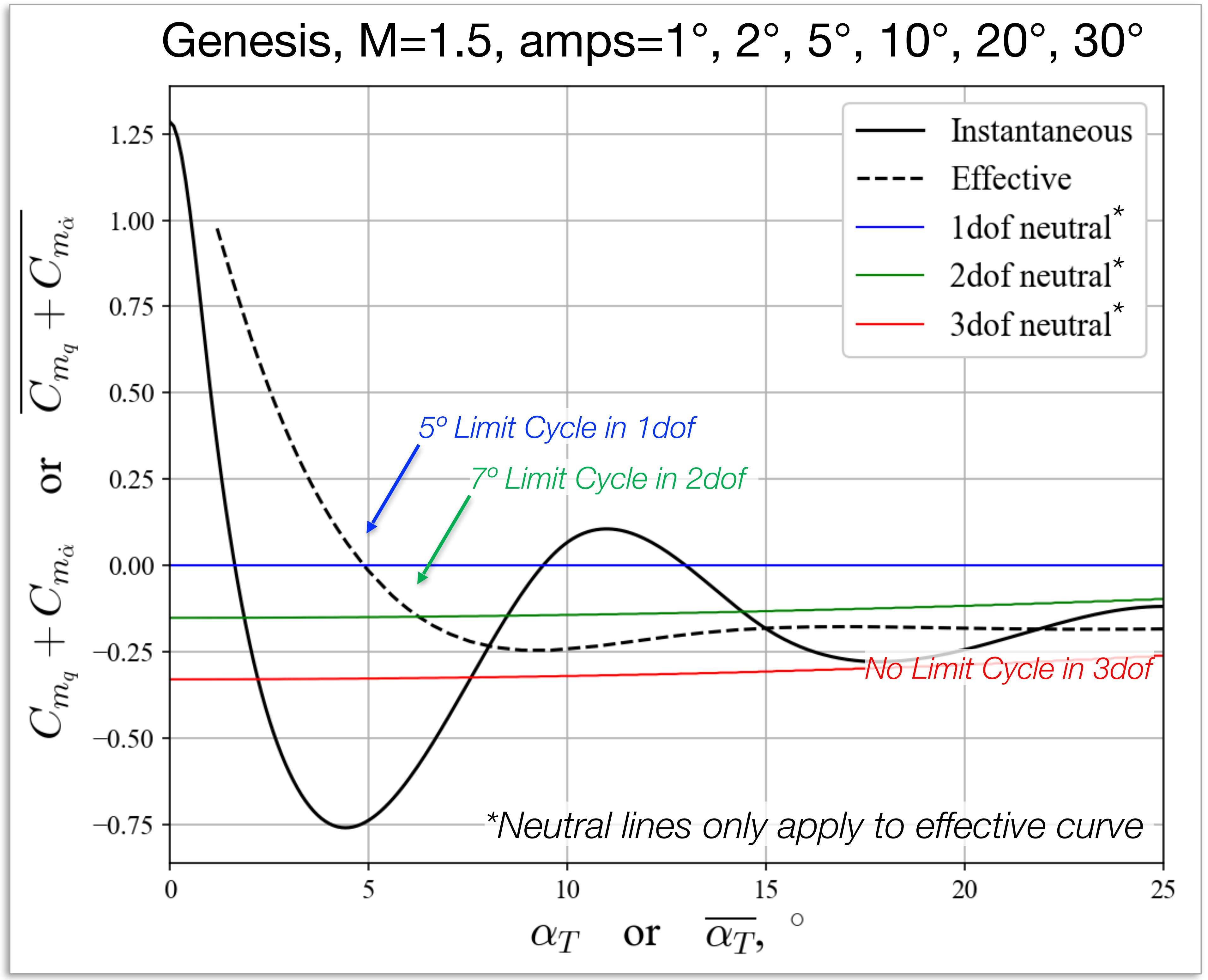

- ESM has invested in Free-Flight CFD capability to bring a computational tool into the portfolio for characterizing dynamic stability
- Extending CFD capability to quantify dynamic stability and perform sensitivity studies for flight projects requires verified and validated tools
  - FF-CFD in US3D has been extensively validated in the supersonic, transonic, and mid-subsonic regime
  - Dynamic simulations provide a new paradigm to simulate as you fly
- Effort in the last 18 months has expanded into developing the data reduction techniques necessary to produce full aerodynamic databases from FF-CFD data
- With a validated tool for modeling the dynamics and an established method for reducing data, computational tools can provide value throughout mission life

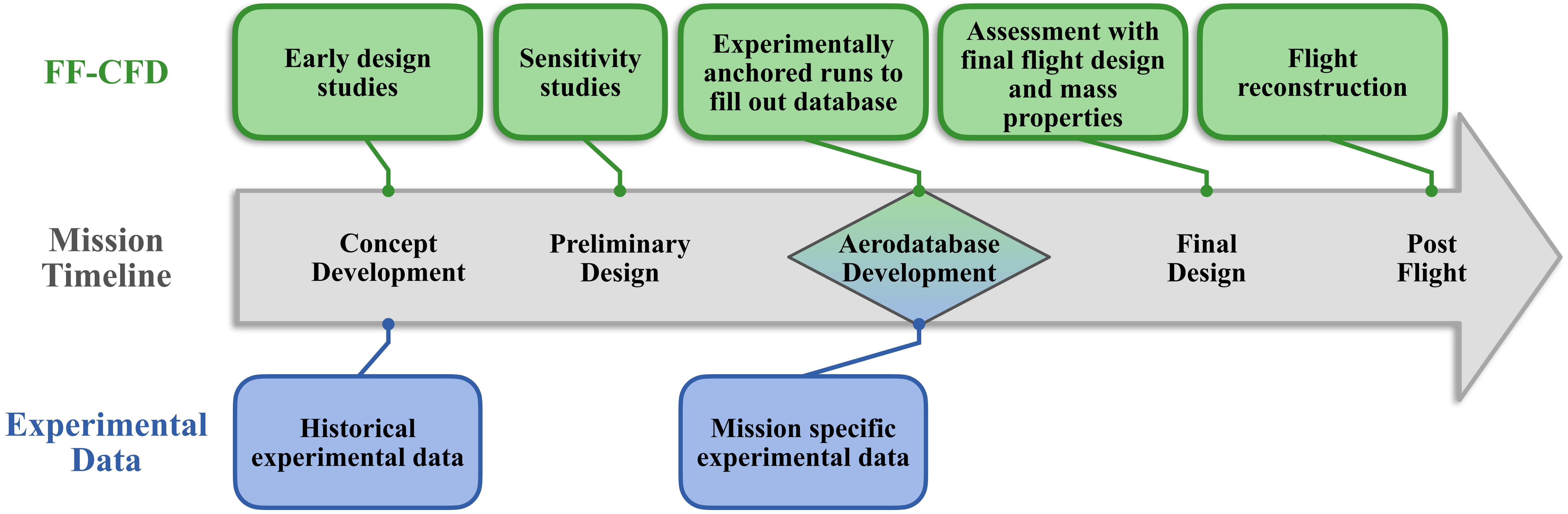

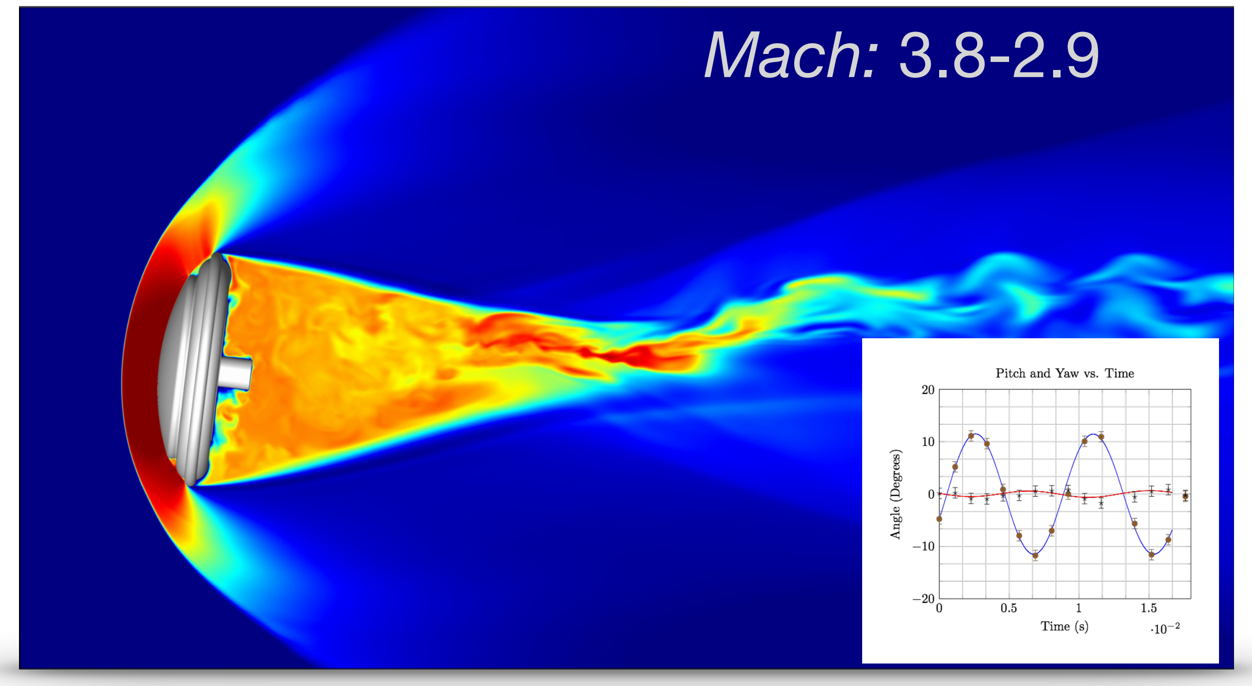

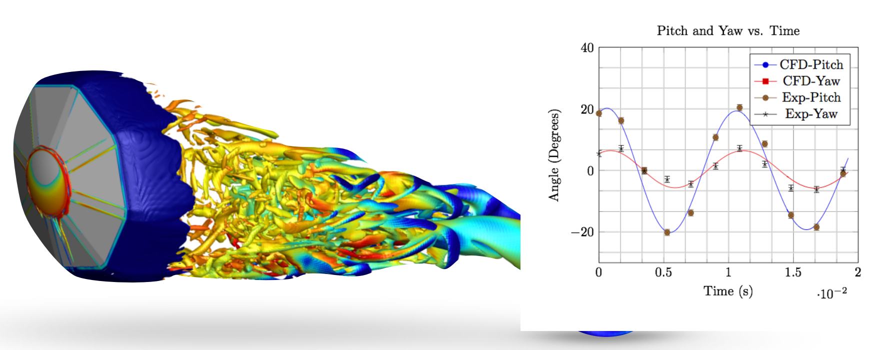

Mach: 2.4-1.2

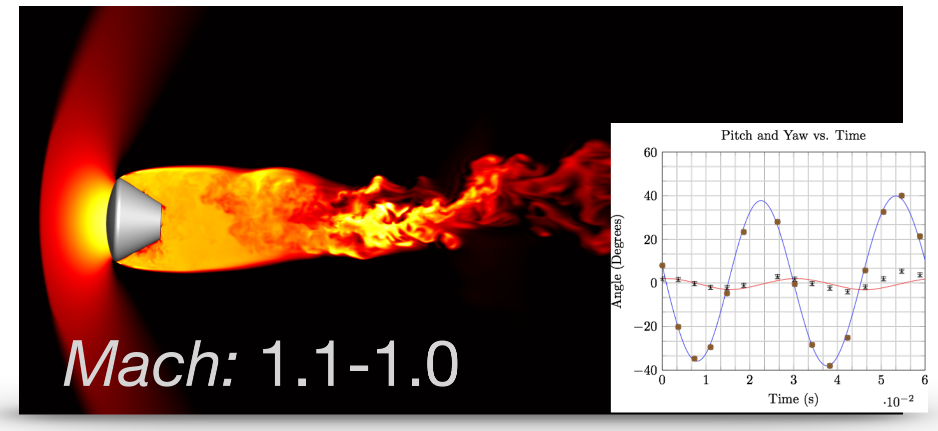

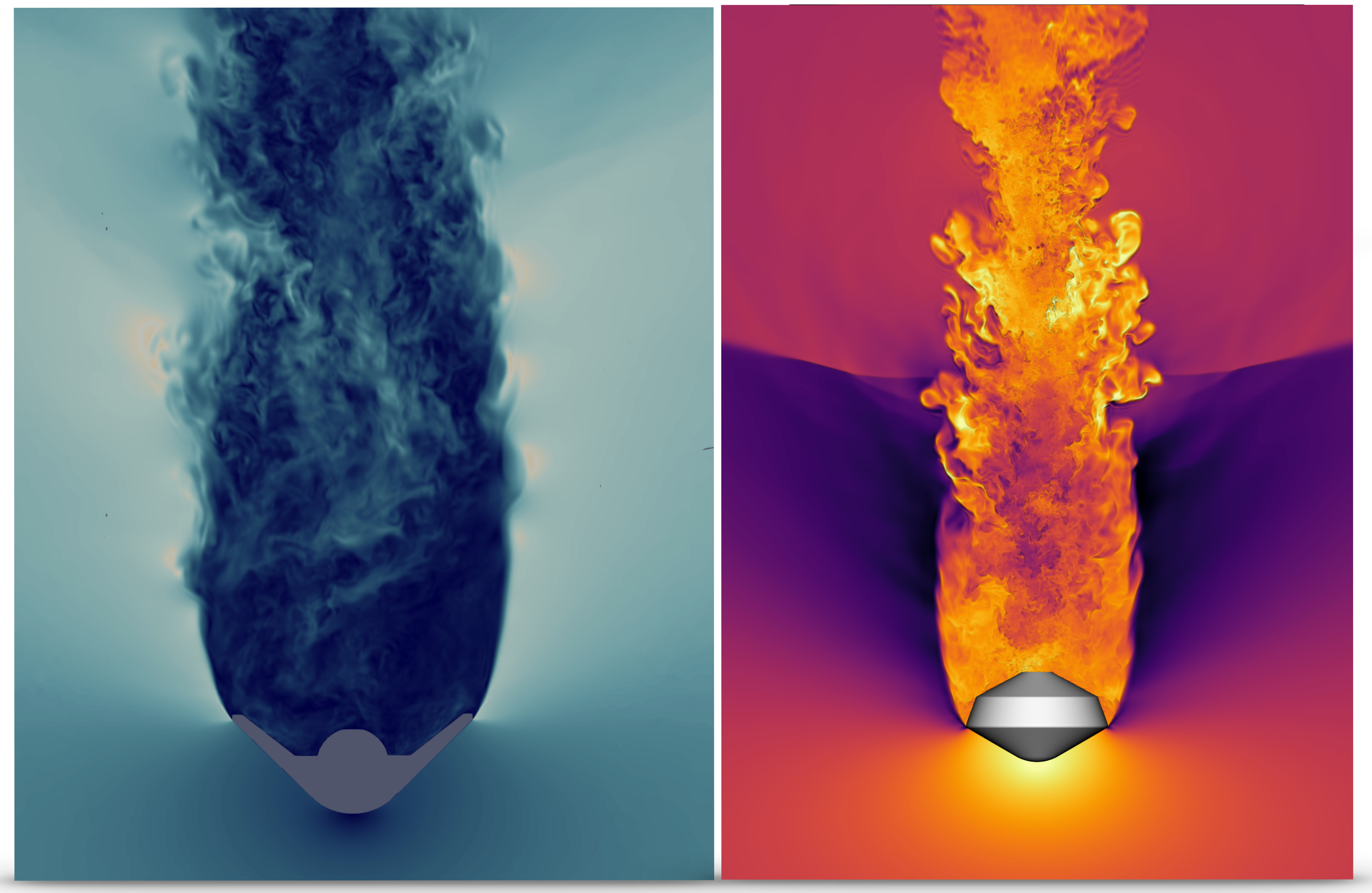


Questions?

References

1. Stern, Eric, et al. "Dynamic CFD Simulations of the MEADS II Ballistic Range Test Model." AIAA Atmospheric Flight Mechanics Conference. 2016.

2. Brock, Joseph M., Eric C. Stern, and Michael C. Wilder. "Computational fluid dynamics simulations of supersonic inflatable aerodynamic decelerator ballistic range tests." Journal of Spacecraft and Rockets 56.2 (2019): 526-535.

3. Hergert, Jakob, et al. "Free-Flight Trajectory Simulation of the ADEPT Sounding Rocket Test Using US3D." *35th AIAA Applied Aerodynamics Conference*. 2017. Brown, Jeffrey D., et al. "Transonic Aerodynamics of a Lifting Orion Crew Capsule from Ballistic Range Data." Journal of Spacecraft and Rockets 47.1 (2010): 36-47.

4. Brock, Joseph M, et al. "Free-Flight CFD Simulations of Transonic MPCV Ballistic Range and Subsonic AA-2 Flight Test". Pending Journal of Spacecraft and Rockets submission

5.Schoenenberger, Mark, and Eric M. Queen. "Limit cycle analysis applied to the oscillations of decelerating blunt-body entry vehicles." NATO RTO Symposium AVT-152 on Limit-Cycle Oscillations and Other Amplitude-Limited, Self-Excited Vibrations. No. RTO-MP-AVT-152. 2008.

6. Stern, Eric, et al. "A Method for Deriving Capsule Pitch-Damping Coefficients from Free-Flight CFD Data". Pending Journal of Spacecraft and Rockets submission

7. McKown, Quincy E., et al. "Attitude Reconstruction of Free-Flight CFD Generated Trajectories Using Non-Linear Pitch Damping Coefficient Curves." AIAA SCITECH 2022 Forum. 2022.